Biochar and pH as Drivers of Greenhouse Gas Production in Denitrification Systems

James Martin Davis, IV

Thesis submitted to the faculty of the Virginia Polytechnic Institute and State University in partial fulfillment of the requirements for the degree of

Master of Science in
Biological Systems Engineering

Zachary M. Easton, Chair
Leigh-Anne Krometis
Brian Badgley

December 4th, 2015
Blacksburg, Virginia

Keywords: (denitrification, biochar, pH, nitrous oxide, N_2O, greenhouse gas, GHG, nitrogen cycle, proximal and distal controls, bioreactor, DNBR, *nirK*, *nirS*, *nosZ*)

Biochar and pH as Drivers of Greenhouse Gas Production in Denitrification Systems

J. Martin Davis, IV

Abstract

Nitrous oxide (N_2O) is a greenhouse gas (GHG) with 300 times the radiative forcing in the atmosphere of carbon dioxide (CO_2), and has recently become a subject of great concern because the nitrogen (N) fertilizers which have been necessary to increase agricultural productivity have also dramatically increased N_2O emissions from agroecosystems. Many N control practices have been suggested and implemented in agroecosystems, but their ability to simultaneously remove reactive N from the environment and prevent the production of N_2O is, at best poorly understood. The goal of this work is to characterize environmental controls on production of N_2O in denitrifying bioreactors. The review portion of this work first discusses the geologic history of the N cycle, how its past and present processes differ, and how it is being affected by human activity. It then explores the N cycle's biochemical pathways, reviews the controls for each of its steps, and discusses the environmental drivers of these controls. The review closes with a discussion of environmental N management strategies. The experimental portion of this work further explores these concepts by observing how biochar amendment and the modification of pH affect N_2O production in the denitrification pathway in denitrifying bioreactors. Both pH and biochar have previously been shown to affect N_2O production and many N management practices utilize biochar or manipulate pH to increase N retention. The objectives of the experiment were to: 1) Examine headspace N_2O concentration in sealed, biochar-amended, denitrifying bioreactors; 2) Determine if the effects of pH on N_2O production differ in biochar-amended systems versus controls (under acidic, unbuffered, and buffered conditions); 3) Quantify key denitrification genes (*nirK*, *nirS*, *nosZ*) in each treatment combination. Experimental results showed biochar treatment to significantly increase N_2O emissions, a result which runs contrary to most, but not all studies regarding its effects on N_2O production. Differences between treatments decreased with increasing pH levels. Biochar did not exhibit significant effects on individual denitrification genes, but it did show influence on the ratios of their populations. On the other hand, pH was found to have significant effects on *nirS* and *nosZ* populations. Differences in N_2O production between biochar and controls were thus explained by biochar's chemical effects, likely its ability to increase denitrification activity. Developing an understanding of the mechanisms behind these differences will require using a combination of isotope tracing, enzyme assays, and mass balance approaches. Future microbial work in biochar-amended systems should attempt to characterize differences in gene expression, overall community structure, and long-term population trends in the genes of interest. The combination of these approaches should allow researchers to better predict where N_2O production will occur and develop strategies to mitigate it while simultaneously increasing food production to meet the demands of a growing population.

I dedicate this work to my family, whose tenacity in the face of hardship remains a constant inspiration.

Acknowledgements

I would like to acknowledge the contributions of my collaborators in the completion of this work, especially the members of the Easton and Badgley research groups. Zach as my advisor you always supported me and you gave me the room to grow in confidence and skill as a researcher. Brian, you taught me how imperfect our understanding of microbial ecology really is, and showed me how important it is to learn from our failures as much as our successes. Emily, you were a voice of reason in all of the crazy times, and your contributions to the gas analysis and sampling in this study were invaluable. Lucas, Josh, Shan, and Tim – thank you for the extensive troubleshooting support in my microbial analysis. Your attention to detail helped to greatly reduce the impact of my laboratory ADHD. To Mark Rogers, thank you for the experimental concept and assistance in the initial setup. To James and Justin, thank you for the help in the initial and replicate runs. To Leigh-Anne and the other members of the Biological Systems Engineering Department, thank you for your support, your advice, your measured criticism, and for all that you have taught me.

To the teachers of my past who had faith in me, thank you for helping me believe in the possibility of my own success. Specifically, I would like to acknowledge Brenda Atkinson, Peter Lustig, Joe LaRocco, Buster White, Bob Butler, Jack Evans, Asim Esen, Bruce Turner, and Eugene Gregory. A special thanks to Drs. Rebecca Ross and Rob DeLong, who were the first to inspire me to pursue a career in applied science.

Finally, I must again acknowledge the contributions of my family, who enabled me to come as far as I have: specifically, I would like to thank my late uncles Bill and Charlie for the example of being true to oneself in the pursuit of dreams, my sister – who listened when no one else did, my mother who refused to ever give up, and my late father who taught me the value of character and whose hard work enabled me to go to college in the first place. Thank you.

Table of Contents

List of Figures

A Synthesis of Microbial Controls in Terrestrial Nitrogen Cycling Systems

Biochar and pH as Drivers of Greenhouse Gas Production in Denitrification Systems

List of Tables

A Synthesis of Microbial Controls in Terrestrial Nitrogen Cycling Systems

Biochar and pH as Drivers of Greenhouse Gas Production in Denitrification Systems

J. Martin Davis, IV
Master's Thesis

A Synthesis of Microbial Controls in Terrestrial Nitrogen Cycling Systems

I - 1. Background

Nitrogen (N) is an essential element for all life as we know it. Dinitrogen gas (N_2) makes up 78% of the Earth's atmosphere, and N is a key component of many biomolecules. Environmental N compounds can exist across a range of oxidation states that cover eight charge equivalents, making it an exceptionally versatile compound. Nevertheless, as most N on Earth is present as inert N_2 gas, its bioavailability is a major constraint for supporting life in a given ecosystem. The transformation of environmental N by microbes into biologically useful molecules forms the backbone of the biogeochemical N Cycle. It is only by virtue of this cycle that sufficient quantities of bioavailable N exist to support complex life on earth. However, imbalances in the N cycle can induce major environmental consequences that include eutrophication, soil and water acidification, ecosystem disruption, ground-level ozone formation, and methomoglobinemia. In order to explore how these effects occur, it is first necessary to examine the processes of the N cycle itself.

The N Cycle is a complex group of oxidation-reduction reactions that convert the various forms of N for the purposes of energy generation, waste excretion, and biosynthesis (Bothe et al., 2007). Figure 1 provides an illustration of its key pathways. The N Cycle begins with N fixation, an energy intensive process that converts N_2 into ammonium (NH_4^+). This ammonium can then be oxidized under aerobic conditions into hydroxylamine (NH_2OH), which is then converted to nitrite (NO_2^-) and finally nitrate (NO_3^-) in the nitrification pathway (Bothe et al., 2007). Under oxygen-limited conditions, NO_3^- can be reduced to NO_2^-, nitric oxide (NO), nitrous oxide (N_2O), and finally dinitrogen gas (N_2), in the denitrification process. Historically, denitrification was understood to be a heterotrophic and anaerobic process, with nitrogenous compounds substituting for oxygen as the terminal electron acceptor in the respiratory oxidation of

carbon (C) (Averill and Tiedje, 1982). However, in the last few decades, aerobic and autotrophic forms of denitrification have been discovered that use unique mechanisms to facilitate the reduction of NO_3^- to N_2 (Burgin and Hamilton, 2007). Other biological reactions in the N Cycle include dissimilatory nitrate reduction to ammonium (DNRA), an energy production pathway that converts NO_3^- to NH_4^+; anaerobic ammonium oxidation (Anammox), a series of reactions that combine NH_4^+ and NO_2^- to form N_2 gas; ammonification, which converts organic N into NH_3 in decomposition, and assimilatory pathways, that incorporate reactive N into biomolecules materials (Bothe et al., 2007). Lastly, under some chemical conditions, many forms of reactive N can be transformed by abiotic processes in situ.

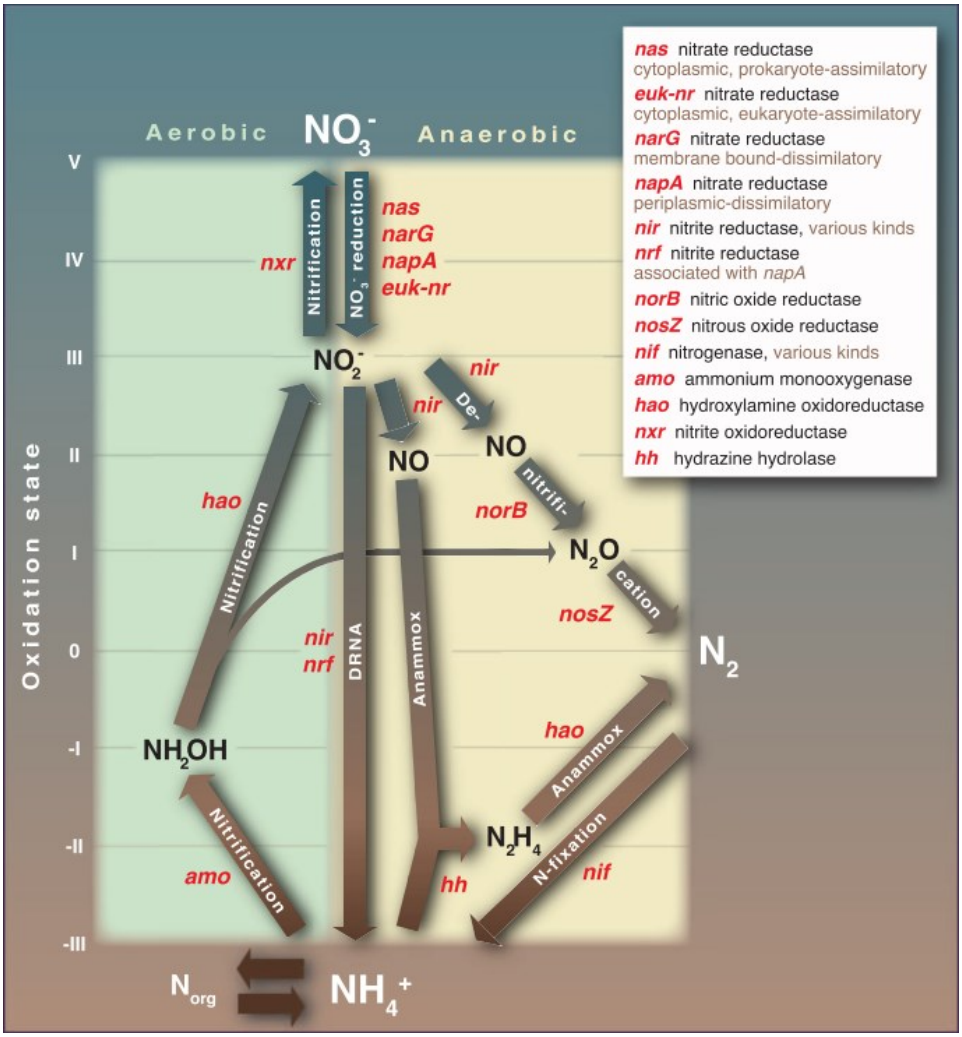

Figure 1: Illustration of the key pathways of the nitrogen cycle. From Canfield, D. E., A. N. Glazer, and P. G. Falkowski. 2010. The evolution and future of Earth's nitrogen cycle. Science 330(6001):192-196. Reprinted with permission from AAAS.

Beyond these natural systems, industrial pathways, such as the Haber-Bosch process, which synthesizes ammonia (NH_3) from N_2 and hydrogen, have had a profound impact on global N balance. In many ways, the changes have been positive, as N is a primary limiting factor to agricultural production. Chemical fertilizers have allowed us to grow more food than at any other time in history. Up to 40% of the world's current population would not be supported without these massive N inputs (Erisman, 2004). However, these inputs engender major ecological consequences. Excess reactive N has been linked to acidification of both soils and waters, ecosystem disruption through altered carbon (C) to N ratios, ground-level ozone formation, eutrophication, and methomoglobinemia (Driscoll et al., 2003; Erisman, 2004; Galloway et al., 2003). Additionally, N_2O, a product of several N Cycle reactions, is a greenhouse gas (GHG) 300 times more potent than CO_2 (Canfield et al., 2010). In order to understand and mitigate these impacts, their environmental context must first be explored, and to this end, it is necessary to dissect the N Cycle itself. In doing so, one must explore its evolution, its biochemistry, and its controls. Only when this thorough exploration is complete will it be realistic to develop solutions that address all aspects of the issues surrounding excess reactive N.

1.1 The Nitrogen Cycle's Evolution and why it Matters

The organisms and processes which underlie the current N Cycle have not always been the same. Rather, they evolved over billions of years in the context of changing environmental conditions (Canfield et al., 2010). Indeed, the chemistry of the ancient N Cycle was vastly different than its current incarnation. For example, Archean environmental conditions precluded the evolution of copper (Cu) -dependent N Cycle enzymes (nirK, nor, nosZ, amo) because the solubility of Cu in ancient seas was extremely low due to prevailing redox conditions (Anbar, 2008). However, ancient oceans likely did have an abundance of iron (Fe), sulfur (S), and molybdenum (Mo), which would have supported an early evolution of the nitrate reductase enzymes (nar, nap, nrf) (Moir, 2011; Rothery et al., 2008). Molecular phylogenies also show

differences between modern pathways and those of the Archaean epoch. Gene mapping suggests that many of the these processes evolved independently (Moir, 2011). Partial denitrification may have existed in the Last Universal Common Ancestor (LUCA), but conversion of other N intermediates would have taken place by abiotic processes such as lightning strikes, serpentinization, volcanic eruptions, and meteorite impacts (Moir, 2011). The most important environmental shift to drive the modern N Cycle's evolution was accumulation of molecular oxygen in the atmosphere between 2 and 2.5 million years ago (Allen and Martin, 2007; Tomitani et al., 2006). Aside from the partial denitrification pathway, which was likely present in the LUCA, only a small number of genes (variants of DNRA, ammonification, and N fixation) were likely to have arisen before this event (Moir, 2011). This history paints a picture of a dynamic N Cycle that has changed in response to the chemical, physical, and biological pressures of the past. As we reflect on the ecological changes being brought on as we enter the Anthropocene (Crutzen, 2002a, b; Steffen et al., 2007), we must consider what effect our actions may exert on the N Cycle of the future.

1.2 The Future of Earth's Nitrogen Cycle

Since the development of input intensive agriculture, humans have drastically altered the global N balance in order to support a growing population. The global N balance can be defined as the cumulative outcomes of N_2 fixation (natural and artificial) and the processes which convert reactive N to inert, atmospheric N_2. The combined outputs of the Haber-Bosch process, the cultivation of N fixing organisms, and the burning of fossil fuels account for more than 45% of all reactive nitrogen entering the environment each year (Canfield et al., 2010), and more reactive N enters the terrestrial environment from these processes than all natural sources combined (Crutzen, 2002b; Steffen et al., 2007). When we consider how much N Cycle processes have changed in the past, we have to wonder what the long term effects of a human-altered nitrogen balance will be. As previously mentioned, this excess N often brings multiple environmental problems (Canfield et al., 2010; Driscoll et al., 2003; Erisman, 2004; Seitzinger et al., 2002). A great deal of

recent research has shown that ecological responses to environmental stimuli are often nonlinear, a fact which is particularly difficult for managers to address because they often lack sufficient information to determine the thresholds where nonlinearity begins (Dodds et al., 2010). Because N is critical to sustaining life, we must consider the evolutionary significance of our actions and act before inflicting irreversible damage. By taking an integrated approach that considers each of the processes involved, we can begin to develop solutions to the problem of anthropogenic N while providing food security, protecting environmental quality, and ensuring sustainable access to agricultural resources for years to come.

I - 2. Controls in N-Cycling Systems

The vast majority transformations in the N Cycle are mediated by microbial processes (Bothe et al., 2007; Seitzinger et al., 2006; Sutton, 2011), but there is rarely enough data to link the drivers of N transformation with specific processes across multiple spatial and temporal scales (Richardson et al., 2009). The current nomenclature uses the terms **proximal and distal controls** to classify these factors based on the scale at which they impact the N Cycle (Fig. 2 – from Sagaar et al. 2013). Proximal controls refer to elements that directly affect the microbial processes at the enzyme/substrate level, while distal controls are those that influence the overall composition of the microbial community (Groffman et al., 1988; Saggar et al., 2013; Wallenstein et al., 2006). Both proximal and distal controls frequently show spatial and temporal variability leading to intervals or regions of increased activity, collectively known as "Hot Spots or Hot Moments" (Groffman, 2012; McClain et al., 2003; Sogbedji et al., 2001). As noted by Groffman, 2012, the importance of each controlling factor also changes with scale. At regional scales, geology, climate, and land use are the most important factors, while at the landscape scale, topography, soil texture, and soil moisture dominate. At the micro- and nano- scales, chemical constraints prevail with oxygen, N, and C availability being the most important proximal controls (Groffman et al., 1988). Thus, to develop a robust understanding of what drives N cycling, it is necessary to study both the macro- and the micro-scale

conditions of an environment. Understanding how these controls interact can provide valuable insights for mitigating excess environmental N, and integrating them into management approaches offers the potential to improve water quality, reduce greenhouse gas emissions, and increase agricultural productivity (Eickhout et al., 2006; Erisman, 2004; Schmidt and Clark, 2013).

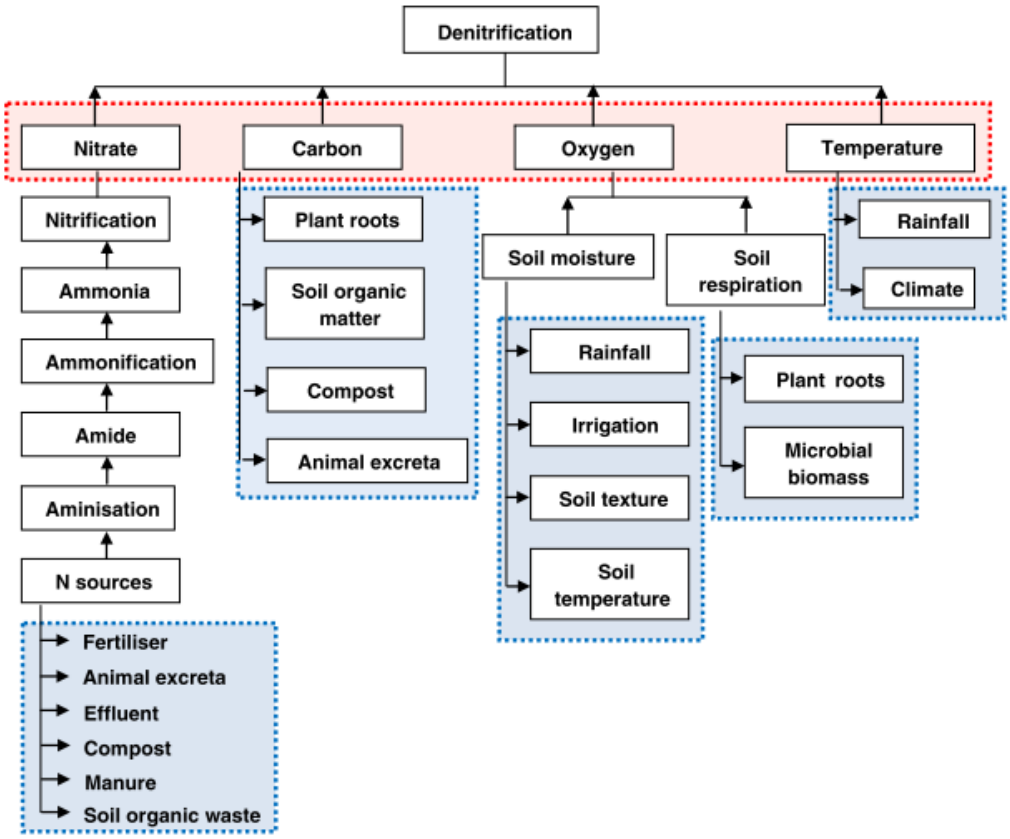

Figure 2: Examples of key proximal and distal factors in N Cycle Regulation. Proximal factors are in red. Distal factors are in blue. Note: pH, which is not included in this figure can act as both a proximal and distal control. From Saggar, S., N. Jha, J. Deslippe, N. S. Bolan, J. Luo, D. L. Giltrap, D. G. Kim, M. Zaman, and R. W. Tillman. 2013. Denitrification and N2O:N2 production in temperate grasslands: Processes, measurements, modelling and mitigating negative impacts. Sci Total Environ 465(0):173-195. Used with permission of Elsevier Limited.

2.1 Proximal Controls: Direct Regulation of N Cycle Enzymes

To begin our analysis of the N Cycle, we must first become familiar each of its key enzymes and their proximal regulators. These enzymes have been characterized, both in-vitro and in-situ, using a wide

variety of techniques including direct assays, structural analysis, and molecular approaches. Some of the more common methods among them include isotope tracing, inhibition, spectroscopy, and chromatography. Newer studies have successfully coupled this data with molecular analysis to identify controls in complex environmental samples. Below, we review current knowledge of N Cycle enzymes and discuss their primary proximal regulators.

Reactive N enters the biosphere as NH_4^+ via N fixation (Bothe et al., 2007; Levy-Booth et al., 2014), a process that is carried out exclusively by diazotrophic prokaryotes using nitrogenase (nif) enzymes. Of these, Mo-nitrogenase is by far the most common (Moir, 2011), and aside from a select group of extreme thermophiles, all N fixing organisms contain this enzyme (Bothe et al., 2007). The genetic sequences that encode for these proteins are highly conserved, with regulation being dependent on three factors: 1) available NH_3 – which suppresses *nif* expression; 2) the presence of O_2, which damages the enzyme (though aerobic N fixers possess ways to internally suppress internal O_2; and 3) access to metal ions – with Mo and Fe being the most important, since they form parts of key enzymatic moieties (Bothe et al., 2007).

Following fixation as NH_4^+, N enters the nitrification pathway, an aerobic process that oxidizes NH_3 or NH_4^+ to NO_2^- by way of NH_2OH, then converts this NO_2^- to NO_3^- (Bothe et al., 2007; Norton and Stark, 2011). This process is facilitated by two groups of organisms: bacterial and archaeal ammonia oxidizers (AOB and AOA), and nitrite oxidizing bacteria. The first stage, ammonium oxidation, is carried out by a sequence of two enzymes, ammonia mono-oxygenase (amo) and hydroxylamine oxidoreductase (hao). The second stage, NO_2^- oxidation to NO_3^- is carried out by the nitrite oxidoreductase (nxr) enzyme. Through mechanisms that are not completely understood, N_2O can also be produced as a by-product of nitrification (Blackmer et al., 1980; Khalil et al., 2004; Sutka et al., 2006). Possible explanations for these include: 1) N_2O as a reaction intermediate in the oxidation of NH_2OH (Khalil et al., 2004; Kool et al., 2011), 2) nitrifier denitrification, where the nitrifiers are also capable of expressing a NO_2 reductase (Khalil et al., 2004; Kool

et al., 2011; Kool et al., 2010; Wrage et al., 2001), and 3) NO_2^- acting as an electron acceptor during NH_4 oxidation under conditions of insufficient O_2 (Khalil et al., 2004; Ritchie and Nicholas, 1972). Indeed, it is likely that all three of these effects may take place under differing chemical conditions. The primary proximal regulators of the nitrification process are 1) ample O_2, CO_2, and NH_3/NH_4^+, 2) sufficient, but not excessive NH_3,,which is toxic at high concentrations, 3) temperature, which affects growth rates and varies by microorganism, and 4) pH where optimum reaction rates are achieved between 7.5 and 8 (Barnard et al., 2005; Bothe et al., 2007; Norton and Stark, 2011).

The NO_3^- generated in nitrification serves as the substrate for the denitrification reactions, a series of reductive reactions that convert NO_3^- to N_2 over the following steps ($NO_3^- \rightarrow NO_2^- \rightarrow NO \rightarrow N_2O \rightarrow N_2$) (Berks et al., 1995; Bothe et al., 2007; Richardson and Watmough, 1999; Weeg-Aerssens et al., 1987; Zumft, 1997). In these reactions, the N compounds act as terminal electron acceptors in an anaerobic respiratory process that oxidizes organic matter to form ATP in (predominantly) heterotrophic bacteria and fungi. The first step of denitrification, the conversion of NO_3^- to NO_2^-, is orchestrated by dissimilatory nitrate reductase enzyme (nar, nap). Both of these are complex iron-sulfur molybdoenzymes, distinguished by being either membrane bound (nar) or periplasmic (nap) varieties (Bothe et al., 2007; Moir, 2011). Regulation of nitrate reductase is accomplished by 1) oxygen, which suppresses transcription in most denitrifiers and acts as a preferred electron acceptor to N compounds, 2) NO_3^- or NO_2^-, which induce expression of *nar* and *nap*, and 3) pH and ORP, which can limit catalysis by altering electrochemical potentials and oxidation states across the cell (Berks et al., 1995; Bothe et al., 2007; Moir, 2011). The second step, reduction of NO_2^- to NO, is carried out in the periplasm by the nitrite reductase enzymes. These are divided into Cu containing (nirK) and cytochrome cd_1 containing (nirS) varieties, only one of which will be present in a given species (Bothe et al., 2007; Moir, 2011). Like the nitrate reductase enzymes, the nitrite reductases are also regulated by oxygen, substrate concentration, and cell pH / ORP

(Bothe et al., 2007; Moir, 2011). *NirK* expression may also be limited by available Cu (Bothe et al., 2007; Granger and Ward, 2003; Moir, 2011). NO produced by the reduction of NO_2^- is rapidly reduced to N_2O in a process catalyzed by the nitric oxide reductase (nor) enzymes. NO is highly reactive and can cause mutations, inactivate metalloprotein ligands, and produce toxins with many intercellular compounds (Richardson et al., 2009; Ye et al., 1994). Perhaps because of this, nor enzymes in bacteria are located on the periplasmic membrane where they act as a barrier to reactive NO entering the cytoplasm (Berks et al., 1995; Hochstein and Tomlinson, 1988; Richardson et al., 2001). The final enzyme in the denitrification process is nitrous oxide reductase (nos), which reduces N_2O to N_2 gas in the periplasm (Ye et al., 1994). Nos is a homodimer whose two catalytic sites each contain six Cu ions (Moir, 2011; Richardson et al., 2009). The system for production and regulation of nos is not completely understood, but of the 50 known genes linked to denitrification, 10 are associated with its assembly and regulation (Bothe et al., 2007). Within this system, the foremost regulators are likely: 1) oxygen, which irreversibly inactivates the enzyme; 2) nitrate, which activates transcription, but at high concentrations is a repressor and preferential electron acceptor to nitrous oxide; 3) pH / ORP, and 4) Cu availability, which, in the event of a shortage, causes a shutdown in *nos* transcription due to its requirement in other essential cell processes (Hochstein and Tomlinson, 1988; Moir, 2011; Richardson et al., 2009). Nos sensitivity to pH is particularly interesting because nitrate, nitrite, and nitric oxide reductases are most active at pH < 7, while nitrous oxide reductase is most active above pH 7 (Richardson et al., 2009). Another feature of pH-mediated regulation of nos is that, near pH 6, while nosZ transcription takes place as normal and existing enzymes remain catalytically active, assembly of functional new proteins is severely inhibited (Bergaust et al., 2010; Cuhel and Simek, 2011a; Liu et al., 2010). Bergaust et al. (2010) noted that nos extracted from a pH 7 culture maintained similar reaction rates when buffered to pH 6.5 and 7.5 and retained 55% catalytic activity as pH approached 6. However, cells from a long-term pH 6 incubation were unable to assemble functional N_2OR, despite measured transcription and translation of precursors. Because of the numerous genes involved in

nos assembly and regulation, it seems logical to suspect that protein assembly is an area where nosZ is uniquely vulnerable to inhibition compared to the other denitrification enzymes.

Like denitrification, DNRA is a form of anaerobic respiration that begins with reduction of NO_3^- to NO_2^-, but instead of proceeding with the formation of gaseous N oxides, it terminates with NO_2^- being directly reduced to NH_4^+ (Bothe et al., 2007; Burgin and Hamilton, 2007). In some cases, DNRA can outcompete denitrification because, in addition to generating ATP, it consumes additional electrons and generates more NAD^+ than denitrification (Bothe et al., 2007; Kaspar et al., 1981). This an advantage in highly reduced environments where generating oxidants like NAD^+ is a necessity. NO_3^- reduction via DNRA uses some of the same enzymes as in denitrification, nar or nap. Above 1mM NO_3^- concentrations, organisms utilize a cytoplasmic process that employs nar for NO_3^- reduction to NO_2^- and the nirB enzyme for NO_2^- reduction to NH_4^+; for lower concentrations, nap and nrf are utilized in an energy-conserving periplasmic process (Wang et al., 1999). Transcription of genes in both pathways is repressed by the presence of O_2 but induced by the presence of NO_3^- or NO_2^- (Bothe et al., 2007). Nap is also employed in the few organisms that are able to reduce NO_2^- but lack the capacity to reduce NO_3^- , as is the case for many sulfate reducers which also carry out DNRA (Bothe et al., 2007). Lastly, sulfides can enhance bacterial preference for the DNRA pathway over denitrification as they both inhibit denitrification (Burgin and Hamilton, 2007; Santoro, 2010; Sorensen et al., 1980) and are employed as an electron donor for DNRA.

The last N Cycle reaction chain to be considered, anaerobic ammonia oxidation, or Anammox, uses NO_2^- to oxidize NH_4^+ into N_2 by way of a hydrazine (N_2H_2) and a possible hydroxylamine (NH_2OH) intermediate (Jetten et al., 2001; Kuenen, 2008). The process has yet to be fully characterized, and debate continues as to what enzymes and substrates are employed in the initial steps (Kuenen, 2008; Moir, 2011; Song and Tobias, 2011). It is thought that NO_2^- is reduced (by an uncharacterized enzyme) to NH_2OH which is reacted with NH_4^+ by hydrazine hydrolase (HH) to form N_2H_2. The final step, the conversion of N_2H_2 to N_2, is known

to be carried out by hydrazine oxidoreductase (hzo), an enzyme that is closely related to the hydroxylamine oxidoreductase enzymes present in ammonia oxidizing bacteria (Li et al., 2010; Moir, 2011). Oxygen concentrations, even as low as 2 µM have been shown to completely inhibit Anammox, although the inhibition is reversible upon resumption of anaerobic conditions (Jetten et al., 2001). Transcriptional regulation underlying the Anammox process has yet to be characterized (Moir, 2011).

2.2 Distal Controls: Effects on Microbial Populations and Functional Genes

Understanding the ecological role of a microbial community requires knowledge of the population structure and the relative abundance of functional genes that code for key enzymes. Techniques used to characterize community structure include terminal restriction fragment length polymorphisms (T-RFLP) or Denaturing Gradient Gel Electrophoresis (DGGE), fatty acid analysis, and metagenomics. Probing individual genes is typically done using Polymerase Chain Reaction (PCR), Fluorescent In-Situ Hybridization (FISH), or clone-and-sequence approaches. Analysis of protein products is done with a variety of enzyme, immunochemical, or stable isotope assays. These techniques can be used in conjunction with physicochemical analysis, tracer studies, and other environmental methods to infer which environmental conditions shape the microbial population that underlies N Cycle processes.

Several laboratory studies have linked changes in microbial community with alterations in C or N input (Gentile et al., 2007; Hai et al., 2009; Han et al., 2014; Van de Pas-Schoonen et al., 2005; Vilar-Sanz et al., 2013; Wang et al., 2013). Even under *in vitro* conditions with a single C source, alterations in N input and changing substrate concentrations were enough to generate complex consortia of microorganisms (Van de Pas-Schoonen et al., 2005). In this study, a co-culture of *A. faecalis* and *Pseudomonas* were tested with nutrient limitations, variant N sources, and assessed for competitiveness in a mixed culture of other denitrifiers. Under C limited conditions with NO_3^- as the electron acceptor, the authors observed <5ppm

N_2O in the headspace and a near 1:1 population ratio. When switched to NO_2^- as electron acceptor, N_2O emissions rose to 164ppm and *Pseudomonas* dropped to 10% of the biomass. Carbon limitation in the mixed cultures shifted the population from (45%) *β*- and (40%) *γ*- proteobacteria, to one dominated by *α*- (65%) and *β*- (10%) with *γ*- (>5%) over a 30-day period. Nitrogen limited conditions resulted in similar community ratios but different organisms in the *α*-proteobacteria fraction. Other work has looked at responses to changing C input in microbial fuel cells (Vilar-Sanz et al., 2013). Cycling the input media from salt only (autotrophic), to a carbonaceous media (heterotrophic), and then back to salt only conditions resulted in major alterations to the microbial community present in the fuel cell. High diversity was observed for nitrate and nitrite reductases (*narG, napA, nirS, nirK*), but 90% of all *nosZ* gene variants were in one taxa across all environmental conditions. Relative abundance of *nir* to *nos* (q*nirS*+q*nirK*)/q*nosZ*, as well as dominance of *nirS* denitrifiers correlated positively with N_2O emissions during the trial. Environmental perturbations have also been shown to create long-term alterations of the microbial community structure (Gentile et al., 2007). In Gentile et al., 2007, six identical chemostats were inoculated with sludge from a stable denitrifying culture in this study. They were maintained for 130 days on ethanol/lactic acid media with 15 mM NO_3^--N and a Chemical Oxygen Demand (COD) to N ratio of 8.2g. On three occasions, influent NO_3^--N was increased to 24 mM for 67 hours. In two of the six replicates, there were major alterations to both the microbial community and reactor performance relative to the other columns. These results illustrate the sensitivity of microbial populations to C and N inputs, and they show a need for engineers to account for C and N fluctuations or risk unwanted alterations in N-Cycling rates, formation of undesirable by-products (N_2O), or even die-off of the microbial community.

Changes in C and N input also induce changes in N cycling communities in the field. Differing fertilizer treatments have been shown to alter the proportions and abundance of rhizosphere soil microbes (Hai et al., 2009; Saggar et al., 2013). Generally, ammonium oxidizers and denitrifiers dominated urea-fertilized

plots, while plots fertilized with organic waste (straw and manure) supported a larger population of N-fixing organisms, though there were small increases in *nirK* denitrifiers as well (Hai et al., 2009). Manure was also associated with larger numbers of denitrifiers carrying the *nosZ* gene, an important finding for researchers seeking to reduce N_2O emissions. Increased *nosZ* gene abundance has be associated with the use of biochar as a C amendment, both in soils, bioreactors, and compost. Biochar is the product of pyrolysis of organic material which is considered a promising tool for carbon sequestration and increasing soil fertility (Lehmann, 2007). Wang et al. (2013) Investigated N_2O emissions and quantified functional denitrification genes in compost amended with biochar versus an unamended control. Compared to the control, the biochar-amended compost had 31% lower N_2O flux, lower abundance of *nirK* denitrifiers, and higher abundance of *nirS* and *nosZ* denitrifiers. All through functional genes were found to be significantly correlated to N_2O emissions with *nirK* being the most significant ($rho = 0.793$, $P < 0.01$). For all of these studies, the relative abundance of bacteria possessing the *nosZ* gene in the total bacterial community was a strong predictor of the N_2O:N_2 product ratio. As in the in vitro studies, environmental research confirms that both the kind and the quantity of C and N are critical controls for the N cycling community structure.

Oxidation / reduction potential (ORP), which is related to pH, oxygen, and the ionic species of the local environment, is another influence on N Cycle community composition. When ORP is stable, highly specialized microbial communities are able to dominate, but under fluctuating conditions, microbial flexibility seems to be more important. One study, which examined tropical forest soils under aerobic, anoxic, and alternating (12h and 4 day intervals) redox conditions, revealed four day fluctuating redox cycles maintained a microbial community very close to that of the source soil, while aerobic and anoxic incubations resulted in significant losses in microbial diversity and shifts toward either nitrifier or denitrifier dominance, respectively (Pett-Ridge et al., 2006). Redox-mediated control of microbial populations has also been noted in wastewater treatment plants (WWTP). In a nine month trial of a staged

membrane bioreactor with both oxic (high ORP) and anoxic (low ORP) stages, the influence of environmental factors was framed by global changes due to redox state (Gomez-Silvan et al., 2014). Under anoxic conditions, C/N ratio, NH_4^+, concentration, and volatile suspended solids (VSS) were positively correlated with greater relative abundance of ammonia oxidizing bacteria and reduced abundance of total bacteria, nitrite oxidizing bacteria, and denitrifiers. In the aerobic system, the strongest controls were inverse correlations between all populations and concentrations of suspended solids. Thus, it appears that redox potential influences a large suite of distal controls. These authors also noted that short-term changes in enzyme activity were more strongly influenced by changes in ORP than changes in population, but noted a need to study multiple aspects of N transformation in a long term (microbial populations, gene expressions, enzymology, and environmental variables). Several of these factors: pH, ORP, and oxygen – can be considered both proximal and distal controls. Because they frequently arise out of macroscopic phenomena, these factors are covered in greater detail in the discussion of environmental drivers (Section 3).

In extreme environments such as those with very low redox potentials or large quantities of Fe or S, pathways such as DNRA and autotrophic denitrification can become dominant forces in N transformation. The microbes that carry out these processes have different environmental requirements than the more common pathways, but they can co-exist under certain circumstances. Of these, autotrophic denitrification is the most likely to be present with more common processes, especially in the presence of Fe or S. These conditions may arise naturally in terrestrial and aquatic ecosystems, but can also be brought about through contamination. Under conditions of low C and high Fe concentrations, autotrophic Fe-based oxidation of NO_3^- can take place (Burgin and Hamilton, 2007). Another type of chemolithoautotrophic nitrate reduction occurs under sulfidic conditions with high C input. These environments support autotrophic sulfur oxidizers with their own versions of denitrification and DNRA,

depending on the S species present (Ahn, 2006; Burgin and Hamilton, 2007, 2008). In highly reduced environments, such as sludge, sediment, thermal vents, and the mammalian gut, DNRA is also a critical pathway (Bothe et al., 2007; Mohan et al., 2004; Pett-Ridge et al., 2006; Revsbech et al., 2005; Santoro, 2010; Scott et al., 2008). Distinctions, however, must be drawn between the fermentative and autotrophic varieties of the process; fermentation requires a high C:N ratio (Kumar and Lin, 2010; Sgouridis et al., 2011), and the autotrophic process demands high levels of sulfides (Burgin and Hamilton, 2007; Scott et al., 2008). A meta-analysis of several DNRA studies using multiple linear regressions found that while high C/N ratios are required for the process to occur, DNRA rates in the field are best predicted using annual precipitation and temperature, whereas the relative contribution of DNRA to $\%NO_3^-$ removal is best explained through a combination of total N and water filled pore space (WFPS) (Rutting et al., 2011). While appreciable levels of DNRA has been observed to occur concurrently with denitrification in activated sludge (Kaspar et al., 1981) and sediment (Scott et al., 2008) in most terrestrial systems, the contribution of DNRA to N transformation is not well characterized (Rutting et al., 2011). Further studies will be required to assess its importance in field-scale N transformation systems.

The conditions that support the Anammox community are the final controls we will consider here. First discovered in a nitrifying wastewater treatment plant, the Anammox process and associated organisms have also been identified in anaerobic marine sediments, particularly in areas with high NO_2^- and NH_4^+ (Kuenen, 2008). Co-occurrence of Anammox and nitrification has been observed under conditions of high ammonium with a limited oxygen supply (Jetten et al., 2001; Schmidt et al., 2002). Nitrifiers remove oxygen as it enters the system, keeping it locally anaerobic. The Anammox organisms then react the NO_2^- generated in the nitrification with the leftover NH_4^+ to generate N_2 gas. Coupled Anammox with denitrification has also been observed in nature (Bothe et al., 2007; Bothe et al., 2000; Erler et al., 2008; Kumar and Lin, 2010), mostly in oceans or marine sediment. Artificial systems exploiting coupled

Anammox / denitrification hold great promise for water treatment, but it is important to note that Anammox organisms grow extremely slowly, are sensitive to the presence of labile C, and are difficult to culture in isolation, all of which reinforce the need for careful environmental controls in the water treatment process (Bothe et al., 2000; Jetten et al., 2001; Kumar and Lin, 2010). However, gaps exist in our knowledge about these processes and the environments that support them are not fully characterized. Understanding that Anammox or other novel processes may be found in unexpected places has the potential to lead to new and exciting discoveries.

2.3 Table of Nitrogen Transformation Controls

Table 1: Proximal and Distal Controls Affecting Nitrogen Transformation

Factor	Effect	Scale of Importance
Nitrogen	NH_3/NH_4^+ suppresses nitrogen fixation, induces nitrification Very High NH_3 is cytotoxic, inhibits ammonia monooxygenase NO_3^- induces: nar, nap, nir High NO_2^- associated with high N2O emissions for denitrifying environments High NO_2^- with High NH_4^+ - associated with Anammox Organic N -> N fixing organisms, nos High Urea -> ammonium oxidizers and denitrifiers	Micro to Landscape / Watershed
Carbon	Labile C, particularly DOC limits many pathways, especially denitrification low labile C, high C:N -> denitrification to N_2; high labile C, high C:N -> DNRA; low C:N -> denitrification. to N_2 high labile C, low C:N -> denitrification to N_2O / Anammox; Type and quantity of C may effect which enzymes/organisms perform best Ample CO_2 required for nitrification	Micro to Global Climate
Biochar	As a soil amendment, associated frequently with lower N_2O emissions, occasionally with increased N_2O emissions Lower nirK, higher nirS, higher nosZ May provide anaerobic microsites necessary for many N-cycle processes	Field Micro
Temperature	Increase denitrification rates with temp up to 30°C. Decrease after 70°C. No denitrification below 5°C or above 85°C Possible C:N ratio changes Microbial community composition alterations	Climate
Oxygen	Suppresses transcription of denitrification, N-fixation, DNRA, Anammox enzymes Inhibits denitrification, N-fixation, DNRA, Anammox Required for nitrification Replaces N-oxides as electron acceptor in respiration when present Induces transcription of nitrification enzymes Destroys redox centers in: nif, nos	Micro to Landscape / Watershed
Soil Moisture	Serves as a proxy for the presence of oxygen Determines availability of soluble nutrients	Field
pH	Influences rates for nitrification and denitrification - optimum between 7.5 and 8.5 Basic pH critical for nos assembly	Micro to Landscape / Watershed
Redox	Frequent fluctuations can increase microbial diversity Low redox potentials required for DNRA and S-mediated denitrification	Micro
Trace Metals	Cu dependence of: nir, nos Mo/Fe dependence of: nif Fe required for some chemolithoautotrophic denitrification	Micro to Landscape / Watershed
Sulfides	Inhibit denitrification, increase microbial preference for DNRA pathway Can act as an electron donor in DNRA	Micro to Landscape / Watershed

I - 3. Environmental Drivers of N Cycle Controls

3.1 Carbon and Nitrogen Availability

Carbon availability is an important limiting factor for many N Cycle enzymes (Bowles et al., 2014; Her and Huang, 1995; Richardson et al., 2009; Schmidt and Clark, 2013). Since the 1970's, researchers have recognized a correlation between an environment's denitrification capacity with total organic C (TOC) and, more importantly, with water-soluble organic C (Burford and Bremner, 1975). As previously discussed, many years of wastewater treatment plant studies have shown that the C source and the C:N ratio affect denitrification reaction rates, end product composition, and N removal efficiency (Her and Huang, 1995; Kampschreur et al., 2009). Studies in soil (Munoz-Leoz et al., 2011; Saggar et al., 2013; Senbayram et al., 2012) and denitrifying bioreactors show similar effects (Cameron and Schipper, 2010; Greenan et al., 2006; Schipper and Vojvodic-Vukovic, 2001; Warneke et al., 2011b). More available C (higher C:N ratio) is associated with higher denitrifying enzyme activity (Richardson et al., 2009), and in the cases of very high C:N ratios, increased NO_3^- transformation via DNRA (Rutting et al., 2011). Research has suggested that in systems receiving exogenous N- input, labile C will determine denitrification rates (Saggar et al., 2013; Zehnder, 1988). In agroecosystems, concentrated application of nitrogenous fertilizer can decouple the N and C cycles (Sharpley et al., 2013; Vitousek, 1997). These systems often exhibit "leakage" of reactive N from the system (Dodds et al., 2010; Evans-White et al., 2009). This can take the form of NO_3^- , NO_2^- , or NH_4^+ in the water supply and NH_3, NO, or N_2O in the atmosphere. Under saturated conditions with high nitrate loading, increasing the available C can induce increased N_2O emissions, due to NO_3^- reduction being energetically favored to N_2O reduction (Blackmer and Bremner, 1978; McKenney et al., 2001; Munoz-Leoz et al., 2011; Richardson et al., 2009; Simek and Cooper, 2002) and the toxic effects of high levels of NO_3^- (Saggar et al., 2013). In aerated systems, increasing C:N ratio has an inverse effect on nitrification rates (Ballinger et al., 2002; Barnard et al., 2005; Hu et al., 2009; Nogueira et al., 2002). All three studies noted

decreasing nitrification rates following an increase in C concentrations in influent. Nogueira et al. (2002) speculated that the rapid increase in carbon led to the growth of large numbers of heterotrophs which subsequently starved the slow-growing nitrifiers of oxygen. Under both nitrification and denitrification conditions, the combination of available C and excess N in conventionally tilled agricultural soils can result in a N_2O flux between five and 20 times that of forest ecosystems (Robertson et al., 2000). Despite this, in agriculture, the primary entry point for anthropogenic N to the environment, these factors are often not considered in management decisions. Indeed, agricultural N usage efficiency is frequently below 40% (Canfield et al., 2010). In agroecosystems, the extent to which we can manipulate C and N is limited, but we can attempt reduce how much N fertilizer is introduced into the environment, and we can alter soil C is availability by changing our tillage practices or using soil amendments. When combined with other management regimes, controlling C and N inputs offers the chance to dramatically reduce N leakage and mitigate environmental impact (Dinnes et al., 2002; Dungait et al., 2012; Sprague and Gronberg, 2012). The greater challenge will be balancing these needs against production systems which naturally prioritize increased crop productivity.

3.2 Physicochemical Drivers

Surface of the Aggregate

We have long known that environmental microstructure and surface charge affect N Cycle reaction rates, as well as nutrient sorption, transport, and storage. Classic denitrification work has shown that microstructure denitrification rates through a combination of diffusion and the creation of anaerobic microsites in the substrate (Groffman and Tiedje, 1991). Low air-filled porosity is associated with less available oxygen and greater the denitrification rates, but even in aerobic environments, locally anaerobic regions often allow denitrification and other anaerobic processes to occur (Betlach and Tiedje, 1981;

Gomez-Silvan et al., 2014; Groffman et al., 1988; Smith and Tiedje, 1979). These systems can give rise to coupled nitrification-denitrification in soils which are aerobic in the bulk phase but contain locally anaerobic sites (Christensen et al., 1990; Groffman et al., 1988; Lloyd et al., 1987; Parkin, 1993). Because the products of the N Cycle processes are consumed in and around the locations where they are produced, the complexity and depth of the pore network directly impacts how much N leakage can occur, especially for gaseous products (Blagodatsky and Smith, 2012). Other important parameters to consider when investigating N fate and transport are hydraulic conductivity, specific surface area, ion exchange capacity, and ion competition (Jahangir et al., 2012; Jellali et al., 2010; Limousin et al., 2007; Matschonat and Matzner, 1995). The latter two mechanisms are also strongly influenced by pH. Sorption is a very important consideration for NH_4^+ availability, which in turn, influences nitrification, Anammox, and assimilatory processes (Bothe et al., 2007). Sorption is less important for NO_3^- because most soils have a negative charge and thus low anion exchange capacity (Hamdi et al., 2013). For an excellent review of techniques which can be used to quantify and model sorption, see the work of Limousin et al. (2007). Despite the difficulty in assessing the importance of these phenomena for a given environment, they should not be neglected – especially for longer term studies concerned with fate and transport. While these properties are restricted by soil type and texture, they can be adjusted through a variety of management practices that are discussed in section 4. These interventions can have large impacts on N retention and should be considered important tools for increasing efficiency and reducing GHG emissions in future agricultural systems (Burgin et al., 2013; Cheng et al., 2012).

Micronutrient availability

Micronutrient availability is a factor for many N Cycle processes (Bowles et al., 2014; Woolfenden et al., 2013), although its effect is complicated by community competition for these micronutrients in addition to their availability. As previously mentioned, a number of N-cycle enzymes are dependent on Cu (nirK,

nor, nosZ, amo), and chemostat studies have confirmed environmental results about its importance as an enzymatic control, particularly for N_2O reductase (Granger and Ward, 2003; Woolfenden et al., 2013). Fe can also play a role as an N Cycle regulator. Fe is found in many N Cycle regulatory proteins, is a component in the structure of several important enzymes (nar, nap, nxr, nirS, nor, nif, nrf) (Bothe et al., 2007; Moir, 2011), and is an important oxidant for autotrophic denitrifiers (Ahn, 2006). The presence of Fe can substantially alter the microbial community in both natural (Burgin and Hamilton, 2007) and artificial denitrifying environments (Huang et al., 2012; Richardson and Nicklow, 2002). Furthermore, in environments with high sulfates and low ORP (< -150mV), Fe III can poise the environmental conditions above the redox potential where sulfate reduction takes place, preventing the formation of sulfides which can lead to the formation of toxic byproducts that disrupt the microbial community (Blowes et al., 1994; Easton et al., 2015). In environments high in sulfides, denitrification can still take place, but autotropic denitrification processes dominate and heterotrophic denitrification is inhibited (Shao et al., 2011; Sorensen et al., 1980; Xu et al., 2014). Since nosZ is particularly sensitive to environmental factors, including the presence of sulfides, these conditions often result in a higher N_2O:N_2 product ratio (Shao et al., 2011). Nevertheless, if it is carefully controlled, combined heterotrophic / autotrophic denitrification shows great promise for simultaneous removal of NO_3^-, organics, and sulfides in the denitrifying sulfide removal (DSR) process (Chen et al., 2010; Lee and Wong, 2014; Shao et al., 2011; Xu et al., 2014).

The role of pH

One of the most important environmental influences on N Cycle processes is pH, which has important proximal and distal effects on its own, and influences a large number of other controls (Bothe et al., 2007; Moir, 2011; Richardson et al., 2009; Wallenstein et al., 2006). N-cycling communities are typically found at environmental pHs ranging from 5.5 to 8, although some extremophiles do exist outside that range (Bothe et al., 2007). It has long been known that denitrifying enzyme activity decreases with decreasing

pH, essentially ceasing below pH 6 (Richardson et al., 2009; Simek and Cooper, 2002; Wan et al., 2000). More recent studies have found denitrifying microbial communities that remain active at low (sub 5.5) pH, but these populations tend to emit larger N_2O fluxes than their counterparts (Cuhel and Simek, 2011a, b; Dannenmann et al., 2008; Simek and Cooper, 2002), despite acidic conditions normally being associated with lower overall denitrification (Saggar et al., 2013; Van Den Heuvel et al., 2011). Liu et al. (2010) and Simek et al. (2002) note that the pH at which a soil achieves optimum denitrification may be as much a function of a soil's microbial community as its chemistry. However, later work by (Cuhel and Simek, 2011a) found maximum denitrifying enzyme activity was found at the same pH (8.4) for three soil samples whose natural pH ranged from 5.31 to 6.93. In general, the most important effect of pH on N-cycling is the inverse relationship between pH and N_2O:N_2 production ratio (Cuhel and Simek, 2011b; Firestone et al., 1980; Liu et al., 2010; Rochester, 2003; Simek et al., 2002; Van Den Heuvel et al., 2011). Various groups have documented both linear (Liu et al., 2010), and exponential (Rochester, 2003; Van Den Heuvel et al., 2011) responses of N_2O:N_2 ratio to pH. It is also important to note that N_2O released as a temporal response to a liming / acidification proceeds from different microbial sources than production in systems maintained at a steady-state pH (Baggs et al., 2010; Bergaust et al., 2010). Using $^{14}NH_4{}^{15}NO_3$ or $^{15}NH_4{}^{15}NO_3$ Baggs et al. (2010) found that unadjusted pH 7 soil emitted most of its N_2O from denitrification, while soil limed to pH 7 with $CaCO_3$ derived a majority of its N_2O from nitrification and emitted four times the N_2O flux in a 41 day incubation. Thus, it is extremely likely that many environmental factors (release of C, NH_3 volatilization, microbial community fluctuations) act in concert with pH to produce its overall effect on the N Cycle.

Possible mechanisms for reduced N_2O emission at high pH may be N_2O reductase (nosZ) being most active at pH > 8 (Dannenmann et al., 2008; Richardson et al., 2009), nos sensitivity to low pH (Liu et al., 2010), or pH-driven changes in functional gene expression (Cuhel et al., 2010; Liu et al., 2010). N_2O reduction is

not noted to take place below pH 4.5 as long as long as NO_3^- is present, but it is able to occur at pH 5 or greater, a finding which suggests pH's influence on transcription regulation of *nosZ* (Van Den Heuvel et al., 2011). For nitrification, the abundance of *amoA* is also linked to higher pH; currently culturable strains of ammonia oxidizers grow best at a pH of 7.5-8, while growth ceases at pH<6.5 for the vast majority of species (Bothe et al., 2007; Hayden et al., 2010; Norton and Stark, 2011). Careful review of the literature shows that pH acts both as a proximal control for enzymatic rates and a distal control for the organization of the N cycling community. However, because of the limited operating range of the enzymes involved in N Cycle processes, distal effects are likely to be dominated by proximal ones. Because of its far-reaching effects, its frequent adjustments in management decisions, and its associations with biogeochemical "hot spots" (Groffman, 2012; McClain et al., 2003; Van Den Heuvel et al., 2011), pH should be considered a key element in future models for the prediction of GHG emissions and water quality. Additionally, long-term studies should be undertaken in a variety of ecosystems to reveal the response of microbial communities to changing pH over extended timescales. Such studies could offer key insights to microbial ecologists, agronomists, and environmental engineers seeking to better understand or manipulate the N Cycle.

3.3 Climate and the Nitrogen Cycle

Temperature-mediated effects on N Cycle processes are well known (Akratos and Tsihrintzis, 2007; Bailey and Beauchamp, 1973; Bonnett et al., 2013; Braker et al., 2010; Das et al., 2011; Holtan-Hartwig et al., 2002; Singh et al., 2010; Stres et al., 2008) but not necessarily well-characterized. In general, both heterotrophic and autotrophic respiration will increase (to a point) with rising temperatures (French et al., 2009). More importantly, rising temperatures have been linked with increased emissions of N_2O, a potent GHG which can create feedback in a cycle of rising temperatures (Canfield et al., 2010). Since the 1970's it has been hypothesized that denitrification increases with temperature up to 30°C and then levels off before decreasing past 70°C. Below 5°C and above 85°C, no denitrification is thought to take place

(Bailey and Beauchamp, 1973). Contemporary experiments have reproduced similar results. Wetland soil studies using NO_3^--enriched water have shown increased N_2O emissions and denitrification rates in response to increased temperatures across multiple soil types (Bonnett et al., 2013; Munoz-Leoz et al., 2011). In the warm summer months, N_2O production may account for up to 40% of equivalent GHG emissions from organic-rich histosols (Bonnett et al., 2013). Another recent study incubated soil slurries on a gradient between 4 and 37 °C and found linearly increasing denitrifying enzyme activity between 4 and 25 °C which then stayed constant through the 37°C incubation (Braker et al., 2010). The same study performed T-RFLP analysis on the slurries to assess microbial diversity. In contrast to the low temperature incubations, which showed > 90% similarity for *nirK* and *nirS* genotypes compared to the source soil, the 37 °C incubation showed major shifts in both gene variants, suggesting that temperature may act as a distal control in addition to its known proximal influence. These observed changes in the N-Cycling microbial community contrast with the findings of (Stres et al., 2008) who found no significant differences between 16S rRNA and *nosZ* in fen soil samples when profiled at 4 and 28°C. Other studies hypothesized that enzymatic temperature dependence is the cause of temperature-mediated changes in N_2O:N_2 ratio, especially for cold-weather N_2O emissions (Holtan-Hartwig et al., 2002; Maag and Vinther, 1996). Results from the above studies are clearly conflicting. It is not known if these divergent results are due to increases in respiration altering C:N ratio (Das et al., 2011; Kammann et al., 2008), expanded microbial biomass (French et al., 2009), altered enzyme kinetics (Holtan-Hartwig et al., 2002; Huang et al., 2012), or changes in the microbial community structure (Braker et al., 2010; Stres et al., 2008). Many soil microbes can tolerate a wide variety of temperatures, and the relatively narrow temperature gradients which were tested may have been within the habitable range of the existing soil flora. Additionally, most enzymes exhibit linear responses to temperature up to a threshold and then denature beyond it. We certainly don't know boundary conditions for every possible scenario. Further investigating the effect of temperature on the N Cycle will require carefully designed studies across a wide number of environments and nutrient

regimes. Despite difficulties in obtaining sufficient data, evidence suggests that feedback between temperature and N_2O production could accelerate the already worrisome pace of climate change (Singh et al., 2010). This is a case that clearly demand further study.

In addition to temperature, elevated atmospheric CO_2 levels associated with climate change can also impact N Cycle controls. Increased CO_2 is associated with elevated soil respiration (Adair et al., 2011; Freeman et al., 2004; French et al., 2009), likely the results of plant-mediated mechanisms that increase available carbon in the soil. This combination of factors could function as a driver for increased N_2O emissions, as noted in two grasslands Free Air CO_2 Enrichment (FACE) studies which observed the effects of elevated ambient CO_2 on N_2O production (Baggs et al., 2003; Kammann et al., 2008). Kammann et al. (2008) found a more than two-fold increase in N_2O emissions over an eight-year experimental period with 20% atmospheric CO_2 enrichment and Baggs noted more than three times greater emissions with 67% enrichment. It is important to note that Kammann's 2008 findings were under N limited conditions while Baggs' 2003 study took place under conditions of excess N. Other major reviews suggested that when N is limited, increasing CO_2 can actually reduce N_2O emissions by decreasing denitrification activity (Barnard et al., 2004; Barnard et al., 2005; Singh et al., 2010). A possible explanation for this may be found in data from N tracer studies at two multi-year FACE sites (Muller et al., 2009; Rutting et al., 2010) which showed CO_2 enrichment of 25 and 30% above atmospheric concentration stimulated DNRA (44% and 140% respectively) and reduced NH_4^+ oxidation (26%, 15%). Another possibility is that CO_2 may be responsible for increasing N in soil microbial biomass (Freeman et al., 2004). Freeman et al. (2004) also noted conflicting CO_2-mediated impacts on N-Cycling microbial populations and their enzyme activities. The findings of these studies indicate that substantial gaps remain in our knowledge of how atmospheric CO_2 influences the N-cycling microbial community (Freeman et al., 2004; French et al., 2009; Singh et al., 2010).

More research is needed using molecular methods to determine what effect CO_2 is having on these systems and investigate its long-term impacts.

Climate change will also undoubtedly also where and when soils can become saturated. This is an important consideration because soil moisture has long been known to influence N transformation (Smith and Tiedje, 1979). Climate projections have predicted both increased frequency and severity of precipitation in Northern Europe and the Eastern United States (Butterbach-Bahl and Dannenmann, 2011; Hayhoe et al., 2008; Lettenmaier et al., 1999; Najjar et al., 2010; Neff et al., 2000). At the landscape scale, saturation functions as a proxy for the presence of oxygen, with water content and aggregate size directly influencing how and where the anaerobic microsites that are necessary for denitrification may arise (Blagodatsky and Smith, 2012; Myrold and Tiedje, 1985). Because of this, saturated areas (along with areas of enriched organic matter or increased temperature) can develop into denitrification "Hot Spots," which frequently account for a large proportion of N_2 and N_2O emissions in terrestrial ecosystems (Groffman, 2012; McClain et al., 2003; Vidon et al., 2010). Changes in the saturation status can also cause rapid shifts between nitrification and denitrification (Bergsma et al., 2002; Webster and Hopkins, 1996). As soon as water losses cause pore space oxygen concentration to rise, most denitrification ceases and nitrification rapidly becomes the dominant N transformation process. Return to anaerobic conditions causes a similar reversal to denitrification. These periods of transition often coincide with peak periods of N_2O flux, especially in agricultural soils (Butterbach-Bahl and Dannenmann, 2011). For agricultural soils that were only wetted at the time of NO_3^- exposure, the ratio of N_2O to (N_2O+N_2) was found to be 2.5 times greater than that of soil which had been wet for two days prior to NO_3^- incubation (Bergsma et al., 2002). This contrasts with forest soils that exhibited nearly identical product ratios under the two wetting regimes. The authors speculated this was due to persistence of nosZ in forest soils, which we note are frequently N limited. In some cases, precipitation associated hot moments bring about highly significant nutrient

fluxes, which sometimes account for more than 50% of annual carbon transport in watersheds (Vidon et al., 2010). Such nutrient fluxes carry the potential for massive fluctuations in N cycling. Where and when saturation becomes a dominant control is determined by a combination of climate, soil, land use, and topography. Due to its powerful role as a driver of N transformation, we must consider soil moisture in these contexts for future N Cycle models at the landscape scale (Anderson et al., 2014b; Billen et al., 2013; Blagodatsky and Smith, 2012; Butterbach-Bahl et al., 2013; Faulkner et al., 2010; Groffman et al., 2009b). Such models will provide valuable insight for researchers and managers alike.

Particularly in areas that are highly affected by climate change, managers must consider environmental drivers in their efforts to reduce environmental N losses (Burgin et al., 2013; Pennock et al., 1992). Once we recognize how they come together to produce "hot spots" and "hot moments", landscape-sensitive approaches can be developed that utilize these features to protect environmental quality and reduce fertilizer inefficiency (Burgin et al., 2013; McClain et al., 2003; Pennock et al., 1992; Vidon et al., 2010).

3.4 N Cycle Control Interactions

Growing evidence shows that the past assumption that different microbial communities will perform equivalent functions when compared in identical environments is incorrect (Strickland et al., 2009). Changes in the N-Cycling community can and do occur in response to climate, management, and physiochemical variability; even in seemingly homogenous landscapes, studies have shown significant temporal and spatial variation in community structure (Bowles et al., 2014; Wallenstein et al., 2006). Vidon et al. (2010) identifies four kinds of hot spots and moments 1) Biogeochemical Hot Spots – e.g. areas with high soil C, pH, or active local biota, 2) Biogeochemical Hot Moments – e.g. nutrient rich zones with transient activity such as decaying organic matter, floodplains, etc., 3) Transport-Driven Hot Spots – e.g. areas of high hydraulic conductivity or prone to saturation, 4) Transport-Driven Hot Moments – e.g. storm

events, snowmelt, fertilizer runoff. These phenomena are not controls in and of themselves, but rather, they are influences that determine which controls ultimately come to dominate local N Cycle. Even in landscapes with similar environmental drivers, there it is considerable variability soil nutrient content, moisture, temperature, oxygen, pH, and ORP; thus it is reasonable to assume that there is a high degree of uncharacterized microbial variability in N-Cycling ecosystems. While temporal variability is difficult to visualize, many beautiful examples of spatial variability have been produced over the years. One of the first was presented in a paper by (Parkin, 1987) which demonstrated that more than 85% of denitrification activity in a soil core was occurring in a region that comprised less than 0.1% of its mass (Fig. 3 – From Parkin et al. 1987).

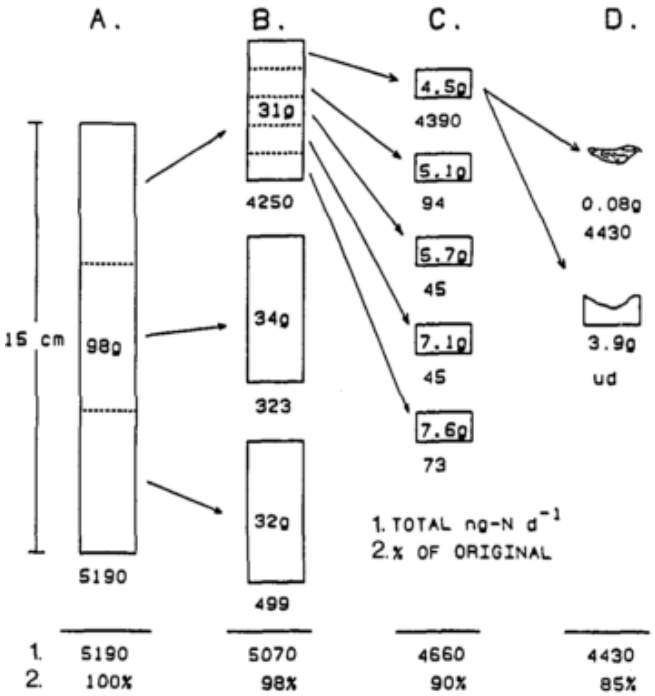

Fig. 3. Results of a core segmentation experiment to identify active denitrifying sites in soil. All incubations were conducted under a headspace atmosphere of 18-kPa O_2 and 10-kPa C_2H_2.

Figure 3: Spatial variability of denitrification activity in a soil core. From Parkin, T. B. 1987. Soil Microsites as a Source of Denitrification Variability. Soil Science Society of America Journal 51(5):1194-1199. Used with permission of ACSESS-Alliance of Crop, Soil, and Environmental Science Societies.

The future of N Cycle research will require multidisciplinary efforts to understand how environmental drivers influence the microbial community over various spatial and temporal scales (Bowles et al., 2014; Wallenstein et al., 2006)**.** While the impact of climate change cannot be understated, its effects are not equal everywhere. An approach which integrates climate forecasting, soil science, hydrology, molecular biology, and environmental chemistry will be necessary if we are to understand what forces underlie the key controls of the N Cycle – and develop effective management strategies. Of particular concern is the feedback between nitrous oxide and climate change (Singh et al., 2010). If we can find ways to reliably reduce N_2O emissions, we can reduce a major contributor to global warming. And while climate change will not be reversed through N work alone, we can tailor management approaches to eliminate a substantial portion of the processes that accelerate it. The challenge for future practitioners will be to control the when and how of these interactions in a way which produces desired outcomes for the environment. In order to do this, comprehensive site surveys and extensive, long-term, data collection are essential. It is not enough to merely calculate rates; in order to understand larger trends, we must consider proximal and distal controls to the N Cycle, their environmental drivers, and the microbial community as a complex ensemble.

3.5 Table of Environmental Drivers for Nitrogen Transformation

Table 2: Environmental Drivers of Nitrogen Transformation

Factor	Level of Influence	Human Ability to Modify	Scales of Importance
Temperature	Proximal and Distal	Human-driven climate change drives temperature changes. In most areas, this means increases Limited ability to alter in the field through shade, planting arrangements, irrigation	Global Climate to Micro
Precipitation	Distal	Human-driven climate change affects where precipitation takes place Almost no ability to influence beyond this	Global Climate to Field
Hydrology	Proximal and Distal	Surface contours can be adjusted in the field, but must be protected from erosion Drainage can be altered by tillage, land-use, and planting schemes Much of the ability to alter these factors depends on the underlying soil characteristics	Landscape to Aggregate
Soil Moisture	Proximal	Influenced by climate, which humans are affecting but have limited ability to control Influenced by hydrology, which humans can alter substantially Land cover can alter available moisture	Aggregate to Micro
Environmental Nitrogen	Proximal and Distal	Heavily influenced by fertilizer application Heavily influenced by overall land use	Landscape, Watershed to Micro
Environmental Carbon	Proximal and Distal	Limited ability to alter available carbon through tillage and other management practices Human-driven climate change increases atmospheric CO_2 which affects soil carbon Aquatic C tied directly to organic pollution	Global Climate to Micro
Aggregate Surface Characteristics	Proximal and Distal	Determined first by geology, can be modified by humans	Landscape to Micro
Trace Metals	Mostly Proximal	Limited ability to influence through soil amendments Heavily influenced in waters by leachate from human activities	Landscape to Micro

I - 4. Nitrogen Mitigation Strategies

Our deepening understanding of the impacts of N on the environment shows that without careful management, anthropogenic N poses serious environmental risks (Canfield et al., 2010; Driscoll et al., 2003; Erisman, 2004; Rao et al., 2009). Despite this, improved engineering and management offer a means to mitigate this impact to a certain extent. In agricultural systems, engineered N controls have existed for many years in the form of drainage structures, tillage practices, and soil additives. Most WWTPs also employ biological processes to achieve nutrient reduction targets. Governments are increasingly recognizing the potential for in situ N control technology to reduce nutrient export in new developments. Future engineering goals should aim to develop precision technologies and management strategies that manipulate N Cycle controls in order to achieve desirable environmental outcomes. Below, we discuss several common terrestrial N control approaches in the context of their current applications, research needs, and the future of each technology.

4.1 Agricultural Management Practices

As previously discussed, the modern agricultural paradigm carries with it a heavy burden of reactive N. Synthetic fertilizer and intensive cultivation of N fixers account for the majority of anthropogenic reactive N entering into the environment (Canfield et al., 2010). Despite agriculture's current burden on water quality and GHG budgets, there is great potential to reduce the current N leakage and improve N use efficiency. Some of the most promising of these strategies include 1) using soil amendments to manipulate soil properties such as pH or C:N ratio, 2) alternative cropping strategies and tillage practices, 3) new approaches to livestock management, and 4) controlling drainage to manipulate where ground is saturated or exposed to nutrients. Though there are many other management practices in for N control,

we chose to focus on these because they directly impact agricultural productivity, deal with excess N at its source, closely affect microbial controls, and are the subject of several of our ongoing research efforts.

4.1a Soil Amendments for Nitrogen Control

Soil amendments are a common strategy to increase productivity in agroecosystems. Recent years have also seen an increase in using soil amendments for bioremediation and pollution control. According to the EPA, the primary functions of soil amendments employed in this context are 1) to address nutrient availability, and 2) improve soil health and ecosystem function (United States Environmental Protection Agency, 2007). In the context of production systems, fertilizers that alter soil organic matter, N, and pH (all critical N Cycle controls), are the most likely to impact N transformation rates or microbial community structure (Baggs et al., 2010; Groffman et al., 1988; Richardson et al., 2009). These are each briefly assessed here with regards to their effects on soil N balance.

Soil pH is frequently adjusted to suit the needs of a particular crop, either through acidification (to lower soil pH) or liming (to raise soil pH) (Baggs et al., 2010; Bolan et al., 2003). Acidification affects N balance in soils by reducing nitrification and denitrification, leading to accumulation of NH_4^+ over time (Baggs et al., 2010; Bolan et al., 2003; United States Environmental Protection Agency, 2007). Liming, on the other hand, increases N transformation reaction rates and availability of several N compounds. In N fertilized ecosystems, this frequently results in N losses through the following routes: 1) N_2O release by nitrification in aerated soils, 2) denitrification emissions of N_2 / N_2O in saturated soils, 3) NH_4^+ volatilization to NH_3 gas, 4) NO_3^- leaching into groundwater (Baggs et al., 2010; Bolan et al., 2003; United States Environmental Protection Agency, 2007).

How and when soils are fertilized has both immediate, and long-term, effects on N balance in agroecosystems. Key management actions to consider on this subject include the following: 1) Variable

fertilizer application rates, 2) Adjusted timing of fertilizer application, 3) Improving delivery method of fertilizer (to reduce runoff), 4) Using biological inhibitors to reduce unwanted transformations (Dinnes et al., 2002; Hoeft, 2004; Reetz, 2004; Sartain et al., 2004). Variable application rates ensure N is available where it is needed, and not fed into hot spots where it is lost to biological processes. Timing applications closer to planting can reduce over-season losses to leaching. Improving fertilizer delivery methods simultaneously increases bioavailability and reduces runoff. Lastly, biological inhibitors can keep fertilizers in less mobile forms like NH_4^- as opposed to forms like NO_3^- which are prone to leaching. The effect of these actions ensures that fertilizer is available to crops when it is needed, but isn't available to be washed out or lost due to microbial processes, and they form a core part of precision agriculture.

Biochar is another material that has received much attention as a soil amendment in recent years. In addition to its potential as a C sink, biochar has shown potential to reduce GHG emissions and N leakage in agricultural soils (Clough et al., 2013; Zhang et al., 2014). It has been linked with increased soil biomass and alterations to N-cycling microbial community composition (Anderson et al., 2011; Anderson et al., 2014a; Steinbeiss et al., 2009; Wang et al., 2013). Biochar's suitability for a particular application is directly related to the feedstock and pyrolysis temperature, which influence its surface characteristics and carbon profile (Ippolito et al., 2012). High temperature biochars, in particular have been associated with reduced GHG when added to N-Cycling systems (Bock et al., 2015c; Cayuela et al., 2013; Ippolito et al., 2012). Despite promising work, the dynamics of how biochar affects N transformations are not well understood. Biochar could function as an electron shuttle or liming agent (Cayuela et al., 2013), or its effects could be realized through increased water holding capacity and micronutrient availability (Ippolito et al., 2014). Despite these knowledge gaps, when an environmental amendment provides N control, fertility benefits, and simultaneously offers the possibility of C sequestration, the case for large-scale trials becomes extremely compelling.

4.1b Alternative Tillage and Cropping Schemes

Conservation tillage is a strategy to reduce runoff, increase retention of organic matter, and improve infiltration potential in agricultural soils by leaving at least 30% of a previous year's crop residue on the surface of a field (Sprague and Gronberg, 2012). In contrast with conventional tillage practices, less O_2 is available for nitrification, and more N is retained in organic forms (Dinnes et al., 2002). In addition to reducing N export in groundwater, conservation tillage has been shown to limit gaseous N_2O emissions. A no-till approach in a three-decade long experiment on corn cultivation was linked with a 40% reduction in N_2O emissions, and the same study showed that rotation could offer 20% N_2O emission reductions (Omonode et al., 2011).

4.1c Livestock Management

Livestock provide essential income for millions of people around the world, but they require large quantities of land to be raised. Up to two-thirds of all agricultural land is utilized in some form of animal production (De Haan et al., 1997). In the United States, Comprehensive Nutrient Management Plans (CNMP) are set of management activities that concentrated animal feeding operations (CAFOs) must employ to minimize their ecological impact (United States Natural Resources Conservation Service, 2000). Practices required by CNMPs include management of manure, wastewater, pastures, feed, and nutrient budgeting. Manure from animal cultivation can be used as a fertilizer, but is frequently stored on-site at CAFOs (Burkholder, 2007). These waste storage sites are often locations of extremely high N export, both from wastewater leaching – up to 143 mg inorganic N / L, and from N_2O production –with dissolved gas concentrations sometimes exceeding 40 ppm (Burkholder, 2007; Makris et al., 2009). High concentrations of cattle in many grazing strategies can also lead to N export into watersheds when concentrated waste overwhelms an ecosystem's ability to respond to N inputs (McGechan and Topp, 2004). Pastureland management is critical in livestock systems, not only to reduce concentrated waste deposition, but to

prevent long-term N depletion from destructive grazing practices (De Haan et al., 1997; Schuman et al., 1999). In the past, pasture soils were heavily fertilized to avoid this, but this came with the side effects of N_2O emissions. Increasingly, recommendations for utilizing N fixing cover crops have come to prominence (Andrews et al., 2007; De Haan et al., 1997). Lastly, feed and nutrient management can be used to ensure that animals do not receive excess nutrients in their feed which are then excreted to the environment in their manure. While animal husbandry brings a number of other challenges to agricultural management, these recommendations provide a means for livestock managers to reduce N export to surrounding ecosystems and simultaneously reduce inefficiency in their operations.

4.1d Controlled Drainage

Because NO_3^- does not readily sorb in most soil profiles, it is rapidly exported to agricultural watersheds along surface or subsurface flow paths. Conventional drainage management emphasizes the removal of water, rather than the prudent management of local water tables, generally resulting in excessive drainage. In addition, routine ditch management practices, including dredging (clean outs) and vegetation management, can minimize internal cycling of nutrients in ditch vegetation and destabilize ditch walls, resulting in bank erosion. Improved drainage management systems aim to reduce nutrient export by establishing conditions necessary for denitrification to take place and remove NO_3^- before it reaches surrounding waters. Drainage control structures work by reducing peak flow in agricultural drainage systems by routing water through channels which slow it down, and provide increased contact time with biologically, physically, and chemically active surfaces. Anderson et al. (2015) measured lower ^{15}N at sample locations located directly over tile drains (e.g., aerobic soil) than at adjacent locations not overlaying a tile (e.g., anaerobic soils). Their findings suggest lower denitrification over the tile drains and this pattern coincides with similar patterns in N_2O emissions. However, when there is decreased denitrification over tile drains, there is a risk of NO_3^- washout during rain or irrigation events. Effective

drainage control reduces offsite transport of agro-nutrients, improving both offsite water quality and the potential for target crop uptake, as well as providing root zone soil water for plants to use during intra-rainfall events.

Variations of controlled drainage structures can provide increased N removal from outflow by routing water through active nutrient removal systems. One example of this kind of technology is the Denitrifying Bioreactor (DNBR). In a DNBR, water is channeled through a carbonaceous filter under saturated conditions (Fig. 4 - from Easton and Lassiter, 2014). Microorganisms in the filter feed on matrix material and facilitate NO_3^- removal through a combination of heterotrophic denitrification and assimilation into microbial biomass. Site constraints, environmental chemistry, and hydrologic conditions determine the removal efficacy. With the right combination of environmental data, the DNBR itself can be tuned for differing remediation targets by adjusting its internal hydrology, (e.g., residence time) C substrate, or pH (Dalahmeh et al., 2012).

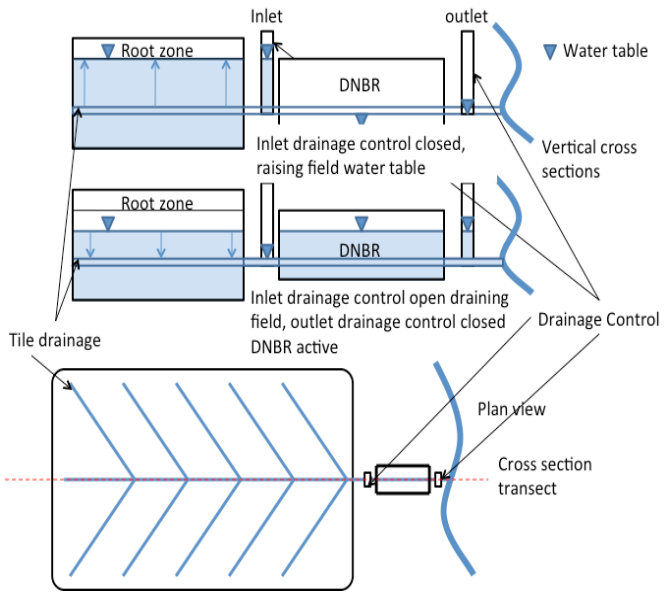

Figure 4: Schematic of bed style bioreactor installed in a tile drainage network.

4.2 Conventional Wastewater Treatment Plants

Though they are not the primary focus of this paper, WWTPs have been employing biological nutrient removal (BNR) technology for years and offer some important insights for the control of terrestrial N. Compared to chemical N removal technologies, BNR is less cost and input intensive (Ahn, 2006). Traditionally, BNR in WWTPs has taken the form of ammonium oxidation followed by anaerobic denitrification. However, the equilibrium of these processes must continuously monitored by skilled technicians, and they often requires the input of an external C source to drive the reactions and prevent instability in microbial populations (Gentile et al., 2007). New designs utilizing the Anammox and other autotrophic processes are promising technologies that reduce the need to supplement available C but which are challenging to implement due to slow microbial growth and increased sensitivity to environmental fluctuations (Jetten et al., 2001; Kuenen, 2008; Kumar and Lin, 2010). Unfortunately, the required infrastructure and costs associated with wastewater treatment plants also makes them unsuitable for remote regions or non-point source pollution control (Blowes et al., 1994). Nevertheless, wastewater treatment plants are well-studied entities and because of their central role in our infrastructure, WWTPs will continue to provide excellent sources of data and test beds for new biotechnology for many years in the future. Perhaps most importantly, wastewater treatment plants offer a virtually untapped frontier for technology transfer and new studies of N Cycle microbial ecology (Daims et al., 2006).

I - 5. Broader Applications of Nitrogen Control, Future Research, and Concluding Remarks

Best management practices can produce major improvements in field-level N control but are frequently are ignored because of lack of access to information, economic constraints, and manager bias (Stuart et al., 2014). Improved communication will be necessary for disseminating research findings in a way which readily adapted by stakeholders. New economics methods can be used to determine cost/benefit for these practices and develop guidelines that balance productivity and environmental goals across the entire life cycle of the production process (Brentrup et al., 2004).

Precision land management offers the potential for removing key sources of N before they reach receiving waters in addition to improving crop productivity. Future research in this field will integrate knowledge from many diverse fields to understand how the drivers for N cycling change over spatial and temporal scales. Efforts to maintain or increase production while reducing the export of reactive N will require extensive understanding of microbial controls combined with topographic, climate, soil, and land use data. The ultimate goal of this work would be the construction of decision support systems which could be tuned for greenhouse gas emissions, water quality, or agricultural productivity targets using sophisticated models. While this may seem a long ways off, with the right understanding of the controls, the design challenges are not insurmountable.

Biochar and pH as Drivers of Greenhouse Gas Production in Denitrification Systems

Martin Davis*[1], Emily Bock[1],
Brian Badgley[2], and Zachary M. Easton[1]

[1] Biological Systems Engineering, Virginia Tech, Blacksburg, VA 24060
[2] Crop and Soil Environmental Science, Virginia Tech, Blacksburg, VA 24060
*Corresponding Author: jmdavis4@vt.edu

Keywords: denitrification, biochar, pH, nitrous oxide, N_2O, greenhouse gas, GHG, nitrogen cycle, proximal and distal controls, bioreactor, DNBR, *nirK*, *nirS*, *nosZ*

II - Abstract

Biochar, or the product or the pyrolysis of organic matter under low oxygen conditions, is a compound that has demonstrated potential for carbon sequestration, improved crop productivity, and environmental nitrogen (N) management. However, interactions between biochar and N cycle processes are not well understood. Recent research has produced conflicting results on biochar's ability to mitigate the microbial production of nitrous oxide, a potent greenhouse gas in agricultural soils. This experiment was designed to determine whether the addition of biochar to a standard woodchip denitrifying bioreactors (DNBR) could reduce N_2O emissions or alter the proportion of key denitrification genes in a week-long study under buffered (BU), unbuffered (UB), and acidified (AC) conditions. Columns containing either woodchips (WC) or biochar + woodchips (BC) were primed for one week with a solution containing 15 mg L^{-1} NO_3-N and 2 mg L^{-1} NH_4-N and then observed for an additional week using an identical solution. Concurrent measurements of aqueous pH and headspace N_2O were taken every 3 hrs gradually slowing to 12 hrs over the sampling period. Three denitrification genes: *nirK*, *nirS*, and *nosZ* were analyzed by quantitative polymerase chain reaction (qPCR) to determine the impact of treatments on denitrifying microbial populations. Contrary to the hypothesis that biochar reduces N_2O production, the biochar-amended columns produced significantly greater N_2O concentrations in the headspace than the woodchip controls at all pH ranges tested. N_2O concentrations were highest in the acidic columns, with concentration curves suggesting no reduction of N_2O was taking place. Although the pH in these microcosms was quite low, the results reflect similar findings from DNBRs in acidic environments and lab-based studies. Within microbial populations, biochar-treatment did not produce changes in denitrification gene copy number, although the combination of altered pH in addition to the presence of biochar showed significant effects on biota. While the literature suggests that biochar remains a promising soil amendment for carbon sequestration, this study demonstrates that it is not necessarily a cure for N_2O emissions. Given the conflict between these results and other studies that show reduced N_2O emissions

in the presence of biochar, there is a need for future research to determine the chemical nature of the biochar – N cycle interactions so that planners do not inadvertently exchange CO_2 for N_2O.

II - 1. Introduction

Intensive use of nitrogen (N) fertilizer lies at the heart of many of the increases to agricultural productivity made during the 20th century (Erisman, 2004). However, excess reactive N resulting from fertilizer application poses significant consequences to the environment and public health that include eutrophication, soil and water acidification, ecosystem disruption, ground level ozone formation, and infant methomoglobinemia (Canfield et al., 2010; Driscoll et al., 2003; Erisman, 2004). Perhaps more important, is the contribution of agricultural N to the production of nitrous oxide (N_2O), a greenhouse gas (GHG) 300 times more potent than CO_2. The Intergovernmental Panel on Climate Change has identified agriculture as the source of 60% of all anthropogenic N_2O production (Metz et al., 2007). In response to these challenges, N control has become a topic of international importance, and the United States National Academy of Engineering has named N management one of its fourteen "Grand Challenges" (Erisman, 2004). Unfortunately, many of the solutions to address excess reactive N in soil and water result in the production of large quantities of N_2O (Bock et al., 2015c; Moorman et al., 2010; Warneke et al., 2011a), and its production is often difficult to predict or manage (Li et al., 2013; Nangia et al., 2013). Furthermore, even natural systems exhibit a high degree of spatial and temporal variability in their N_2O production, which makes modeling future N_2O-related climate impacts extremely challenging (Groffman, 2012; Groffman et al., 2009b; McClain et al., 2003; Sogbedji et al., 2001). In order to address these problems, there is an urgent need to investigate what controls underlie N_2O production. Only then will we be able to develop strategies for N control that do not trade increased GHG emissions for improved water quality (Eickhout et al., 2006; Erisman, 2004; Schmidt and Clark, 2013).

1.1. Production and Management of N_2O

Unlike other biogeochemical cycles, where processes like net primary production (C-cycling) and physical weathering (P-cycling) are dominant forces, the key processes of the N Cycle are microbially-mediated and extremely sensitive to environmental controls (Bothe et al., 2007; Seitzinger et al., 2002; Sutton, 2011). The main microbial processes that produce N_2O are nitrification, which takes place under aerobic conditions, and denitrification, which takes place under anaerobic conditions and is the focus of this study. The denitrification pathway facilitates the stepwise reduction of NO_3^- to N_2 through the following intermediates: nitrite (NO_2^-), nitric oxide (NO), and N_2O (Bothe et al., 2007). In many systems, it accounts for the bulk of N_2O that is produced (Webster and Hopkins, 1996). Several of the enzymes in this process (Nap, Nir, N_2OR) are extremely sensitive to physicochemical controls (pH, ORP, and the availability of C, N, and O) (Richardson et al., 2009), and the associated reaction rates are somewhat predictable based on these parameters. Additionally, many of these controls are relevant to land managers for their relationships to crop productivity and water quality. An important example of these is pH. Adjusting pH is commonplace in agriculture and water treatment; though, most protocols do not consider N_2O emissions. Yet because the practice is so widespread, modifying current protocols with the goal of reducing N_2O emissions would likely be met with less resistance than introducing new practices.

Other controls of N_2O production come in the form of amendments to soils, waters, and wastes. One such additive is biochar, a carbonaceous material produced via pyrolysis of organic matter in a process that also yields bio-oil and synthetic natural gas (Lehmann, 2007; Sohi et al., 2010). In recent years, biochar has garnered a great deal of interest for use as a carbon (C) sink as well as an additive to agricultural and wastewater treatment processes (Amonette et al., 2010; Lehmann, 2007; Liang et al., 2014). Biochar amendment is associated with local alterations to the N cycle, including both reductions (Cayuela et al., 2013; Saarnio et al., 2013; van Zwieten et al., 2010; Wang et al., 2011) and increases (Anderson et al.,

2014a; Clough et al., 2010; Obia et al., 2015; Sanchez-Garcia et al., 2014; Yoo and Kang, 2012) of N_2O emissions. However, because biochar's primary purpose is C sequestration, interactions with the N cycle are often not considered during its use. Additionally, biochar's interaction with the surrounding environment may elicit differing responses in N cycle processes under different conditions, so experimental results may not account for a full range of potential effects. Before the potential of biochar is oversold, there is a need to determine the nature of its N cycle interactions under a variety of environmental conditions.

1.2. pH as a Regulator of N_2O Production

pH has long been known as a master variable in the N cycle, and its effects on N_2O production are no exception. The manner in which it affects N_2O production is both as a proximal control, through altered enzyme kinetics, gene expression, and inhibition (Groffman and Tiedje, 1989; Groffman et al., 1988; Richardson et al., 2009; Wallenstein et al., 2006), and as a distal control, through its influence on long-term environmental conditions that shape the structure of the microbial community (Cuhel and Simek, 2011a; Cuhel et al., 2010; Philippot et al., 2009; Wallenstein et al., 2006). These effects are realized through several routes, not all of which are well-characterized (Bothe et al., 2007; Cuhel et al., 2010; Richardson et al., 2009; Simek and Cooper, 2002). In the field, pH interacts with a host of other environmental variables to determine the suitability of a particular environment for the local microbial community. For N_2O production, this effect can be realized through differing fitness of nitrous oxide reducing (*nosZ*) organisms relative to nitrite reducing organisms (*nirK, nirS*) at different pH levels. As the ratio of *nosZ* organisms increases relative to *nirK* and *nirS* organisms, potentially more N_2O can be removed relative to production (Cuhel et al., 2010; Liu et al., 2010; Philippot et al., 2009). However, because of differences in gene expression, the importance of these ratios is always fixed. Indeed, short-term versus long-term changes in pH may elicit different responses in the microbial community (Baggs et

al., 2010). In general, acidic pH reduces reaction rates throughout denitrification, but its effect is greatest on N_2O reduction to N_2, and low pH is frequently associated with higher N_2O production (Cuhel and Simek, 2011a; Richardson et al., 2009; Simek and Cooper, 2002). However, like with distal regulation, there are many possible effects that could give rise to this outcome. Proposed explanations this include: N_2O reductase (N_2OR) protein assembly (Bergaust et al., 2010), altered enzyme kinetics (Dannenmann et al., 2008; Liu et al., 2010; Richardson et al., 2009), and pH-dependent transcription regulation (Van Den Heuvel et al., 2011). However, because of both microbial and environmental diversity in denitrifying systems, it is critical to understand that any pH-mediated effects on N_2O are operating in a larger context. pH's importance as a regulator of N cycle processes cannot be understated, but any conclusions which are drawn from a study must be carefully rooted in that study's environmental frame of reference.

1.3. Biochar's Potential to Alter N_2O Production

Biochars have half-lives ranging from 10^2 to 10^7 years in soil (Zimmerman, 2010), but differ in physicochemical properties beyond this recalcitrance depending on their manufacturing temperature and feedstock (Amonette et al., 2010; Kloss et al., 2012; Mayer et al., 2014; Ronsse et al., 2013). Using pH as an example, biochars can be manufactured with pHs ranging from less than 4 to greater than 12 (Lehmann, 2007) – a range which spans vastly different microenvironments. When amended to an environment, biochar induces effects such as: increases in biomass, cation exchange, and water retention, as well as changes in local microbial communities (Lehmann et al., 2011; Warnock et al., 2007). Biochar amendment to soil is also frequently associated with increased abundance of *nirS* and *nosZ*-encoding microorganisms (Anderson et al., 2014a; Ducey et al., 2013; Harter et al., 2014) and reduced N_2O emissions (Cayuela et al., 2013; Saarnio et al., 2013; van Zwieten et al., 2010; Wang et al., 2011). Biochars addition to compost has also been shown produce similar effects (reduced *nirK,* and increased *nirS* / *nosZ* resulting in less N_2O emitted*)* (Wang et al., 2013). Additionally, when combined with slurry from an

anaerobic digester as a fertilizer, wheat straw biochar was shown to decrease soil N_2O emissions by 47% compared to slurry alone (Bruun et al., 2011). However, other studies have shown that, under certain environmental conditions, such as under pasture urine patches, or in rice paddy soils, biochar amendment can actually lead to increase N_2O emissions (Anderson et al., 2014a; Clough et al., 2010; Obia et al., 2015; Sanchez-Garcia et al., 2014; Yoo and Kang, 2012).

For many of these studies, biochar-associated alterations to N_2O emissions coincided with enhanced soil microbial activity and N- immobilization. High-temperature biochars in particular are able to adsorb ammonium (NH_4^+) and nitrate (NO_3^-), which could both reduce N losses via leaching and increase N bioavailability in its micropores (Clough et al., 2013; Ippolito et al., 2012; Taghizadeh-Toosi et al., 2011). For agriculture, it is obviously preferable to retain as much N as possible in root zone soil, but if such a mechanism leads to denitrification, it could inadvertently trade groundwater N losses for gaseous N_2O losses or reductions in CO_2 for increases in N_2O (Ippolito et al., 2012). By contrast, in water treatment, it is desirable to remove as much N as possible from the water, but complete denitrification to N_2 is far more desirable than partial denitrification to N_2O. One technology which has application for N control in both the agricultural and wastewater realms is the denitrifying bioreactor (DNBR), a technology that uses stable organic carbon supplies to fuel natural denitrification of influent water (Blowes et al., 1994; Robertson and Merkley, 2009; Schipper et al., 2010). DNBRs utilizing biochar as an adjunct to a conventional C sources have recently begun to be tested (Bock et al., 2015c; Bock et al., 2015d; Christianson et al., 2011; Easton et al., 2015; Zhang, 2015). Exploring N_2O dynamics in these systems is a major goal of this study.

1.4. Denitrifying Bioreactors and N_2O

The last several years have seen DNBRs become a popular alternative approach to mitigate excessive environmental N. In agricultural systems, they represent a valuable tool to reducing export of NO_3^- to

receiving waters by intercepting tile drainage, groundwater, or runoff in a space which is constructed to favor denitrification conditions (Schipper et al., 2010). In most field applications, the C supply of DNBRs is provided by wood chips, due to their low cost, stable long-term performance, and widespread availability (Bock et al., 2015d; Schipper et al., 2010). Though they are quite effective at removal of N from influent water, DNBRs have been noted as a source of GHG emissions, particularly N_2O (Bock et al., 2015c; Easton et al., 2015; Elgood et al., 2010; Moorman et al., 2010). Additionally, the design criteria of these systems is typically focused on water quality, not GHG emissions. As with the amendment of biochar it is important to understand what factors are associated with these emissions so that mechanisms can be derived and future engineering solutions do not simply trade the problem of NO_3^- for the problem of N_2O.

1.5. Experimental Objectives

Knowledge gaps currently exist in understanding how the N_2O production of biochar-amended DNBR systems may vary with differing pH. Biochar is commonly used in environments which diverge considerably in pH. Indeed, most studies of N_2O production in biochar-amended systems do not account for differences in pH. This experiment was designed to address this gap by monitoring N_2O in biochar-amended DNBRs that were operated under a three different pH levels. This simultaneously addresses gaps in basic science and offers insights that could be applied to improving DNBR performance.

This experiment utilized lab-scale, biochar-amended DNBRs, operated at three pH levels to explore the following objectives: 1) Examination of N_2O production behavior through analysis of headspace gas 2) Quantification of key denitrification genes (*nirK, nirS, nosZ*) in DNBR column media; 3) Determination of whether any biochar-induced differences in the above objectives exhibit pH-dependent behavior.

II - 2. Methods

2.1. Experimental Design and Setup

Eighteen denitrification experiments were carried out in bioreactor columns constructed from PVC pipe (61cm L X 10cm D) and fitted with ports for aqueous and gaseous sampling (Fig. 1). Columns were filled with either wood chips, or a combination of wood chips and biochar, and examined at three pH levels.

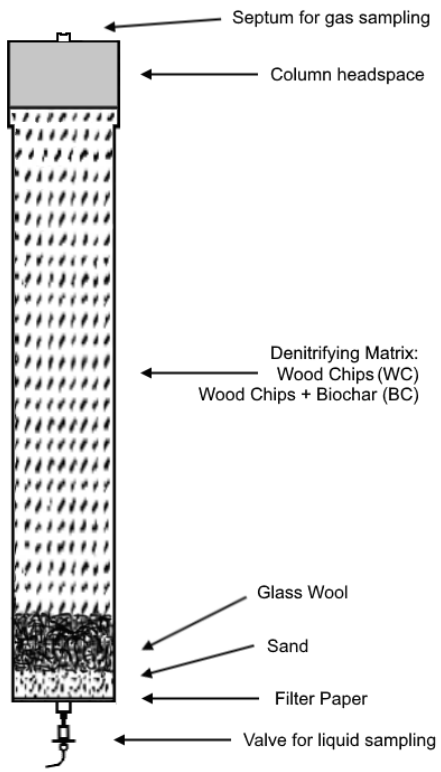

Figure 1: Schematic of denitrification columns. Treatments consisted of a matrix of wood chips (WC) or wood chips amended with 10% biochar by volume (BC). Within each treatment, N_2O concentrations were observed at three experimentally imposed pH levels: unbuffered (UB), buffered (BU), and acidified (AC).

The end cap and the threaded plug were attached with PVC-primer and cement, and columns were tested for gas and water tightness before use. Wire mesh followed by 50-µm filter paper (VWR Filter Paper), glass wool, and 5cm of washed, quartz sand, was placed at the bottom end cap to prevent solids from washing into the sampling tube. Columns were filled with the denitrifying matrix material, using one of

two treatments: wood chips as a control (WC, Timberland Mulch, Ferrum, VA), and wood chips amended with 26-mesh hardwood biochar in a 10:1 volumetric ratio (BC, Biochar Now, Berthod, CO). Biochar was mixed into the wood chips to achieve a near uniform distribution, and because the biochar filled the interstitial spaces between the wood chips, the total volume occupied by substrate in each column was not increased. Total matrix volume within each column was 5000 cm^3 while headspace volume was 600 cm^3. Columns were stored vertically at room temperature for the duration of the experiment.

2.2. Test Solution, Priming, and Sampling Schedule

Before running any experimental trials, columns were primed for one week with the test solutions to establish conditions favorable for denitrification. The test solution consisted of 15 mg L^{-1} NO_3^- -N and 2 mg L^{-1} NH_4^+ -N. Columns received approximately 3.5 L of solution. These concentrations were selected as values relevant to those found in soil water (Schipper et al., 2005) and tile-drained effluent (Schipper et al., 2010; Warneke et al., 2011). One third of the solution was buffered to pH 8 with carbonate-bicarbonate (BU), one third was left unbuffered (UB), and the remainder was acidified with HCl (AC). Following the one week priming, the columns were drained, washed twice with ultrapure water (>10 mΩ) to minimize the effects of the first flush of dissolved organic carbon and other issues associated with new matrix material (Schipper et al., 2010) and refilled with the 15 mg L^{-1} NO_3^- -N and 2 mg L^{-1} NH_4^+ -N solution. Experimental trials were carried out in triplicate at all three pH ranges, yielding 6 matrix-pH combinations over 18 total trials. Due to differences in interstitial space and a need to preserve a constant headspace volume across replicates, the exact volume of solution added to each column varied approximately 5% between replicates. This was considered necessary because differences in headspace volume would have a far greater impact on gas concentrations than slight differences in solution or matrix volume.

Aqueous and gaseous samples were collected concurrently at 0.5 hrs, 3 hrs, 6 hrs and again every 6 hrs for the first 3 days of the experiment. This was followed by a gradual reduction in sample frequency to every 12 hrs from day 5 to the end of the experimental period. These intervals were selected based on the rate of NO_3^- removal observed in previous experiments (Bock et al., 2015c; Easton et al., 2015).

2.3. Aqueous Sample Analysis

Aqueous samples were collected to verify that pH did not change throughout the duration of the experiment and remained within the ranges set in the experimental design. Samples were drawn from the base of each column in 20 mL acid-washed beakers. Immediately after sampling, these were filtered using 0.45 µm pore diameter nylon syringe filters (Restek Corporation, Bellefonte, PA) and assayed for pH using an Orion Versa Star electrochemistry meter (Thermo-Fisher Scientific, Waltham, MA).

2.4. Gas Sampling and GC/MS Analysis

Quantification of headspace N_2O was carried out using a Shimadzu QP2010ultra GC/MS (Shimadzu Scientific Instruments Inc., Columbia, MD). Though N_2O was the only gas being analyzed, the protocol employed is being developed for simultaneous quantification of CH_4, CO_2, and N_2O. GC utilized a 60 m Carboxen® 1010 PLOT carbon molecular sieve with a 32 µm inner diameter (Sigma-Aldrich Corporation, St. Louis, MO). 500 µL headspace gas samples were withdrawn through column septa using gastight syringes (Hamilton Laboratory Products, Reno, NV) and manually injected onto the GC column using a split ratio of 10:1 carrier to sample. Grade 5.5 ultra-pure He (Airgas, Inc., Radnor Township, PA) was used as the carrier gas with an inlet pressure of 500 kPa and flow set to a constant linear velocity of 45 cm/s. Injection port temperature was 200 ˚C. From starting point of 100 ˚C, GC temperature was increased at a rate of 35 ˚C min^{-1} until reaching 180 ˚C for complete elution into the MS interface. Interface and ion source were set to 220 ˚C and 200 ˚C, respectively. Tuning electron multiplier voltage was set to 1.07 kV

and then adjusted to an absolute voltage of 0.85 kV between 3.5 and 3.9 min to encompass elution of CH_4 at 3.59 min. CH_4 was detected using SIM for m/z 16 and 15. Absolute voltage of 0.7 was used from 3.9 to 4.2 min during a scan from m/z 35 to m/z 50 to encompass CO_2 elution at 3.99 min. The voltage was then increased to 1.25 kV from 4.2 to 4.49 min to encompass N_2O elution at 4.34 min. N_2O detection utilized SIM at m/z 30 and using m/z 44 as a reference ion. Total sample run time was 4.49 min. N_2O standards were prepared by mixing ultra-pure N_2O and N_2 in a 1 L gas bulb (N_2O and N_2 were Grade-5, Ultra High Purity, obtained from Praxair, Inc., Danbury, CT and Airgas, Inc., Radnor Township, PA, respectively). The calibration curve included eight standards ranging from 0.1 to 50 ppm and was plotted as signal versus 1/c. Dilutions were prepared individually with the exceptions of the 0.5 and 0.1 ppm concentrations, which were serially diluted. An R^2 value of 0.9994 with a RSD of 12% was obtained. A custom greenhouse gas (GHG) gas standard consisting of 610 ppm CO_2, 5ppm CH_4, and 1ppm N_2O (Air Liquide America Specialty Gasses LLC, Plumsteadville, PA) was used to independently validate the standard curve with the long-term goal of simultaneous quantification (Bock et al., 2015b).

2.5. Column Matrix Sampling and DNA Extraction

Column matrix material (woodchip or woodchip+biochar) was sampled for DNA extraction before and after the incubation period. Columns were emptied into a bucket and mixed to ensure that samples were homogenous and representative of multiple strata in the column. Because of the necessity of unsealing the columns to take samples, the process was destructive to the denitrifying environment and could only be undertaken at pre- and post- stages of incubation. Matrix specimens were withdrawn by hand, placed into 30mL Nalgene sample bottles, and stored at -15 ˚C until DNA extraction took place. All bottles, tools, and gloves, were washed with 90% Et-OH and rinsed at each step to avoid contamination.

Matrix samples were then processed for DNA extraction using a modification of methods from Leite et al. (2014). Large wood chips from each sample were broken into smaller pieces using an ethanol-washed scalpel and tweezers. From these samples, 250 mg sub-samples were weighed into bead tubes and disrupted using a BioSpec Mini-Beadbeater-24 (BioSpec Products, Inc., Bartlesville, OK) for 10 minutes. Remaining matrix material was re-frozen for storage. The disrupted samples were then extracted with a MoBio PowerSoil® DNA Isolation Kit (MoBio, Inc., Carlsbad, CA, USA) and eluted with 75 µL of PCR grade water. DNA concentration in extracts was quantified using a Qubit® 2.0 Fluorimeter and a dsDNA BR Assay kit (Thermo-Fisher Scientific, Waltham, MA). Extracts were then diluted to concentrations of 3 ng DNA / µL for downstream qPCR application and stored at 4 ˚C. Samples with less than this concentration were left undiluted during qPCR. The remainder of the extracts were stored at -15 ˚C for long-term use.

2.6. Molecular Analysis Procedures

Quantitative PCR (qPCR) was employed to assess copy number of the genes coding for the denitrification enzymes: Cu-dependent nitrite reductase (*nirK*), Cytochrome cd_1 nitrite reductase (*nirS*), and nitrous oxide reductase (*nosZ*) using the standard curve method. These genes were selected on the basis of functional relevance to N_2O production. *nirK* and *nirS* lead to N_2O accumulation, and *nosZ* facilitates N_2O removal. While obtaining copy number does not indicate activity or expression, it is a good baseline measure for assessing the potential for denitrification to occur within a microbial population. The ratio of denitrification genes present in a microbial community has also been linked to differences in denitrification products. In particular, the ratios of *nosZ/(nirK+nirS)* and *nosZ/nirS* have been shown to affect both total gas production as well as the proportion of N_2O produced relative to N_2 (Cuhel et al., 2010; Liu et al., 2010; Philippot et al., 2009).

Samples were assayed against a calibration curve using clones that had been previously prepared from environmental amplicons using an Invitrogen TOPO® TA Cloning® Kit (Thermo-Fisher Scientific, Waltham, MA) and sequenced to confirm their identity. From these clones, standards were serially diluted and run with each qPCR assay to obtain Ct values for the curve. The following primers were employed in the analysis: nirK-876, nirK-1040 (Henry et al., 2006); nirS-cd3af, nirS-R3cd (Hallin and Lindgren, 1999; Throback et al., 2004); and nosZ2F, nosZ2R (Henry et al., 2006). PCR preparations were made using Bio-Rad SsoAdvanced™ Universal SYBR® Green Supermix reagents (Bio-Rad Laboratories, Inc., Hercules, CA). Analysis was carried out on an Eppendorf Mastercycler® RealPlex^2 thermal cycler using Eppendorf's RealPlex software to determine Ct values.

Assays were carried out with three technical replicates sample to ensure the validity of the method. No template controls were included with each plate to calibrate measures for non-specific amplification. Gel electrophoresis and melting curve analysis were used to validate PCR products. Standard curves were constructed over 7 orders of magnitude and were required to have efficiency within +/- 20% from ideal. Curves not falling into this range were re-run. Additionally, if more than two technical replicates on the in the standard curve had to be excluded, then the plate was re-run. These thresholds reflect realistic performance boundaries for environmental data generated with the selected primers (Wei et al., 2015).

2.7. Statistical Approach

Treatments consisted of 2 matrix materials (WC or BC) at three treatment levels (UB, BU, AC). Data was analyzed in the R statistical programing environment (R Core Team, 2015) and plotted using the ggplot2 and gridExtra packages (Auguie, 2015; Wickham, 2009). Time series data was collected for pH and N_2O headspace concentration and binned using the following factors: *timestep (n=19), column number (n=18), matrix treatment (n=2), pH level (n=3), and a combined matrix-pH effect (n=6)*. Q-Q plots and Shapiro-Wilk

tests were employed to check the normality of pH for each level over the course of the study. One and two way Liner Mixed Effects (LME) Analyses of Variance (ANOVA) were used to determine overall differences in N_2O production within treatment groups (N_2O production was the response variable and matrix material, along with pH grouping, were predictor variables). Time-wise sections of these results were then analyzed by differencing followed by pairwise comparisons using a Tukey's Honest Significant Difference (HSD) test. These results were plotted and compared with differences indicated by a locally weighted polynomial regression (LOESS) applied to a time-series of headspace N_2O concentrations. Microbial data was collected as pre- and post- treatment copy numbers for the genes of interest, which were checked for normality and then averaged to give a single value for each column. The choice to analyze copy number in this manner (as opposed to as a time series) was due to the requirement of maintaining a sealed sample chamber for the duration of the study. The microbial data was then binned using the same factors as time series data. One and 2-way ANOVAs were also used to analyze sensitivity of microbial populations to the matrix material and pH conditions. Tukey's HSD tests were then employed to perform post hoc comparisons of effects (matrix, pH, and joint) on microbial populations.

II - 3. Results

The results of this study are presented as follows: 1) pH measurements are discussed with respect to the three levels (AC, BU, UB), 2) N_2O production is assessed as a function of matrix material at each pH level, and 3) analysis of the denitrification genes: *nirK, nirS,* and *nosZ* is presented for each treatment and level.

3.1. Stability of pH Levels

Normality of pH treatment levels was assayed by Shapiro-Wilk test and Q-Q plots at a 95% significance interval. Buffered (BU) and unbuffered (UB) levels exhibited normal distribution of pH over the experimental duration, but the acidified (AC) level was not normally distributed (Fig. 2). When examined

within the six possible pairs of matrix and pH, all combinations were found to be normally distributed. Additionally, the LME ANOVA used to analyze the data is relatively robust against moderate deviations from normality (McDonald, 2014), thus this did not have an impact on the overall conclusions of this study.

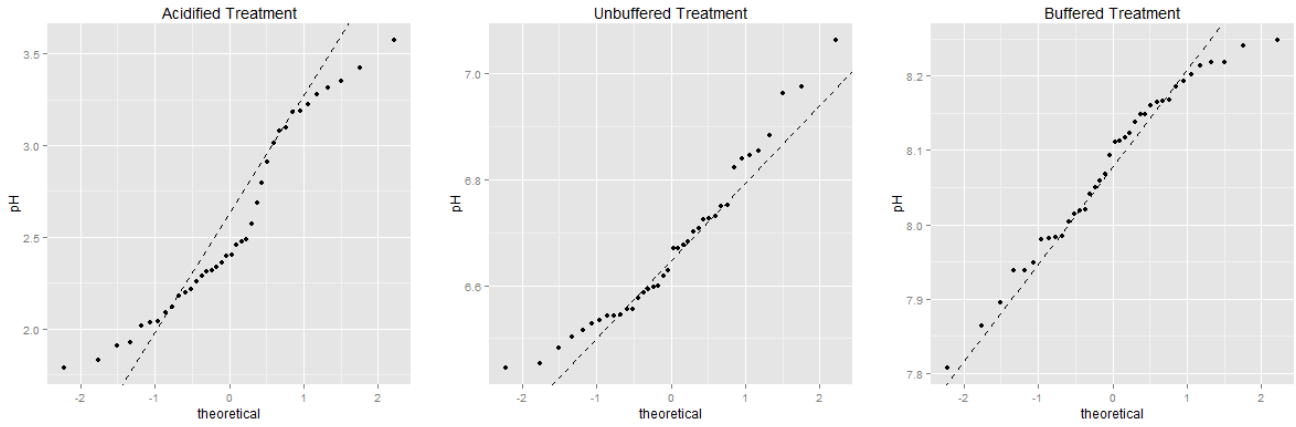

Figure 2: Q-Q plots of pH data by treatment level.

The acid that was added to the AC treatment level reduced effluent pH to a value lower than anticipated – around 2.5. Although this value is outside those typically found in agricultural soils, it is relevant to conditions found in engineered denitrifying environments, including bioreactors (Bock et al., 2015a; Partheeban et al., 2014; Rivett et al., 2008). pH values remained stable for the full duration of the experiment for both the BU and UB levels, never varying by more than 10% (Fig. 3); however, the AC pH exhibited an increasing trend and was more variable overall, perhaps as a result of natural buffering provided by the matrix material (residual standard deviation = 0.200 compared to 0.023 and 0.014 for UB and BU groups, respectively).

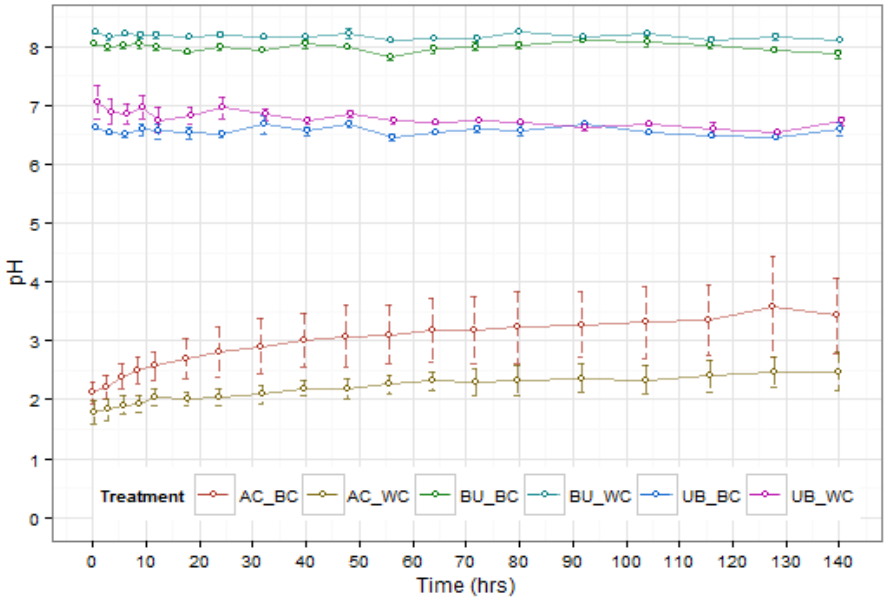

Figure 3: Time series of pH during the experiment

3.2. Nitrous Oxide Production

Figures 4 and 5 present time series of mean headspace N_2O concentrations analyzed using the LOESS non-parametric procedure (span = 0.40) to visualize the data and test treatment differences at each time step (Grosjean and Ibanez, 2014; Loader, 2013).

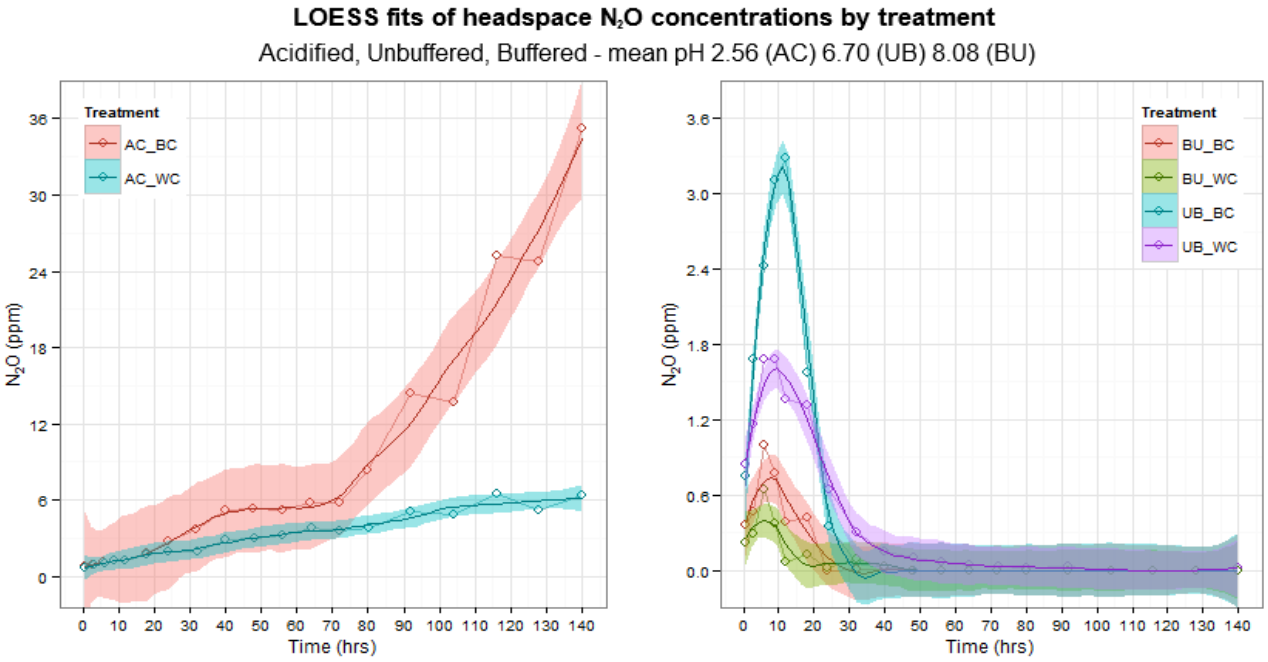

Figure 4: LOESS fits for N_2O production by treatment (alpha=0.40) Open points represent mean data values (note the y-axis scales differ by an order of magnitude). Wood Chips (WC), Biochar (BC) Acidified (AC) Unbuffered (UB) Buffered (BU)

Figure 4 shows that headspace N_2O varied considerably by pH level, with BC treatments having higher concentrations at all pHs tested, although the biochar treatment's N_2O concentrations generally declined more rapidly as well. For both the BU and UB levels, N_2O concentrations approached peak values within the first 12 hrs and then decreased rapidly over the next 24 hrs. BU columns reached zero ppm N_2O within 48 hrs while the UB treatments took slightly longer to achieve zero values (30-70 hrs depending on treatment, Fig. 4). By contrast, at the AC level both the WC and BC treatments showed continuous increases in headspace N_2O concentration throughout the experiment's duration (Fig. 4).

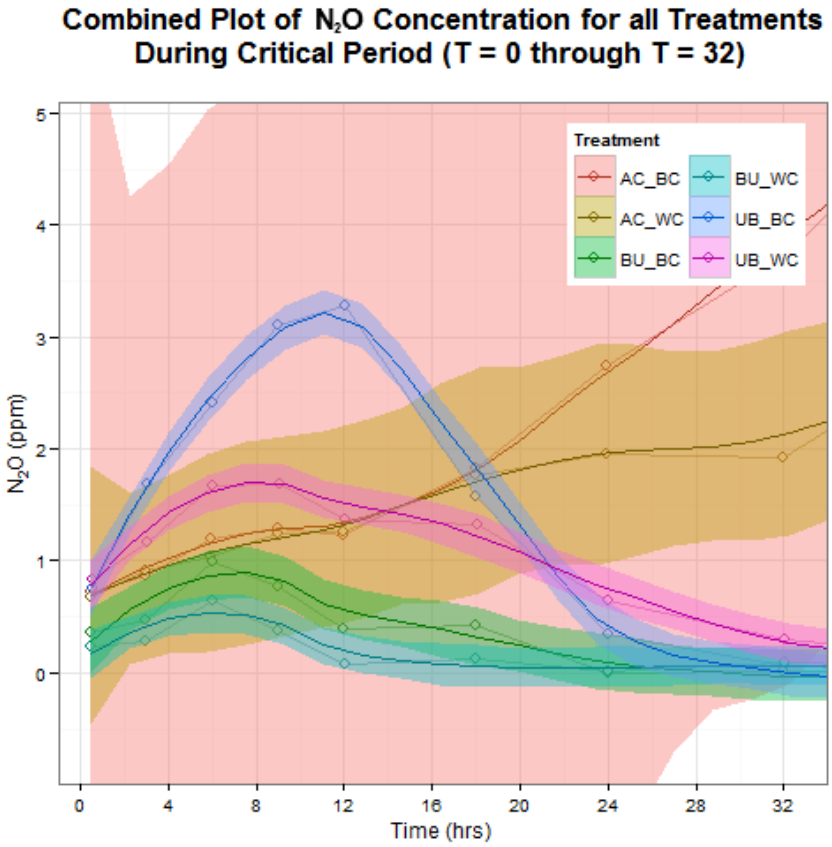

Figure 5: LOESS fits for the critical period (T=0-32) of N_2O concentration (alpha=0.40) Axes are truncated at 5 ppm and 32 hrs to highlight the differences between treatments. Wood Chips (WC), Biochar (BC) Acidified (AC) Unbuffered (UB) Buffered (BU)

Significant differences between the BU and UB levels were only apparent during the initial peak time period (0-32 hrs), after which the LOESS indicated statistical equivalence at 0 ppm (Fig. 5). For the AC level,

significant divergence occurred at the 75 hr mark when headspace N_2O for the BC treatment began to increase at a much faster rate than the WC treatment (Fig. 4).

Peak N_2O values measured were 6.363 ppm (AC_WC) and 35.231 (AC_BC). These peak values were more than an order of magnitude greater than the concentrations of N_2O produced by the same matrix material at the other pH ranges (Table 1). The peak N_2O values and the time it took to reach them were then analyzed by ANOVA and compared to each other using Tukey's HSD test. Post-hoc testing (Table 2) indicated significant differences in peak height and time to reach peak by pH (but only with the AC level). No significant differences were seen in the treatment comparison.

Table 1: LOESS regression fits of peak headspace N_2O concentrations by treatment group with mean pH and time data for peak and zero values

Treatment	Mean pH	Peak N_2O (ppm)	Time to Peak N_2O (hrs)	Time to Zero N_2O (hrs)
AC_WC	2.168	6.363	140	NA
UB_WC	6.777	1.680	9	104
BU_WC	8.171	0.643	6	48
AC_BC	2.941	35.231	140	NA
UB_BC	6.560	3.283	12	48
BU_BC	7.984	0.996	6	48

Table 2: Tukey's HSD comparing N_2O headspace concentrations peak values and times across treatments and levels

Tukey's HSD Pair	Time to Peak N_2O, P-Value	Peak N_2O Concentration, P-Value
BU-AC (Level)	0	0.035
UB-AC (Level)	0	0.061
UB-BU (Level)	0.832	0.956
WC-BC (Treat)	0.931	0.187

Pairwise comparisons between matrix and pH combinations were then made at each timestep by pairwise differencing and plotting the results of each treatment combination (Fig. 6). Statistically significant differences between N_2O concentrations in the pairwise comparisons were determined by ANOVA

followed by Tukey's HSD tests. Significant differences are indicated in Fig. 6 at the timestep during which they occurred.

The LOESS and Tukey's HSD timewise differencing procedure revealed some differences on when divergence of N_2O production occurred between the treatments. While the LOESS procedure indicated differences between the AC_BC and UB/BU groups emerging after 34 hrs, the differencing method revealed significant differences occurring slightly earlier, at T=32. Between the two treatments at the AC level, differencing only provided a single, statistically significant divergence at 140 hrs, while the LOESS procedure indicated differences emerging between WC and BC treatments after T=75. Between the AC_WC and the BU/UB treatments, timewise differencing found no significant divergence in N_2O concentration, but LOESS indicated differences beginning at T=24 and continuing through the duration of the experiment. Between the BU and UB treatment combinations, the differencing found no significant deviation in N_2O concentration throughout the course of the study. By contrast, LOESS showed differences in N_2O concentration occurring at many time intervals (Table 3, Fig. 5).

Table 3: Periods of significant divergence in headspace N_2O concentrations. Comparisons between treatment combinations are presented side-by-side with significant periods from both analysis.

Treatment 1	Treatment 2	Divergence Periods (LOESS)	Divergence Periods (Differencing)
AC_BC	AC_WC	T:83-T:140	T:140
AC_BC	UB_BC	T:34-T:140	T:32-T:40, T:64, T:92, T:116-T:140
AC_BC	UB_WC	T:35-T:140	T:40, T:64, T:92, T:116-T:140
AC_BC	BU_BC	T:34-T:140	T:32-T:40, T:64, T:92, T:116-T:140
AC_BC	BU_WC	T:34-T:140	T:24-T:40, T:64, T:92, T:116-T:140
AC_WC	All UB/BU	T:24-T:140	NA
UB_BC	UB_WC	T:3-T:23, BC > WC T:23-T:29, WC > BC	NA
UB_BC	All BU	T:0.5-T:23	NA
UB_WC	All BU	T:0.5-T:29	NA
BU_BC	BU_WC	T:8-T:11	NA

These differences are likely accounted for by the variance structure of each method. While the LOESS accounts for variance between timesteps and from one replicate to another within treatments, the differencing only considers variance within treatment. The combination of variance between timesteps and within treatment appears to be what caused the discrepancy between the two analyses conducted in this study.

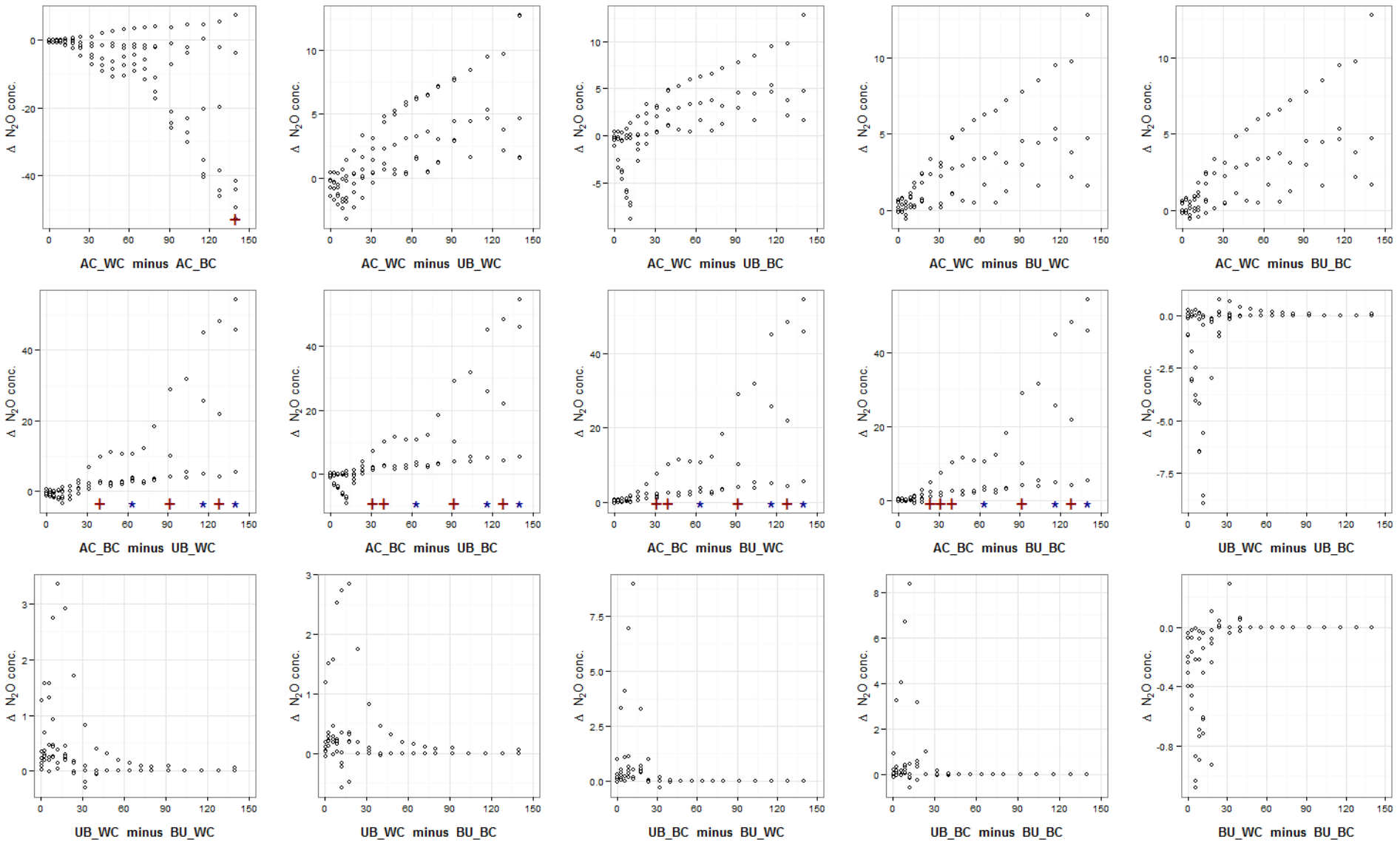

Figure 6: Pairwise differencing of N_2O concentrations at each timestep (X axis, hrs.) Differencing was conducted pair-wise with each replicate subtracted from the others (six replicate combinations). Significant differences determined by a Tukey HSD test at (α=0.05) were plotted at each timestep using a '+' to indicate a P-Value of less than 0.10 and a '' to indicate a P-Value of less than 0.05.*

Using the ez package (Lawrence, 2013), repeated measure ANOVA was used to compare the effect of the experimental factors on N_2O production over time (Table 4). Matrix material, pH category, and matrix by pH interaction were all found to have significant effects on peak N_2O concentrations (F statistics of 9.693, 15.240, and 7.705 with p-values of 6.022×10^{-3}, 1.603×10^{-5}, and 1.639×10^{-3} for matrix, pH group, and matrix x pH, respectively). When the six possible combinations were analyzed individually, instead of by treatment, the differences were also statistically significant (F statistic = 12.441, p-value = 3.490×10^{-9}).

These measures were then repeated excluding the data from the acidified columns (Table 4). The results showed similar trends to those which included the AC data. As before, the combination of treatment and pH produced the most significant relation to N_2O peaks (F statistic = 6.972, p-value = 4.752×10^{-4}). This was followed by the effect of pH alone (BU vs UB) – (F statistic = 8.740, p-value = 8.003×10^{-3}). Matrix material was shown to have a weak effect (F statistic = 2.996, p-value = 0.100). Matrix by pH interactions were not found to have significant interactions with N_2O (F statistics of 1.230, p-value = 0.282).

Table 4: Linear Mixed Effects (LME) ANOVA tables for assessing N_2O production relative to treatment factors by time

Including AC	**Factor**	**DFn**	**DFd**	**F stat.**	**P-value**
Within pH by Matrix	pH Category	2	36	15.240	1.603×10^{-5}
	Matrix Material	1	18	9.683	6.022×10^{-3}
	pH Category : Matrix Material	2	36	7.705	1.639×10^{-3}
Single Variable	Treatment Pairings	5	90	12.441	3.490×10^{-9}
Excluding AC	**Factor**	**DFn**	**DFd**	**F stat.**	**P-value**
Within pH by Matrix	pH Category	1	18	8.740	8.003×10^{-3}
	Matrix Material	1	18	2.996	0.100
	pH Category : Matrix Material	1	18	1.230	0.282
Single Variable	Treatment Pairings	4	54	6.972	4.752×10^{-4}

These results suggest that while the AC pH level certainly skewed the importance of the relationships between treatment, pH level, and N_2O production, they did not produce trends which were vastly different from those between BU and UB levels alone. Individual pairs still produced the most significant

differences and within the multi-level analysis, pH was the most important factor, followed by matrix and then matrix by pH. While the significance was not as high, the identical order of importance reinforces the idea that pH is dominating matrix effects for N_2O production in this particular system.

N_2O peak values were then used to construct an interaction plot to visualize the effects of pH and matrix material on N_2O concentrations (Fig. 7). Figure 7 depicts the peak N_2O concentration and confidence intervals for each treatment level. The plot corroborates the results of the ANOVA, namely, that BC treatments were associated with more N_2O than their WC counterparts. Outside the AC pH level, these differences are less pronounced, but still statistically significant. For both matrices, decreasing pH is the factor most significantly correlated with increased headspace N_2O, but it is important to note that this concentration is a combination of production and consumption of N_2O over time – without a mass balance approach, it is impossible to derive details about the mechanisms behind these differences.

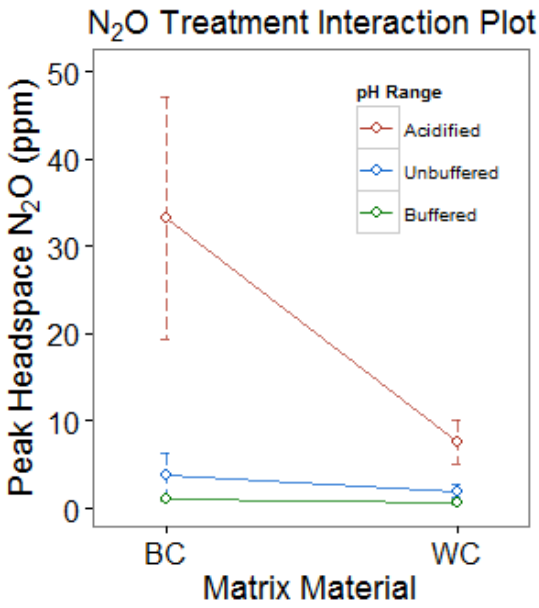

Figure 7: Interactions plot of peak headspace N_2O and treatment factors (95% CI)

3.3. Denitrifying Gene Abundance

Mean copy numbers of the three genes of interest (*nirK, nirS, nosZ*) were quantified by PCR. Standard curves obtained a mean efficiency of 105.33%, and a mean R^2 value of 99.4%. Fig. 8 and Table 5 present the results normalized per gram of matrix material and sorted by treatment and pH level.

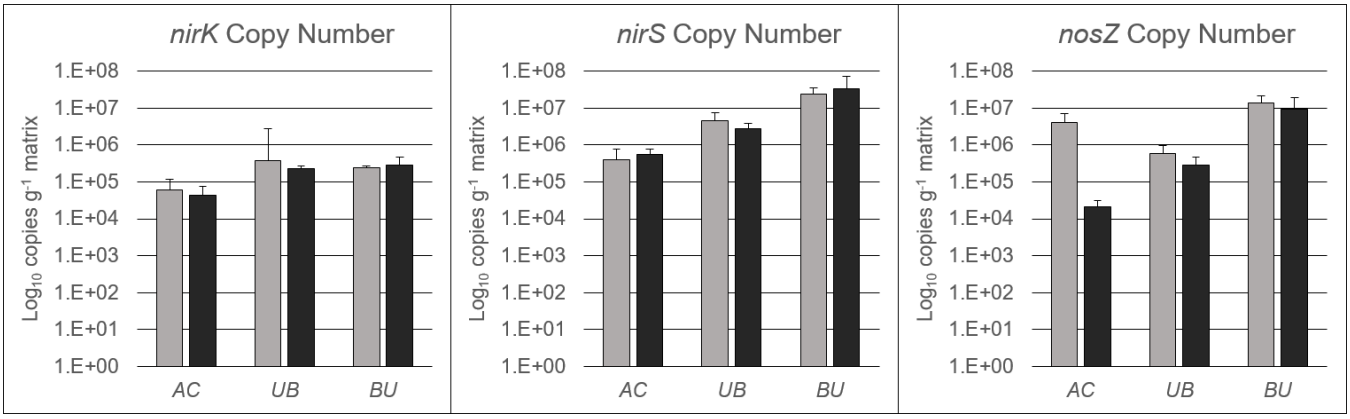

Figure 8: Denitrifying gene quantification plot: mean of pre- and post- sampling with standard deviations as error bars. Treatments shown by color – WC: light grey; BC: dark grey. Plots are sorted by gene (nirK, nirS, nosZ) and pH level (AC, UB, BU). Units are log_{10} copy number per gram of matrix. Significant differences determined by Tukey's HSD test are noted in Figure 9.

Table 5: Mean copy numbers of denitrification gene targets (nirK, nirS, and nosZ)

Gene Target	WC_AC	WC_UB	WC_BU	BC_AC	BC_UB	BC_BU
nirK copies	4.61×10^4	1.60×10^6	2.08×10^5	2.89×10^4	2.2×10^5	2.47×10^5
nirS copies	3.48×10^5	3.91×10^6	1.68×10^7	3.45×10^5	2.03×10^6	3.35×10^7
nosZ copies	3.11×10^6	6.08×10^5	7.94×10^6	1.38×10^4	2.89×10^5	5.08×10^6

Gene copy numbers were normally distributed within groups and had no significant differences between pre- and post- experiment conditions. However, three samples out of 108 were shown to be outliers and had to be excluded from the analysis. High spatial variability is common in environmental samples (Christensen et al., 1990; Groffman et al., 2009a; Parkin, 1993), so having a small number of outliers is not unusual. The quantification indicated that *nirS* denitrifiers outnumbered *nirK* denitrifiers by one to two orders of magnitude. The difference appeared to be greatest in the BU pH level, where both *nirS* and *nosZ* populations were an order of magnitude greater than in the UB level.

One-way ANOVA was used to analyze the influence of treatment matrix and pH level on the denitrifying populations (Table 6). Significant interactions were found between the pH group and mean copy number for all three denitrifying gene targets. F statistics of 2.168, 6.777, and 8.171 with p-values 0.0889, 0.0453, and 0.0137, were obtained for *nirK*, *nirS,* and *nosZ,* respectively. The test was also repeated excluding results from the AC columns to test if the extreme conditions were producing bias in the data. The results were similar to the original testing, though the *nirK*-pH effect was no longer significant (F statistics of 2.536, 9.241, and 8.232 with p-values 0.142, 0.0125, and 0.0167, for *nirK*, *nirS,* and *nosZ*).

No interactions were found between individual gene copy number and matrix material in both the complete and AC-excluded analyses. This indicates that in this system, pH, rather than matrix material is the primary driver of gene abundance in these denitrifying populations. Potential alterations to functional gene ratios were also tested with respect to the treatment factors. A weakly significant effect was found between the *nirS*/*nosZ* ratio in the AC-excluded data (F statistic = 3.955, p-value = 0.0748).

Table 6: One-way ANOVA table relating gene targets to treatment factors

Gene Target	Factor	F stat.	p-value	Repeat, excluding AC level	Factor	F stat.	p-value
nirK copies	pH level	2.168	0.0889		pH level	2.536	0.142
nirS copies	pH level	6.777	0.0453		pH level	9.241	0.0125
nosZ copies	pH level	8.171	0.0137		pH level	8.232	0.0167

To further assess the pH level's effects on the functional gene groups, post hoc analysis was performed with a Tukey's HSD test to compare differences in gene copy number for each pH category. The test indicated that there were fewer pH-influenced statistical differences within the treatment pairs than in the population on the whole. No pairwise differences were found in the *nirK* populations. Statistically significant differences were obtained in *nirS* between the BU and UB groups (p-value = 0.0432), and in *nosZ* between the BU and AC levels (p-value = 0.0489), as well as the BU and UB levels (p-value = 0.0156) (Fig. 9). Repeating the testing while excluding the AC level produced the same results: in BU and UB levels,

no differences were found between *nirK* populations (p-value = 0.142) but significant differences were noted in both *nirS* (p-value = 0.0125) and *nosZ* (p-value = 0.0167) populations.

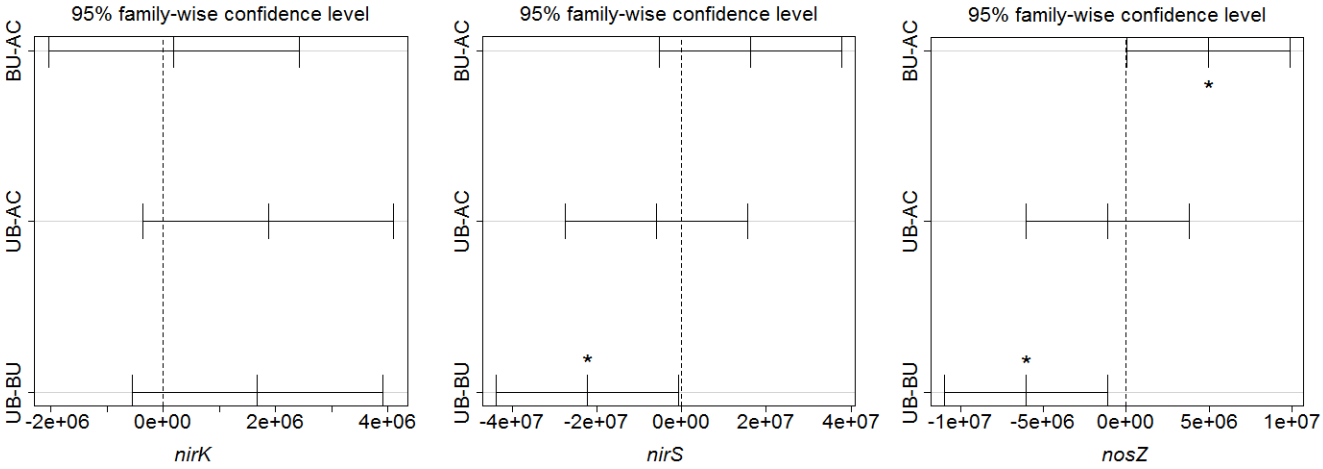

Figure 9: Tukey's HSD Plot of functional gene comparisons between pH levels. Significant differences determined by a Tukey HSD test at (α=0.05) were plotted over means using a '' to indicate a p-value of less than 0.05.*

These results indicate that buffering (from pH 6.70 to 8.08) has a significant, stimulatory effect, on *nirS* populations and *nosZ* populations. When considering the sum of the three populations together, pH did alter total abundance – buffered having the most, acid the least – but while acidification appeared to reduce copy numbers on the whole, the only pairwise significant difference was *nosZ* in the BU to AC comparison. A two-way ANOVA was also used to analyze the combined effects of pH and matrix material on denitrification genes (Table 7). No significant interactions between the *nirK* copy numbers and the combined factors were found. *nirS* populations exhibited a response to pH (F stat. 3.855, p-value = 0.0509) with no response to either matrix material or a combined effect of matrix and pH group. *nosZ* exhibited a strong response to pH (F stat. 5.550, p-value = 0.197) with no response to matrix material or the combination of pH and matrix effects. Repeating these tests without the AC group produced the same results: no *nirK* effects and pH responses in both *nirS* and *nosZ* (F stats. 10.067 and 7.259, p-values = 0.0131 and 0.0273, respectively). Population ratios were influenced by the matrix, but results were less clear for pH (due to the AC level's influence on the analysis). In the AC-included dataset, *nosZ/nirS* ratio was found to be weakly influenced by matrix material and matrix by pH effects (F stats. 3.371 and 2.906, p-values

0.0912 and 0.0935, respectively). The proportion of *nosZ/(nirK+nirS)* was also weakly affected by the matrix material (F stat. 3.213, p-value = 0.0983). When AC was excluded, significant relations emerged in the *nosZ*/*nirK* ratio, and the relative influence of the factors changed. While matrix remained an important effect for *nosZ/nirS*, and *nosZ/(nirK+nirS)*, with p-values of 0.0312 and 0.0188, respectively, pH also emerged as a highly significant factor, especially with respect to *nirK* ratios (Table 7).

Table 7: Two-way ANOVA table relating gene targets to treatment factors. Significant results are indicated in red.

Gene Target (s)	Factors	F stat.	P-value	F stat.	P-value
		AC Included		AC Excluded	
nirK copies	pH Group	2.324	0.1400	2.064	0.189
	Matrix Material	0.074	0.7910	0.078	0.788
	pH Group + Matrix Material	0.067	0.9360	0.060	0.813
nirS copies	pH Group	**3.855**	**0.0509**	**10.067**	**0.0131**
	Matrix Material	1.732	0.2128	1.124	0.320
	pH Group + Matrix Material	0.680	0.5253	1.769	0.220
nosZ copies	pH Group	**5.550**	**0.0197**	**7.259**	**0.0273**
	Matrix Material	1.750	0.2105	0.500	0.500
	pH Group + Matrix Material	0.316	0.7347	0.319	0.588
nosZ/nirK copies	pH Group	1.125	0.357	**25.327**	**0.00101**
	Matrix Material	1.507	0.243	**6.177**	**0.0378**
	pH Group + Matrix Material	1.205	0.333	**6.065**	**0.0392**
nosZ/nirS copies	pH Group	2.686	0.1086	**4.968**	**0.0564**
	Matrix Material	**3.371**	**0.0912**	**6.805**	**0.0312**
	pH Group + Matrix Material	**2.906**	**0.0935**	**4.236**	**0.0736**
nosZ/(nirK+nirS) copies	pH Group	2.606	0.1149	**13.488**	**0.00629**
	Matrix Material	**3.213**	**0.0983**	**8.628**	**0.0188**
	pH Group + Matrix Material	2.764	0.1030	**5.706**	**0.0439**

These findings suggest that pH is an important control for DNBR microbial populations, particularly in the mid pH range (6-8) when other factors such as the presence of O_2, C:N ratio, NO_3 concentration are held constant. Of the three genes, *nosZ* is the most sensitive to the different pH levels and *nirK* the least. Matrix effects seem to be less tied to individual populations and more to the ratios of one gene to another. Weak correlations with respect to BC were observed in the full data set between *nosZ* and both *nirS* and the

sum of *nirK* and *nirS*. When the AC level was removed, these correlations became more significant and a more complex picture emerged where joint effects of matrix and pH were revealed.

II - 4. Discussion

pH is often cited as a master variable controlling N-cycling (Liu et al., 2010; Morkved et al., 2007; Van Den Heuvel et al., 2011). The results of this experiment corroborate these findings and offer insight into how pH influences both N_2O production and functional gene abundance. Lower experimental pH levels were consistently correlated with higher peak N_2O concentrations for both matrix materials. However, between replicates, there was a high degree of variability. For the microbial populations, *nosZ* was the most sensitive to pH, which is critical because *nos* microbes are the organisms that reduce N_2O from the system. Although the proximal effects of pH on N_2OR (the product of the *nos* genes) are likely to be the principal determinants of N_2O accumulation at low, pH (Bergaust et al., 2010; Richardson et al., 2009), the post-hoc testing indicates that short-term distal control of *nosZ* microorganisms may also play a role in the high pH environments. *nirS*, while not as sensitive to low pH as *nosZ*, was also found in increased numbers at high pH. These results corroborate findings suggesting that denitrifying populations that exist at low pH ranges (> pH 5) emit larger N_2O fluxes than their counterparts (Čuhel and Šimek, 2011; Dannenmann et al., 2008; Šimek and Cooper, 2002). Another important point to consider is that under pH 5.5 the abiotic reduction of NO_2^-, or chemodenitrification, is a mechanism that can contribute to N_2O production (Van Cleemput and Samater, 1995). It is reasonable to assume that some of the N_2O produced in the AC columns could have originated through this mechanism.

The kinetics of N_2O concentration changes that were observed in this study may offer important insights for managers who use DNBRs in the field. The timing of the N_2O concentration changes indicate that the denitrification taking place in reactors similar to our own requires around 32 hours to reach equilibrium.

Field systems should be designed with a hydraulic residence time of at least this duration in order to achieve optimum NO_3^- removal. Additionally, the maintenance of saturated conditions will likely be required in order to maintain minimum N_2O production levels. The fact that reactors often run dry in the absence of rain or irrigation means that a re-wetting period may be associated with a bump in N_2O production for 32 hours. Similar N_2O emissions are known to occur following rain events in soil settings. A final point of concern to managers may be that some form of liming is required inside bioreactors themselves in order to provide conditions that reduce N_2O output.

Data from this experiment supports the previous findings that, under certain conditions, biochar can actually increase N_2O emission (Anderson et al., 2014a; Clough et al., 2010; Obia et al., 2015; Sanchez-Garcia et al., 2014), despite the consensus that biochar usually mitigates its production. The pH in these studies varied, but was all acidic in environments where increases in N_2O were observed (Anderson: 5.1-5.9, Clough: 4.9, Obia: 4.0, Sanchez-Garcia: 5.84-6.35). Indeed, a purported ability to support increased N-cycling microorganism abundance (Clough and Condron, 2010; Lehmann et al., 2011) and activity (Cayuela et al., 2013) does not necessarily equate to decreased N_2O emissions, especially if the local pH is inactivating the reduction of N_2O. If N_2O reducing organisms are abundant, but N_2OR is not active, then N_2O will still accumulate. Or, if NO_2^- reducers are more active than N_2O reducers, N_2O will also accumulate. Without a combined assessment of many possible causes (microbial populations, gene expression, enzyme activity, and extensive environmental chemistry measures), it will be difficult to determine the why most systems containing biochar exhibit decreased N_2O production, but others, like the system examined in this study, actually emit more N_2O.

The results show that while the BC treatments exhibited increased N_2O emissions, the influence of matrix material as a predictor for N_2O production is not as strong as that of pH. Biochar was not associated with statistically significant changes in specific denitrifier abundance, although there may be a weak correlation

with changes in the ratios of certain types of denitrifiers: *nosZ/nirS* and *nosZ/(nirK+nirS)*, a factor which was linked to altered N_2O production in several studies (Cuhel et al., 2010; Liu et al., 2010; Philippot et al., 2009). More likely, however, is that the differences in N_2O concentrations between the matrix materials result from chemical effects on the denitrification process rather than a change in the populations. This does not rule out population changes emerging in the long-term, but indicates that one week is not long enough for treatment effects on the population to occur. Indeed, the studies that noted changes in the microbial populations of biochar-amended environments saw differences emerge gradually over time (Anderson et al., 2011; Harter et al., 2014; Wang et al., 2013). Another, less likely possibility is that reactor design could have facilitated rapid shifts in populations, but that differences would only emerge during the peak periods of gas flux. To address these possible scenarios, future microbial work should attempt to capture samples at a greater number of intervals and over a longer overall time period.

Future studies must also consider the interaction between matrix material and pH, a combination that was shown to have highly significant effects on N_2O production. A promising line of inquiry is to consider how changing pH induces physicochemical changes in biochar, particularly with respect to C and N availability (Clough and Condron, 2010; Clough et al., 2013; Lehmann et al., 2011). These factors directly limit denitrification (and in turn, N_2O production) because organic C functions as the electron donor in denitrification, and N oxides as the electron acceptor (Bothe et al., 2007). Increases in C:N ratio have been linked with decreased N_2O production in denitrification systems (Hunt et al., 2007; Itokawa et al., 2001; Richardson et al., 2009; Sobieszuk and Szewczyk, 2006). Because no significant differences in microbial populations were observed between treatments, differences in N_2O production resulting from biochar amendment must be driven by proximal effects. However, it is unclear if this is the result of chemical (direct N_2O generation, increased nutrient availability, electron shuttling) or microbial (gene expression, protein assembly, enzyme kinetics) mechanisms. Investigation of mechanisms behind this interaction

could potentially allow researchers to mitigate high N_2O production and develop N_2O repressive biochars that are tailored to specific environmental conditions or microbial communities (Ippolito et al., 2012; Sohi et al., 2010).

II - 5. Conclusions

This study shows the importance of pH as a control for N_2O production in both of the matrices examined. N_2O production decreased with increasing pH, but significant differences in its production occurred only in the first 32 hrs for the unbuffered and buffered groups. By contrast, a markedly different N_2O emission pattern emerged by the end of the study in the acidified group, though there was high variability in the early emissions. In all groups, BC emitted more N_2O during the periods of significant difference. *nosZ* gene abundance was most sensitive to changes in pH, and it exhibited significant increases in copy number with rising pH. *nirS* copy number was also sensitive to pH, but significant differences were only found between the buffered and unbuffered comparisons. Despite their sensitivity to pH, BC vs WC individually effected none of the microbial populations, though there were weak correlations to altered population ratios. This suggests that in the time period investigated in this experiment, proximal effects dominate over distal ones in the production of N_2O. When examined together, pH and matrix material were shown have highly significant effects on both N_2O production and the abundance of functional denitrification genes. Elucidating the biochemical mechanisms behind this interaction should be the next step in future research.

While the case remains strong for biochar use as a soil amendment for C sequestration, the findings of this study raise doubt as to its potential as a panacea for offsetting N_2O emissions. Particularly in acidic environments, the use of biochar may result in trading one greenhouse gas for another (CO_2 for N_2O), a finding which is echoed by Clough et al. (2010), Obia et al. (2015), and Sanchez-Garcia et al. (2014).

Furthermore, because pH is a factor so frequently adjusted by agricultural management practices, we believe it is critical to continue to investigate how changes in pH might result in increased N_2O flux for biochar amended environments. Because both pH and biochar effects depend on underlying environmental chemistry, it is challenging to generalize conclusions about its influence across different environments. Future studies must attempt to reduce the number of confounding variables while exploring a wide enough range of potential outcomes to encompass relevant field-use scenarios. Developing a complete understanding of these interaction will require many complex experiments involving tracer studies, long-term profiling of the microbial community, enzyme assays, and correlation with both hydrological and meteorological data, but the results could mean the difference between developing a powerful tool to fight climate change and actually making the problem worse.

II - Acknowledgements

This work was supported by a grant from the Institute of Critical Science and Technology at Virginia Tech and the United States Department of Agriculture – Natural Resources Conservation Service.

References

Adair, C. E., P. B. Reich, J. J. Trost, and S. E. Hobbie. 2011. Elevated CO2 stimulates grassland soil respiration by increasing carbon inputs rather than by enhancing soil moisture. *Global Change Biology* 17(12):3546-3563.

Ahn, Y. H. 2006. Sustainable nitrogen elimination biotechnologies: A review. *Process Biochemistry* 41(8):1709-1721.

Akratos, C. S., and V. A. Tsihrintzis. 2007. Effect of temperature, HRT, vegetation and porous media on removal efficiency of pilot-scale horizontal subsurface flow constructed wetlands. *Ecological Engineering* 29(2):173-191.

Allen, J. F., and W. Martin. 2007. Evolutionary biology: out of thin air. *Nature* 445(7128):610-612.

Amonette, J. E., F. A. Street-Perrott, J. Lehmann, S. D. Joseph, and D. Woolf. 2010. Sustainable biochar to mitigate global climate change. *Nature Communications* 1(5):1-9.

Anbar, A. D. 2008. Oceans. Elements and evolution. *Science* 322(5907):1481-1483.

Anderson, C. R., L. M. Condron, T. J. Clough, M. Fiers, A. Stewart, R. A. Hill, and R. R. Sherlock. 2011. Biochar induced soil microbial community change: Implications for biogeochemical cycling of carbon, nitrogen and phosphorus. *Pedobiologia* 54(5-6):309-320.

Anderson, C. R., K. Hamonts, T. J. Clough, and L. M. Condron. 2014a. Biochar does not affect soil N-transformations or microbial community structure under ruminant urine patches but does alter relative proportions of nitrogen cycling bacteria. *Agriculture Ecosystems & Environment* 191:63-72.

Anderson, T. R., C. L. Goodale, P. M. Groffman, and M. T. Walter. 2014b. Assessing denitrification from seasonally saturated soils in an agricultural landscape: A farm-scale mass-balance approach. *Agriculture Ecosystems & Environment* 189:60-69.

Andrews, M., D. Scholefield, M. T. Abberton, B. A. McKenzie, S. Hodge, and J. A. Raven. 2007. Use of white clover as an alternative to nitrogen fertiliser for dairy pastures in nitrate vulnerable zones in the UK: productivity, environmental impact and economic considerations. *Ann Appl Biol* 151(1):11-23.

Auguie, B. 2015. *gridExtra: Miscellaneous Functions for "Grid" Graphics.*

Averill, B. A., and J. M. Tiedje. 1982. The chemical mechanism of microbioal denitrification. *FEBS letters* 138(1):8-12.

Baggs, E. M., M. Richter, G. Cadisch, and U. A. Hartwig. 2003. Denitrification in grass swards is increased under elevated atmospheric CO2. *Soil Biology & Biochemistry* 35(5):729-732.

Baggs, E. M., C. L. Smales, and E. J. Bateman. 2010. Changing pH shifts the microbial sourceas well as the magnitude of N2O emission from soil. *Biology and Fertility of Soils* 46(8):793-805.

Bailey, L. D., and E. G. Beauchamp. 1973. Effects of Temperature on NO3− and NO2− Reduction, Nitrogenous Gas Production, and Redox Potential in a Saturated Soil. *Can J Soil Sci* 53(2):213-218.

Ballinger, S. J., I. M. Head, T. P. Curtis, and A. R. Godley. 2002. The effect of C/N ratio on ammonia oxidising bacteria community structure in a laboratory nitrification-denitrification reactor. *Water Sci Technol* 46(1-2):543-550.

Barnard, R., L. Barthes, X. Le Roux, and P. W. Leadley. 2004. Dynamics of nitrifying activities, denitrifying activities and nitrogen in grassland mesocosms as altered by elevated CO2. *New Phytologist* 162(2):365-376.

Barnard, R., P. W. Leadley, and B. A. Hungate. 2005. Global change, nitrification, and denitrification: A review. *Global Biogeochemical Cycles* 19(1):GB1007.

Bergaust, L., Y. Mao, L. R. Bakken, and A. Frostegard. 2010. Denitrification response patterns during the transition to anoxic respiration and posttranscriptional effects of suboptimal pH on nitrous oxide reductase in Paracoccus denitrificans. *Appl Environ Microbiol* 76(19):6387-6396.

Bergsma, T. T., G. P. Robertson, and N. E. Ostrom. 2002. Influence of soil moisture and land use history on denitrification end-products. *J Environ Qual* 31(3):711-717.

Berks, B. C., S. J. Ferguson, J. W. B. Moir, and D. J. Richardson. 1995. Enzymes and associated electron transport systems that catalyse the respiratory reduction of nitrogen oxides and oxyanions. *Biochimica Et Biophysica Acta-Bioenergetics* 1232(3):97-173.

Betlach, M. R., and J. M. Tiedje. 1981. Kinetic explanation for accumulation of nitrite, nitric oxide, and nitrous oxide during bacterial denitrification. *Appl Environ Microbiol* 42(6):1074-1084.

Billen, G., J. Garnier, and L. Lassaletta. 2013. The nitrogen cascade from agricultural soils to the sea: modelling nitrogen transfers at regional watershed and global scales. *Philos Trans R Soc Lond B Biol Sci* 368(1621):20130123.

Blackmer, A. M., and J. M. Bremner. 1978. Inhibitory Effect of Nitrate on Reduction of N2O to N2 by Soil-Microorganisms. *Soil Biology & Biochemistry* 10(3):187-191.

Blackmer, A. M., J. M. Bremner, and E. L. Schmidt. 1980. Production of Nitrous Oxide by Ammonia-Oxidizing Chemoautotrophic Microorganisms in Soil. *Appl Environ Microbiol* 40(6):1060-1066.

Blagodatsky, S., and P. Smith. 2012. Soil physics meets soil biology: Towards better mechanistic prediction of greenhouse gas emissions from soil. *Soil Biology & Biochemistry* 47:78-92.

Blowes, D. W., W. D. Robertson, C. J. Ptacek, and C. Merkley. 1994. Removal of Agricultural Nitrate from Tile-Drainage Effluent Water Using in-Line Bioreactors. *Journal of Contaminant Hydrology* 15(3):207-221.

Bock, E., M. Davis, B. Coleman, and Z. M. Easton. Unpublished Work. 2015a.

Bock, E., P. Macek, and Z. M. Easton. Unpublished Work. 2015b.

Bock, E., N. Smith, M. Rogers, B. Coleman, M. Reiter, B. Benham, and Z. M. Easton. 2015c. Enhanced Nitrate and Phosphate Removal in a Denitrifying Bioreactor with Biochar. *J Environ Qual* 44(2):605-613.

Bock, E. M., B. Coleman, and Z. M. Easton. 2015d. Effect of Biochar on Nitrate Removal in a Pilot-Scale Denitrifying Bioreactor. *J Environ Qual*.

Bolan, N. S., D. C. Adriano, and D. Curtin. 2003. Soil acidification and liming interactions with nutrient and heavy metal transformation and bioavailability. 215-272. San Diego: Academic Press Inc.

Bonnett, S. A., M. S. Blackwell, R. Leah, V. Cook, M. O'Connor, and E. Maltby. 2013. Temperature response of denitrification rate and greenhouse gas production in agricultural river marginal wetland soils. *Geobiology* 11(3):252-267.

Bothe, H., S. J. Ferguson, and W. E. Newton. 2007. *Biology of the nitrogen cycle*. No. Book, Whole. Elsevier, Amsterdam; Oxford.

Bothe, H., G. Jost, M. Schloter, B. B. Ward, and K. Witzel. 2000. Molecular analysis of ammonia oxidation and denitrification in natural environments. *FEMS Microbiol Rev* 24(5):673-690.

Bowles, T. M., V. Acosta-Martinez, F. Calderon, and L. E. Jackson. 2014. Soil enzyme activities, microbial communities, and carbon and nitrogen availability in organic agroecosystems across an intensively-managed agricultural landscape. *Soil Biology & Biochemistry* 68:252-262.

Braker, G., J. Schwarz, and R. Conrad. 2010. Influence of temperature on the composition and activity of denitrifying soil communities. *FEMS Microbiol Ecol* 73(1):134-148.

Brentrup, F., J. Küsters, J. Lammel, P. Barraclough, and H. Kuhlmann. 2004. Environmental impact assessment of agricultural production systems using the life cycle assessment (LCA) methodology II. The application to N fertilizer use in winter wheat production systems. *European Journal of Agronomy* 20(3):265-279.

Bruun, E. W., D. Muller-Stover, P. Ambus, and H. Hauggaard-Nielsen. 2011. Application of biochar to soil and N2O emissions: potential effects of blending fast-pyrolysis biochar with anaerobically digested slurry. *European Journal of Soil Science* 62(4):581-589.

Burford, J. R., and J. M. Bremner. 1975. Relationships between the denitrification capacities of soils and total, water-soluble and readily decomposable soil organic matter. *Soil Biology & Biochemistry* 7(6):389-394.

Burgin, A., J. G. Lazar, P. M. Groffman, A. J. Gold, and D. Q. Kellogg. 2013. Balancing nitrogen retention ecosystem services and greenhouse gas disservices at the landscape scale. *Ecological Engineering* 56:26-35.

Burgin, A. J., and S. K. Hamilton. 2007. Have we overemphasized the role of denitrification in aquatic ecosystems? A review of nitrate removal pathways. *Frontiers in Ecology and the Environment* 5(2):89-96.

Burgin, A. J., and S. K. Hamilton. 2008. NO3 −-Driven SO4 2− Production in Freshwater Ecosystems: Implications for N and S Cycling. *Ecosystems* 11:908-922.

Burkholder, J. 2007. *Impacts of Waste from Concentrated Animal Feeding Operations on Water Quality*. Environmental health perspectives No. 2. National Institute of Environmental Health Sciences. National Institutes of Health. Department of Health, Education and Welfare, Res Triangle Pk.

Butterbach-Bahl, K., E. M. Baggs, M. Dannenmann, R. Kiese, and S. Zechmeister-Boltenstern. 2013. Nitrous oxide emissions from soils: how well do we understand the processes and their controls? *Philos Trans R Soc Lond B Biol Sci* 368(1621):20130122.

Butterbach-Bahl, K., and M. Dannenmann. 2011. Denitrification and associated soil N2O emissions due to agricultural activities in a changing climate. *Current Opinion in Environmental Sustainability* 3(5):389-395.

Cameron, S. G., and L. A. Schipper. 2010. Nitrate removal and hydraulic performance of organic carbon for use in denitrification beds. *Ecological Engineering* 36(11):1588-1595.

Canfield, D. E., A. N. Glazer, and P. G. Falkowski. 2010. The evolution and future of Earth's nitrogen cycle. *Science* 330(6001):192-196.

Cayuela, M. L., M. A. Sanchez-Monedero, A. Roig, K. Hanley, A. Enders, and J. Lehmann. 2013. Biochar and denitrification in soils: when, how much and why does biochar reduce N(2)O emissions? *Sci Rep* 3:1732.

Chen, C., N. Ren, A. Wang, L. Liu, and D. J. Lee. 2010. Functional consortium for denitrifying sulfide removal process. *Appl Microbiol Biotechnol* 86(1):353-358.

Cheng, Y., Z. C. Cai, S. X. Chang, J. Wang, and J. B. Zhang. 2012. Wheat straw and its biochar have contrasting effects on inorganic N retention and N2O production in a cultivated Black Chernozem. *Biology and Fertility of Soils* 48(8):941-946.

Christensen, S., S. Simkins, and J. M. Tiedje. 1990. Spatial Variation in Denitrification - Dependency of Activity Centers on the Soil Environment. *Soil Science Society of America Journal* 54(6):1608-1613.

Christianson, L., M. Hedley, M. Camps, H. Free, and S. Saggar. 2011. Influence of Biochar Amendments on Denitrification Bioreactor Performance.

Clough, T. J., J. E. Bertram, J. L. Ray, L. M. Condron, M. O'Callaghan, R. R. Sherlock, and N. S. Wells. 2010. Unweathered Wood Biochar Impact on Nitrous Oxide Emissions from a Bovine-Urine-Amended Pasture Soil. *Soil Science Society of America Journal* 74(3):852-860.

Clough, T. J., and L. M. Condron. 2010. Biochar and the nitrogen cycle: introduction. *J Environ Qual* 39(4):1218-1223.

Clough, T. J., L. M. Condron, C. Kammann, and C. Müller. 2013. A Review of Biochar and Soil Nitrogen Dynamics. *Agronomy* 3(Generic):275-293.

Crutzen, P. J. 2002a. The "anthropocene". *J Phys IV France* 12(10):1-5.

Crutzen, P. J. 2002b. Geology of mankind. *Nature* 415(6867):23-23.

Cuhel, J., and M. Simek. 2011a. Effect of pH on the denitrifying enzyme activity in pasture soils in relation to the intrinsic differences in denitrifier communities. *Folia Microbiol* 56(3):230-235.

Cuhel, J., and M. Simek. 2011b. Proximal and distal control by pH of denitrification rate in a pasture soil. *Agriculture, Ecosystems & Environment* 141(1-2):230-233.

Cuhel, J., M. Simek, R. J. Laughlin, D. Bru, D. Cheneby, C. J. Watson, and L. Philippot. 2010. Insights into the effect of soil pH on N(2)O and N(2) emissions and denitrifier community size and activity. *Appl Environ Microbiol* 76(6):1870-1878.

Daims, H., M. W. Taylor, and M. Wagner. 2006. Wastewater treatment: a model system for microbial ecology. *Trends Biotechnol* 24(11):483-489.

Dalahmeh, S. S., M. Pell, B. Vinneras, L. D. Hylander, I. Oborn, and H. Jonsson. 2012. Efficiency of Bark, Activated Charcoal, Foam and Sand Filters in Reducing Pollutants from Greywater. *Water Air Soil Pollut* 223(7):3657-3671.

Dannenmann, M., K. Butterbach-Bahl, R. Gasche, G. Willibald, and H. Papen. 2008. Dinitrogen emissions and the N2:N2O emission ratio of a Rendzic Leptosol as influenced by pH and forest thinning. *Soil Biology & Biochemistry* 40(9):2317-2323.

Das, S., P. Bhattacharyya, and T. K. Adhya. 2011. Interaction effects of elevated CO(2) and temperature on microbial biomass and enzyme activities in tropical rice soils. *Environ Monit Assess* 182(1-4):555-569.

De Haan, C., H. Steinfeld, H. Blackburn, and U. Europea. 1997. *Livestock & the environment: Finding a balance*. European Commission Directorate-General for Development, Development Policy Sustainable Development and Natural Resources Rome,, Italy.

Dinnes, D. L., D. L. Karlen, D. B. Jaynes, T. C. Kaspar, J. L. Hatfield, T. S. Colvin, and C. A. Cambardella. 2002. Review and Interpretation: Nitrogen Management Strategies to Reduce Nitrate Leaching in Tile-Drained Midwestern Soils. *Agronomy Journal* 94(1):153-171.

Dodds, W. K., W. H. Clements, K. Gido, R. H. Hilderbrand, and R. S. King. 2010. Thresholds, breakpoints, and nonlinearity in freshwaters as related to management. *Journal of the North American Benthological Society* 29(3):988-997.

Driscoll, C. T., D. Whitall, J. Aber, E. Boyer, M. Castro, C. Cronan, C. L. Goodale, P. Groffman, C. Hopkinson, K. Lambert, G. Lawrence, and S. Ollinger. 2003. Nitrogen pollution in the northeastern United States: Sources, effects, and management options. *Bioscience* 53(4):357-374.

Ducey, T. F., J. A. Ippolito, K. B. Cantrell, J. M. Novak, and R. D. Lentz. 2013. Addition of activated switchgrass biochar to an aridic subsoil increases microbial nitrogen cycling gene abundances. *Applied Soil Ecology* 65:65-72.

Dungait, J. A., L. M. Cardenas, M. S. Blackwell, L. Wu, P. J. Withers, D. R. Chadwick, R. Bol, P. J. Murray, A. J. Macdonald, A. P. Whitmore, and K. W. Goulding. 2012. Advances in the understanding of nutrient dynamics and management in UK agriculture. *Sci Total Environ* 434:39-50.

Easton, Z. M., M. Rogers, M. Davis, J. Wade, M. Eick, and E. Bock. 2015. Mitigation of sulfate reduction and nitrous oxide emission in denitrifying environments with amorphous iron oxide and biochar. *Ecological Engineering* 82:605-613.

Eickhout, B., A. F. Bouwman, and H. van Zeijts. 2006. The role of nitrogen in world food production and environmental sustainability. *Agriculture Ecosystems & Environment* 116(1-2):4-14.

Elgood, Z., W. D. Robertson, S. L. Schiff, and R. Elgood. 2010. Nitrate removal and greenhouse gas production in a stream-bed denitrifying bioreactor. *Ecological Engineering* 36(11):1575-1580.

Erisman, J. W. 2004. The Nanjing declaration on management of reactive nitrogen. *Bioscience* 54(4):286-287.

Erler, D. V., B. D. Eyre, and L. Davison. 2008. The contribution of anammox and denitrification to sediment N2 production in a surface flow constructed wetland. *Environ Sci Technol* 42(24):9144-9150.

Faulkner, J. W., Z. M. Easton, W. Zhang, L. D. Geohring, and T. S. Steenhuis. 2010. Design and risk assessment tool for vegetative treatment areas receiving agricultural wastewater: preliminary results. *J Environ Manage* 91(8):1794-1801.

Firestone, M. K., R. B. Firestone, and J. M. Tiedje. 1980. Nitrous oxide from soil denitrification: factors controlling its biological production. *Science* 208(4445):749-751.

Freeman, C., S. Y. Kim, S. H. Lee, and H. Kang. 2004. Effects of elevated atmospheric CO2 concentrations on soil microorganisms. *J Microbiol* 42(4):267-277.

French, S., D. Levy-Booth, A. Samarajeewa, K. E. Shannon, J. Smith, and J. T. Trevors. 2009. Elevated temperatures and carbon dioxide concentrations: effects on selected microbial activities in temperate agricultural soils. *World J Microbiol Biotechnol* 25(11):1887-1900.

Galloway, J. N., J. D. Aber, J. W. Erisman, S. P. Seitzinger, R. W. Howarth, E. B. Cowling, and B. J. Cosby. 2003. The Nitrogen Cascade. *Bioscience* 53(4):341.

Gentile, M. E., J. L. Nyman, and C. S. Criddle. 2007. Correlation of patterns of denitrification instability in replicated bioreactor communities with shifts in the relative abundance and the denitrification patterns of specific populations. *ISME J* 1(8):714-728.

Gomez-Silvan, C., R. Vilchez-Vargas, J. Arevalo, M. A. Gomez, J. Gonzalez-Lopez, D. H. Pieper, and B. Rodelas. 2014. Quantitative response of nitrifying and denitrifying communities to environmental variables in a full-scale membrane bioreactor. *Bioresour Technol* 169:126-133.

Granger, J., and B. B. Ward. 2003. Accumulation of nitrogen oxides in copper-limited cultures of denitrifying bacteria. *Limnology and Oceanography* 48(1):313-318.

Greenan, C. M., T. B. Moorman, T. C. Kaspar, T. B. Parkin, and D. B. Jaynes. 2006. Comparing carbon substrates for denitrification of subsurface drainage water. *J Environ Qual* 35(3):824-829.

Groffman, P. M. 2012. Terrestrial denitrification: challenges and opportunities. *Ecological Processes* 1(1):11.

Groffman, P. M., K. Butterbach-Bahl, R. W. Fulweiler, A. J. Gold, J. L. Morse, E. K. Stander, C. Tague, C. Tonitto, and P. Vidon. 2009a. Challenges to incorporating spatially and temporally explicit phenomena (hotspots and hot moments) in denitrification models. *Biogeochemistry* 93(1-2):49-77.

Groffman, P. M., E. A. Davidson, and S. Seitzinger. 2009b. New approaches to modeling denitrification. *Biogeochemistry* 93:1-5.

Groffman, P. M., and J. M. Tiedje. 1989. Denitrification in North Temperate Forest Soils - Relationships between Denitrification and Environmental-Factors at the Landscape Scale. *Soil Biology & Biochemistry* 21(5):621-626.

Groffman, P. M., and J. M. Tiedje. 1991. Relationships between Denitrification, CO2 Production and Air-Filled Porosity in Soils of Different Texture and Drainage. *Soil Biology & Biochemistry* 23(3):299-302.

Groffman, P. M., J. M. Tiedje, and S. Christensen. 1988. Denitrification at different temporal and geographical scales: proximal and distal controls. In *Advances in Nitrogen Cycling in Agricultural Systems*, 174-192. J. R. Wilson, ed. Wallingford, U. K.: CAB International.

Grosjean, P., and F. Ibanez. 2014. *pastecs: Package for Analysis of Space-Time Ecological Series.*

Hai, B., N. H. Diallo, S. Sall, F. Haesler, K. Schauss, M. Bonzi, K. Assigbetse, J. L. Chotte, J. C. Munch, and M. Schloter. 2009. Quantification of key genes steering the microbial nitrogen cycle in the rhizosphere of sorghum cultivars in tropical agroecosystems. *Appl Environ Microbiol* 75(15):4993-5000.

Hallin, S., and P. E. Lindgren. 1999. PCR detection of genes encoding nitrite reductase in denitrifying bacteria. *Appl Environ Microbiol* 65(4):1652-1657.

Hamdi, W., F. Gamaoun, D. E. Pelster, and M. Seffen. 2013. Nitrate Sorption in an Agricultural Soil Profile. *Appl Environ Microbiol* 2013:1-7.

Han, J. G., L. S. Dou, Y. L. Zhu, and P. P. Li. 2014. Estimates of potential nitrate reductase activity in sediments: comparisons of two incubation methods and four inhibitors. *Environmental Earth Sciences* 71(1):419-425.

Harter, J., H. M. Krause, S. Schuettler, R. Ruser, M. Fromme, T. Scholten, A. Kappler, and S. Behrens. 2014. Linking N2O emissions from biochar-amended soil to the structure and function of the N-cycling microbial community. *ISME J* 8(3):660-674.

Hayden, H. L., J. Drake, M. Imhof, A. P. A. Oxley, S. Norng, and P. M. Mele. 2010. The abundance of nitrogen cycle genes amoA and nifH depends on land-uses and soil types in South-Eastern Australia. *Soil Biology & Biochemistry* 42(10):1774-1783.

Hayhoe, K., C. Wake, B. Anderson, X. Z. Liang, E. Maurer, J. H. Zhu, J. Bradbury, A. DeGaetano, A. M. Stoner, and D. Wuebbles. 2008. Regional climate change projections for the Northeast USA. *Mitig Adapt Strat Glob Change* 13(5-6):425-436.

Henry, S., D. Bru, B. Stres, S. Hallet, and L. Philippot. 2006. Quantitative detection of the nosZ gene, encoding nitrous oxide reductase, and comparison of the abundances of 16S rRNA, narG, nirK, and nosZ genes in soils. *Appl Environ Microbiol* 72(8):5181-5189.

Her, J. J., and J. S. Huang. 1995. Influences of carbon source and C/N ratio on nitrate/nitrite denitrification and carbon breakthrough. *Bioresour Technol* 54(1):45-51.

Hochstein, L. I., and G. A. Tomlinson. 1988. The enzymes associated with denitrification. *Annu Rev Microbiol* 42:231-261.

Hoeft, R. G. 2004. Environmental and Agronomic Fate of Fertilizer Nitrogen. In *Environmental Impact of Fertilizer on Soil and Water*, 235-243. Washington: Amer Chemical Soc.

Holtan-Hartwig, L., P. Dorsch, and L. R. Bakken. 2002. Low temperature control of soil denitrifying communities: kinetics of N2O production and reduction. *Soil Biology & Biochemistry* 34(11):1797-1806.

Hu, J., D. Li, Q. Liu, Y. Tao, X. He, X. Wang, X. Li, and P. Gao. 2009. Effect of organic carbon on nitrification efficiency and community composition of nitrifying biofilms. *J Environ Sci (China)* 21(3):387-394.

Huang, G. X., H. Fallowfield, H. D. Guan, and F. Liu. 2012. Remediation of Nitrate-Nitrogen Contaminated Groundwater by a Heterotrophic-Autotrophic Denitrification Approach in an Aerobic Environment. *Water Air Soil Pollut* 223(7):4029-4038.

Hunt, P. G., T. A. Matheny, and K. S. Ro. 2007. Nitrous oxide accumulation in soils from riparian buffers of a coastal plain watershed carbon/nitrogen ratio control. *J Environ Qual* 36(5):1368-1376.

Ippolito, J. A., D. A. Laird, and W. J. Busscher. 2012. Environmental benefits of biochar. *J Environ Qual* 41(4):967-972.

Ippolito, J. A., M. E. Stromberger, R. D. Lentz, and R. S. Dungan. 2014. Hardwood biochar influences calcareous soil physicochemical and microbiological status. *J Environ Qual* 43(2):681-689.

Itokawa, H., K. Hanaki, and T. Matsuo. 2001. Nitrous oxide production in high-loading biological nitrogen removal process under low COD/N ratio condition. *Water Res* 35(3):657-664.

Jahangir, M. M. R., P. Johnston, M. I. Khalil, D. Hennessy, J. Humphreys, O. Fenton, and K. G. Richards. 2012. Groundwater: A pathway for terrestrial C and N losses and indirect greenhouse gas emissions. *Agriculture Ecosystems & Environment* 159:40-48.

Jellali, S., E. Diamantopoulos, H. Kallali, S. Bennaceur, M. Anane, and N. Jedidi. 2010. Dynamic sorption of ammonium by sandy soil in fixed bed columns: Evaluation of equilibrium and non-equilibrium transport processes. *J Environ Manage* 91(4):897-905.

Jetten, M. S. M., M. Wagner, J. Fuerst, M. van Loosdrecht, G. Kuenen, and M. Strous. 2001. Microbiology and application of the anaerobic ammonium oxidation ('anammox') process. *Current Opinion in Biotechnology* 12(3):283-288.

Kammann, C., C. Muller, L. Grunhage, and H. J. Jager. 2008. Elevated CO2 stimulates N2O emissions in permanent grassland. *Soil Biology & Biochemistry* 40(9):2194-2205.

Kampschreur, M. J., H. Temmink, R. Kleerebezem, M. S. Jetten, and M. C. van Loosdrecht. 2009. Nitrous oxide emission during wastewater treatment. *Water Res* 43(17):4093-4103.

Kaspar, H. F., J. M. Tiedje, and R. B. Firestone. 1981. Denitrification and dissimilatory nitrate reduction to ammonium in digested sludge. *Can J Microbiol* 27(9):878-885.

Khalil, K., B. Mary, and P. Renault. 2004. Nitrous oxide production by nitrification and denitrification in soil aggregates as affected by O2 concentration. *Soil Biology & Biochemistry* 36(4):687-699.

Kloss, S., F. Zehetner, A. Dellantonio, R. Hamid, F. Ottner, V. Liedtke, M. Schwanninger, M. H. Gerzabek, and G. Soja. 2012. Characterization of slow pyrolysis biochars: effects of feedstocks and pyrolysis temperature on biochar properties. *J Environ Qual* 41(4):990-1000.

Kool, D. M., J. Dolfing, N. Wrage, and J. W. Van Groenigen. 2011. Nitrifier denitrification as a distinct and significant source of nitrous oxide from soil. *Soil Biology & Biochemistry* 43(1):174-178.

Kool, D. M., N. Wrage, S. Zechmeister-Boltenstern, M. Pfeffer, D. Brus, O. Oenema, and J. W. Van Groenigen. 2010. Nitrifier denitrification can be a source of N2O from soil: a revised approach to the dual-isotope labelling method. *European Journal of Soil Science* 61(5):759-772.

Kuenen, J. G. 2008. Anammox bacteria: from discovery to application. *Nat Rev Microbiol* 6(4):320-326.

Kumar, M., and J. G. Lin. 2010. Co-existence of anammox and denitrification for simultaneous nitrogen and carbon removal--Strategies and issues. *J Hazard Mater* 178(1-3):1-9.

Lawrence, M. A. 2013. *ez: Easy analysis and visualization of factorial experiments.*

Lee, D. J., and B. T. Wong. 2014. Denitrifying sulfide removal by enriched microbial consortium: kinetic diagram. *Bioresour Technol* 164:386-393.

Lehmann, J. 2007. Bio-Energy in the Black. *Frontiers in Ecology and the Environment* 5(7):381-387.

Lehmann, J., M. C. Rillig, J. Thies, C. A. Masiello, W. C. Hockaday, and D. Crowley. 2011. Biochar effects on soil biota – A review. *Soil Biology & Biochemistry* 43(9):1812-1836.

Leite, D. C., F. C. Balieiro, C. A. Pires, B. E. Madari, A. S. Rosado, H. L. Coutinho, and R. S. Peixoto. 2014. Comparison of DNA extraction protocols for microbial communities from soil treated with biochar. *Braz J Microbiol* 45(1):175-183.

Lettenmaier, D. P., A. W. Wood, R. N. Palmer, E. F. Wood, and E. Z. Stakhiv. 1999. Water Resources Implications of Global Warming: A U.S. Regional Perspective. *Climatic Change* 43(3):537-579.

Levy-Booth, D. J., C. E. Prescott, and S. J. Grayston. 2014. Microbial functional genes involved in nitrogen fixation, nitrification and denitrification in forest ecosystems. *Soil Biology & Biochemistry* 75:11-25.

Li, D., C. J. Watson, M. J. Yan, S. Lalor, R. Rafique, B. Hyde, G. Lanigan, K. G. Richards, N. M. Holden, and J. Humphreys. 2013. A review of nitrous oxide mitigation by farm nitrogen management in temperate grassland-based agriculture. *J Environ Manage* 128:893-903.

Li, M., Y. Hong, M. G. Klotz, and J. D. Gu. 2010. A comparison of primer sets for detecting 16S rRNA and hydrazine oxidoreductase genes of anaerobic ammonium-oxidizing bacteria in marine sediments. *Appl Microbiol Biotechnol* 86(2):781-790.

Liang, Y., X. Cao, L. Zhao, and E. Arellano. 2014. Biochar- and phosphate-induced immobilization of heavy metals in contaminated soil and water: implication on simultaneous remediation of contaminated soil and groundwater. *Environ Sci Pollut Res Int* 21(6):4665-4674.

Limousin, G., J. P. Gaudet, L. Charlet, S. Szenknect, V. Barthès, and M. Krimissa. 2007. Sorption isotherms: A review on physical bases, modeling and measurement. *Applied Geochemistry* 22(2):249-275.

Liu, B. B., P. T. Morkved, A. Frostegard, and L. R. Bakken. 2010. Denitrification gene pools, transcription and kinetics of NO, N2O and N2 production as affected by soil pH. *FEMS Microbiol Ecol* 72:407-417.

Lloyd, D., L. Boddy, and K. J. P. Davies. 1987. Persistence of Bacterial Denitrification Capacity under Aerobic Conditions - the Rule Rather Than the Exception. *FEMS Microbiol Ecol* 45(3):185-190.

Loader, C. 2013. *locfit: Local Regression, Likelihood and Density Estimation.*

Maag, M., and F. P. Vinther. 1996. Nitrous oxide emission by nitrification and denitrification in different soil types and at different soil moisture contents and temperatures. *Applied Soil Ecology* 4(1):5-14.

Makris, K. C., D. Sarkar, S. S. Andra, S. B. Bach, and R. Datta. 2009. Do lagoons near concentrated animal feeding operations promote nitrous oxide supersaturation? *Environ Pollut* 157(6):1957-1960.

Matschonat, G., and E. Matzner. 1995. Quantification of ammonium sorption in acid forest soils by sorption isotherms. *Plant and Soil* 168/169(1):95-101.

Mayer, Z. A., Y. Eltom, D. Stennett, E. Schröder, A. Apfelbacher, and A. Hornung. 2014. Characterization of engineered biochar for soil management. *Environmental Progress & Sustainable Energy* 33(2):490-496.

McClain, M. E., E. W. Boyer, C. L. Dent, S. E. Gergel, N. B. Grimm, P. M. Groffman, S. C. Hart, J. W. Harvey, C. A. Johnston, E. Mayorga, W. H. McDowell, and G. Pinay. 2003. Biogeochemical Hot Spots and Hot Moments at the Interface of Terrestrial and Aquatic Ecosystems. *Ecosystems* 6(4):301-312.

McDonald, J. H. 2014. *Handbook of Biological Statistics*. 3rd Edition ed. Sparky House Publishing, Baltimore, MD.

McGechan, M. B., and C. F. E. Topp. 2004. Modelling environmental impacts of deposition of excreted nitrogen by grazing dairy cows. *Agriculture, Ecosystems & Environment* 103(1):149-164.

McKenney, D. J., C. F. Drury, and S. W. Wang. 2001. Effects of Oxygen on Denitrification Inhibition, Repression, and Derepression in Soil Columns. *Soil Science Society of America Journal* 65(1):126.

Metz, B., G. Intergovernmental Panel on Climate Change. Working, III, and C. Intergovernmental Panel on Climate. 2007. *Climate change 2007: mitigation of climate change : contribution of Working Group III to the Fourth Assessment Report of the Intergovernmental Panel on Climate Change*. No. Book, Whole. Cambridge University Press, Cambridge;New York;.

Mohan, S. B., M. Schmid, M. Jetten, and J. Cole. 2004. Detection and widespread distribution of the nrfA gene encoding nitrite reduction to ammonia, a short circuit in the biological nitrogen cycle that competes with denitrification. *FEMS Microbiol Ecol* 49(3):433-443.

Moir, J. W. B. 2011. *Nitrogen cycling in bacteria: molecular analysis*. No. Book, Whole. Caister Academic Press, Norfolk, UK.

Moorman, T. B., T. B. Parkin, T. C. Kaspar, and D. B. Jaynes. 2010. Denitrification activity, wood loss, and N2O emissions over 9 years from a wood chip bioreactor. *Ecological Engineering* 36(11):1567-1574.

Morkved, P. T., P. Dorsch, and L. R. Bakken. 2007. The N2O product ratio of nitrification and its dependence on long-term changes in soil pH. *Soil Biology & Biochemistry* 39(8):2048-2057.

Muller, C., T. Rutting, M. K. Abbasi, R. J. Laughlin, C. Kammann, T. J. Clough, R. R. Sherlock, J. Kattge, H. J. Jager, C. J. Watson, and R. J. Stevens. 2009. Effect of elevated CO2 on soil N dynamics in a temperate grassland soil. *Soil Biology & Biochemistry* 41(9):1996-2001.

Munoz-Leoz, B., I. Antiguedad, C. Garbisu, and E. Ruiz-Romera. 2011. Nitrogen transformations and greenhouse gas emissions from a riparian wetland soil: an undisturbed soil column study. *Sci Total Environ* 409(4):763-770.

Myrold, D. D., and J. M. Tiedje. 1985. Establishment of denitrification capacity in soil: Effects of carbon, nitrate and moisture. *Soil Biology & Biochemistry* 17(6):819-822.

Najjar, R. G., C. R. Pyke, M. B. Adams, D. Breitburg, C. Hershner, M. Kemp, R. W. Howarth, M. R. Mulholland, M. Paolisso, D. Secor, K. Sellner, D. Wardrop, and R. Wood. 2010. Potential climate-change impacts on the Chesapeake Bay. *Estuarine, Coastal and Shelf Science* 86(1):1-20.

Nangia, V., M. D. Sunohara, E. Topp, E. G. Gregorich, C. F. Drury, N. Gottschall, and D. R. Lapen. 2013. Measuring and modeling the effects of drainage water management on soil greenhouse gas fluxes from corn and soybean fields. *J Environ Manage* 129:652-664.

Neff, R., H. J. Chang, C. G. Knight, R. G. Najjar, B. Yarnal, and H. A. Walker. 2000. Impact of climate variation and change on Mid-Atlantic Region hydrology and water resources. *Climate Research* 14(3):207-218.

Nogueira, R., L. s. F. Melo, U. Purkhold, S. Wuertz, and M. Wagner. 2002. Nitrifying and heterotrophic population dynamics in biofilm reactors: effects of hydraulic retention time and the presence of organic carbon. *Water Res* 36(2):469-481.

Norton, J. M., and J. M. Stark. 2011. Chapter 15 - Regulation and Measurement of Nitrification in Terrestrial Systems. In *Methods in Enzymology*, 343-368. G. K. Martin, ed: Academic Press.

Obia, A., G. Cornelissen, J. Mulder, and P. Dorsch. 2015. Effect of Soil pH Increase by Biochar on NO, N2O and N2 Production during Denitrification in Acid Soils. *PLoS One* 10(9):e0138781.

Omonode, R. A., D. R. Smith, A. Gal, and T. J. Vyn. 2011. Soil Nitrous Oxide Emissions in Corn following Three Decades of Tillage and Rotation Treatments. *Soil Science Society of America Journal* 75(1):152-163.

Parkin, T. B. 1987. Soil Microsites as a Source of Denitrification Variability. *Soil Science Society of America Journal* 51(5):1194-1199.

Parkin, T. B. 1993. Spatial Variability of Microbial Processes in Soil—A Review. *J Environ Qual* 22:409-417.

Partheeban, C., J. Kjaersgaard, C. Hay, and T. Trooien. 2014. A Review of the factors controlling the performance of denitrifying woodchip bioreactors ASABE.

Pennock, D. J., C. Vankessel, R. E. Farrell, and R. A. Sutherland. 1992. Landscape-Scale Variations in Denitrification. *Soil Science Society of America Journal* 56(3):770-776.

Pett-Ridge, J., W. L. Silver, and M. K. Firestone. 2006. Redox Fluctuations Frame Microbial Community Impacts on N-cycling Rates in a Humid Tropical Forest Soil. *Biogeochemistry* 81(1):95-110.

Philippot, L., J. Cuhel, N. P. Saby, D. Cheneby, A. Chronakova, D. Bru, D. Arrouays, F. Martin-Laurent, and M. Simek. 2009. Mapping field-scale spatial patterns of size and activity of the denitrifier community. *Environ Microbiol* 11(6):1518-1526.

R Core Team. 2015. *R: A language and environment for statistical computing.* Vienna, Austria: R Foundation for Statistical Computing.

Rao, N. S., Z. M. Easton, E. M. Schneiderman, M. S. Zion, D. R. Lee, and T. S. Steenhuis. 2009. Modeling watershed-scale effectiveness of agricultural best management practices to reduce phosphorus loading. *J Environ Manage* 90(3):1385-1395.

Reetz, H. F. 2004. Impact of High-Yield, Site-Specific Agriculture on Nutrient Efficiency and the Environment. In *Environmental Impact of Fertilizer on Soil and Water*. Cary; Washington: American Chemical Society.

Revsbech, N. P., J. P. Jacobsen, and L. P. Nielsen. 2005. Nitrogen transformations in microenvironments of river beds and riparian zones. *Ecological Engineering* 24(5):447-455.

Richardson, D. J., B. C. Berks, D. A. Russell, S. Spiro, and C. J. Taylor. 2001. Functional, biochemical and genetic diversity of prokaryotic nitrate reductases. *Cell Mol Life Sci* 58(2):165-178.

Richardson, D. J., H. Felgate, N. Watmough, A. Thomson, and E. M. Baggs. 2009. Mitigating release of the potent greenhouse gas N(2)O from the nitrogen cycle - could enzymic regulation hold the key? *Trends Biotechnol* 27(7):388-397.

Richardson, D. J., and N. J. Watmough. 1999. Inorganic nitrogen metabolism in bacteria. *Current Opinion in Chemical Biology* 3(2):207-219.

Richardson, J. P., and J. W. Nicklow. 2002. In situ permeable reactive barriers for groundwater contamination. *Soil & Sediment Contamination* 11(2):241-268.

Ritchie, G. A., and D. J. Nicholas. 1972. Identification of the sources of nitrous oxide produced by oxidative and reductive processes in Nitrosomonas europaea. *Biochem J* 126(5):1181-1191.

Rivett, M. O., S. R. Buss, P. Morgan, J. W. Smith, and C. D. Bemment. 2008. Nitrate attenuation in groundwater: a review of biogeochemical controlling processes. *Water Res* 42(16):4215-4232.

Robertson, G. P., E. A. Paul, and R. R. Harwood. 2000. Greenhouse Gases in Intensive Agriculture: Contributions of Individual Gases to the Radiative Forcing of the Atmosphere. *Science* 289(5486):1922-1925.

Robertson, W. D., and L. C. Merkley. 2009. In-stream bioreactor for agricultural nitrate treatment. *J Environ Qual* 38(1):230-237.

Rochester, I. J. 2003. Estimating nitrous oxide emissions from flood-irrigated alkaline grey clays. *Australian Journal of Soil Research* 41(2):197-206.

Ronsse, F., S. van Hecke, D. Dickinson, and W. Prins. 2013. Production and characterization of slow pyrolysis biochar: influence of feedstock type and pyrolysis conditions. *Global Change Biology Bioenergy* 5(2):104-115.

Rothery, R. A., G. J. Workun, and J. H. Weiner. 2008. The prokaryotic complex iron-sulfur molybdoenzyme family. *Biochim Biophys Acta* 1778(9):1897-1929.

Rutting, T., P. Boeckx, C. Muller, and L. Klemedtsson. 2011. Assessment of the importance of dissimilatory nitrate reduction to ammonium for the terrestrial nitrogen cycle. *Biogeosciences* 8(7):1779-1791.

Rutting, T., T. J. Clough, C. Muller, M. Lieffering, and P. C. D. Newton. 2010. Ten years of elevated atmospheric carbon dioxide alters soil nitrogen transformations in a sheep-grazed pasture. *Global Change Biology* 16(9):2530-2542.

Saarnio, S., K. Heimonen, and R. Kettunen. 2013. Biochar addition indirectly affects N2O emissions via soil moisture and plant N uptake. *Soil Biology & Biochemistry* 58:99-106.

Saggar, S., N. Jha, J. Deslippe, N. S. Bolan, J. Luo, D. L. Giltrap, D. G. Kim, M. Zaman, and R. W. Tillman. 2013. Denitrification and N2O:N2 production in temperate grasslands: Processes, measurements, modelling and mitigating negative impacts. *Sci Total Environ* 465(0):173-195.

Sanchez-Garcia, M., A. Roig, M. A. Sanchez-Monedero, and M. L. Cayuela. 2014. Biochar increases soil N2O emissions produced by nitrification-mediated pathways. *Frontiers in Environmental Science* 2.

Santoro, A. 2010. Microbial nitrogen cycling at the saltwater–freshwater interface. *Hydrogeology Journal* 18:187-202.

Sartain, J. B., W. L. Hall, R. C. Littell, and E. W. Hopwood. 2004. New tools for the analysis and characterization of slow-release fertilizers. In *Environmental Impact of Fertilizer on Soil and Water*, 180-195. Washington: Amer Chem Soc.

Schipper, L. A., W. D. Robertson, A. J. Gold, D. B. Jaynes, and S. C. Cameron. 2010. Denitrifying bioreactors—An approach for reducing nitrate loads to receiving waters. *Ecological Engineering* 36(11):1532-1543.

Schipper, L. A., and M. Vojvodic-Vukovic. 2001. Five years of nitrate removal, denitrification and carbon dynamics in a denitrification wall. *Water Res* 35(14):3473-3477.

Schmidt, C. A., and M. W. Clark. 2013. Deciphering and modeling the physicochemical drivers of denitrification rates in bioreactors. *Ecological Engineering* 60:276-288.

Schmidt, I., O. Sliekers, M. Schmid, I. Cirpus, M. Strous, E. Bock, J. G. Kuenen, and M. S. Jetten. 2002. Aerobic and anaerobic ammonia oxidizing bacteria--competitors or natural partners? *FEMS Microbiol Ecol* 39(3):175-181.

Schuman, G. E., J. D. Reeder, W. A. Manley, J. T. Manley, and R. H. Hart. 1999. Impact of Grazing Management on the Carbon and Nitrogen Balance of a Mixed-Grass Rangeland. *Ecological Applications* 9(1):65-71.

Scott, J. T., M. J. McCarthy, W. S. Gardner, and R. D. Doyle. 2008. Denitrification, dissimilatory nitrate reduction to ammonium, and nitrogen fixation along a nitrate concentration gradient in a created freshwater wetland. *Biogeochemistry* 87(1):99-111.

Seitzinger, S., J. A. Harrison, J. K. Böhlke, A. F. Bouwman, R. Lowrance, B. Peterson, C. Tobias, and G. V. Drecht. 2006. Denitrification across Landscapes and Waterscapes: A Synthesis. *Ecol Appl* 16(6):2064-2090.

Seitzinger, S. P., C. Kroeze, A. F. Bouwman, N. Caraco, F. Dentener, and R. V. Styles. 2002. Global Patterns of Dissolved Inorganic and Particulate Nitrogen Inputs to Coastal Systems: Recent Conditions and Future Projections. *Estuaries* 25(4):640-655.

Senbayram, M., R. Chen, A. Budai, L. Bakken, and K. Dittert. 2012. N2O emission and the N2O/(N2O+N2) product ratio of denitrification as controlled by available carbon substrates and nitrate concentrations. *Agriculture, Ecosystems & Environment* 147:4-12.

Sgouridis, F., C. M. Heppell, G. Wharton, K. Lansdown, and M. Trimmer. 2011. Denitrification and dissimilatory nitrate reduction to ammonium (DNRA) in a temperate re-connected floodplain. *Water Res* 45(16):4909-4922.

Shao, M. F., T. Zhang, H. H. Fang, and X. Li. 2011. The effect of nitrate concentration on sulfide-driven autotrophic denitrification in marine sediment. *Chemosphere* 83(1):1-6.

Sharpley, A., H. P. Jarvie, A. Buda, L. May, B. Spears, and P. Kleinman. 2013. Phosphorus legacy: overcoming the effects of past management practices to mitigate future water quality impairment. *J Environ Qual* 42(5):1308-1326.

Simek, M., and J. E. Cooper. 2002. The influence of soil pH on denitrification: progress towards the understanding of this interaction over the last 50 years. *European Journal of Soil Science* 53(3):345-354.

Simek, M., L. Jisova, and D. W. Hopkins. 2002. What is the so-called optimum pH for denitrification in soil? *Soil Biology & Biochemistry* 34(9):1227-1234.

Singh, B. K., R. D. Bardgett, P. Smith, and D. S. Reay. 2010. Microorganisms and climate change: terrestrial feedbacks and mitigation options. *Nat Rev Microbiol* 8(11):779-790.

Smith, M. S., and J. M. Tiedje. 1979. Phases of denitrification following oxygen depletion in soil. *Soil Biology & Biochemistry* 11(3):261-267.

Sobieszuk, P., and K. W. Szewczyk. 2006. Estimation of (C/N) ratio for microbial denitrification. *Environ Technol* 27(1):103-108.

Sogbedji, J. M., H. M. van Es, S. D. Klausner, D. R. Bouldin, and W. J. Cox. 2001. Spatial and temporal processes affecting nitrogen availability at the landscape scale. *Soil & Tillage Research* 58(3-4):233-244.

Sohi, S. P., E. Krull, E. Lopez-Capel, and R. Bol. 2010. A Review of Biochar and Its Use and Function in Soil. In *Advances in Agronomy*, 47-82.

Song, B., and C. R. Tobias. 2011. Chapter 3 - Molecular and Stable Isotope Methods to Detect and Measure Anaerobic Ammonium Oxidation (Anammox) in Aquatic Ecosystems. In *Methods in Enzymology*, 63-89. G. K. Martin, and Y. S. Lisa, eds: Academic Press.

Sorensen, J., J. M. Tiedje, and R. B. Firestone. 1980. Inhibition by sulfide of nitric and nitrous oxide reduction by denitrifying Pseudomonas fluorescens. *Appl Environ Microbiol* 39(1):105-108.

Sprague, L. A., and J. A. Gronberg. 2012. Relating management practices and nutrient export in agricultural watersheds of the United States. *J Environ Qual* 41(6):1939-1950.

Steffen, W., P. J. Crutzen, and J. R. McNeill. 2007. The Anthropocene: are humans now overwhelming the great forces of Nature? *Ambio* 36(8):614-621.

Steinbeiss, S., G. Gleixner, and M. Antonietti. 2009. Effect of biochar amendment on soil carbon balance and soil microbial activity. *Soil Biology & Biochemistry* 41(6):1301-1310.

Stres, B., T. Danevcic, L. Pal, M. M. Fuka, L. Resman, S. Leskovec, J. Hacin, D. Stopar, I. Mahne, and I. Mandic-Mulec. 2008. Influence of temperature and soil water content on bacterial, archaeal and denitrifying microbial communities in drained fen grassland soil microcosms. *FEMS Microbiol Ecol* 66(1):110-122.

Strickland, M. S., C. Lauber, N. Fierer, and M. A. Bradford. 2009. Testing the functional significance of microbial community composition. *Ecology* 90(2):441-451.

Stuart, D., R. L. Schewe, and M. McDermott. 2014. Reducing nitrogen fertilizer application as a climate change mitigation strategy: Understanding farmer decision-making and potential barriers to change in the US. *Land Use Policy* 36:210-218.

Sutka, R. L., N. E. Ostrom, P. H. Ostrom, J. A. Breznak, H. Gandhi, A. J. Pitt, and F. Li. 2006. Distinguishing Nitrous Oxide Production from Nitrification and Denitrification on the Basis of Isotopomer Abundances. *Appl Environ Microbiol* 72(1):638-644.

Sutton, M. A. 2011. *The European nitrogen assessment: sources, effects, and policy perspectives*. No. Book, Whole. Cambridge University Press, Cambridge, UK; New York.

Taghizadeh-Toosi, A., T. J. Clough, R. R. Sherlock, and L. M. Condron. 2011. Biochar adsorbed ammonia is bioavailable. *Plant and Soil* 350(1-2):57-69.

Throback, I. N., K. Enwall, A. Jarvis, and S. Hallin. 2004. Reassessing PCR primers targeting nirS, nirK and nosZ genes for community surveys of denitrifying bacteria with DGGE. *FEMS Microbiol Ecol* 49(3):401-417.

Tomitani, A., A. H. Knoll, C. M. Cavanaugh, and T. Ohno. 2006. The evolutionary diversification of cyanobacteria: molecular-phylogenetic and paleontological perspectives. *Proc Natl Acad Sci U S A* 103(14):5442-5447.

United States Environmental Protection Agency. 2007. *The use of soil amendments for remediation, revitalization and reuse*. No. Book, Whole. Solid Waste and Emergency Response, Washington, D.C.

United States Natural Resources Conservation Service. 2000. Comprehensive Nutrient Management Planning - Technical Guidance. In *National Planning Procedures Handbook*.

Van Cleemput, O., and A. H. Samater. 1995. Nitrite in soils: accumulation and role in the formation of gaseous N compounds. *Fertilizer research* 45(1):81-89.

Van de Pas-Schoonen, K. T., S. Schalk-Otte, S. Haaijer, M. Schmid, H. Op den Camp, M. Strous, J. Gijs Kuenen, and M. S. Jetten. 2005. Complete conversion of nitrate into dinitrogen gas in co-cultures of denitrifying bacteria. *Biochem Soc Trans* 33(Pt 1):205-209.

Van Den Heuvel, R. N., S. E. Bakker, M. S. M. Jetten, and M. M. Hefting. 2011. Decreased N2O reduction by low soil pH causes high N2O emissions in a riparian ecosystem. *Geobiology* 9(3):294-300.

van Zwieten, L., S. Kimber, S. Morris, A. Downie, E. Berger, J. Rust, and C. Scheer. 2010. Influence of biochars on flux of N2O and CO2 from Ferrosol. *Australian Journal of Soil Research* 48(7):555.

Vidon, P., C. Allan, D. Burns, T. P. Duval, N. Gurwick, S. Inamdar, R. Lowrance, J. Okay, D. Scott, and S. Sebestyen. 2010. Hot Spots and Hot Moments in Riparian Zones: Potential for Improved Water Quality Management. *JAWRA Journal of the American Water Resources Association* 46(2):278-298.

Vilar-Sanz, A., S. Puig, A. Garcia-Lledo, R. Trias, M. D. Balaguer, J. Colprim, and L. Baneras. 2013. Denitrifying bacterial communities affect current production and nitrous oxide accumulation in a microbial fuel cell. *PLoS One* 8(5):e63460.

Vitousek, P. M. 1997. Human Domination of Earth's Ecosystems. *Science* 277(5325):494-499.

Wallenstein, M. D., D. D. Myrold, M. Firestone, and M. Voytek. 2006. Environmental controls on denitrifying communities and denitrification rates: insights from molecular methods. *Ecol Appl* 16(6):2143-2152.

Wan, X., G. Wan, and M. Snozzi. 2000. Microbiological denitrification and denitrifying activity of Paracoccus Denitrificans. *Chinese Journal of Geochemistry* 19(2):186-192.

Wang, C., H. Lu, D. Dong, H. Deng, P. J. Strong, H. Wang, and W. Wu. 2013. Insight into the effects of biochar on manure composting: evidence supporting the relationship between N2O emission and denitrifying community. *Environ Sci Technol* 47(13):7341-7349.

Wang, H., C. P. Tseng, and R. P. Gunsalus. 1999. The napF and narG nitrate reductase operons in Escherichia coli are differentially expressed in response to submicromolar concentrations of nitrate but not nitrite. *J Bacteriol* 181(17):5303-5308.

Wang, J. Y., M. Zhang, Z. Q. Xiong, P. L. Liu, and G. X. Pan. 2011. Effects of biochar addition on N2O and CO2 emissions from two paddy soils. *Biology and Fertility of Soils* 47(8):887-896.

Warneke, S., L. A. Schipper, D. A. Bruesewitz, I. R. McDonald, and S. Cameron. 2011a. Rates, controls and potential adverse effects of nitrate removal in a denitrification bed. *Ecological Engineering* 37(3):511-522.

Warneke, S., L. A. Schipper, M. G. Matiasek, K. M. Scow, S. Cameron, D. A. Bruesewitz, and I. R. McDonald. 2011b. Nitrate removal, communities of denitrifiers and adverse effects in different carbon substrates for use in denitrification beds. *Water Res* 45(17):5463-5475.

Warnock, D. D., J. Lehmann, T. W. Kuyper, and M. C. Rillig. 2007. Mycorrhizal responses to biochar in soil - concepts and mechanisms. *Plant and Soil* 300(1-2):9-20.

Webster, E. A., and D. W. Hopkins. 1996. Contributions from different microbial processes to N2O emission from soil under different moisture regimes. *Biology and Fertility of Soils* 22(4):331-335.

Weeg-Aerssens, E., J. M. Tiedje, and B. A. Averill. 1987. The mechanism of microbial denitrification. *Journal of the American Chemical Society* 109(23):7214-7215.

Wei, W., K. Isobe, T. Nishizawa, L. Zhu, Y. Shiratori, N. Ohte, K. Koba, S. Otsuka, and K. Senoo. 2015. Higher diversity and abundance of denitrifying microorganisms in environments than considered previously. *ISME J* 9(9):1954-1965.

Wickham, H. 2009. *ggplot2: elegant graphics for data analysis*. UseR! Springer-Verlag, New York, NY.

Woolfenden, H. C., A. J. Gates, C. Bocking, M. G. Blyth, D. J. Richardson, and V. Moulton. 2013. Modeling the effect of copper availability on bacterial denitrification. *MicrobiologyOpen* 2(5):756-765.

Wrage, N., G. L. Velthof, M. L. van Beusichem, and O. Oenema. 2001. Role of nitrifier denitrification in the production of nitrous oxide. *Soil Biology & Biochemistry* 33(12-13):1723-1732.

Xu, X., C. Chen, A. Wang, W. Guo, X. Zhou, D. J. Lee, N. Ren, and J. S. Chang. 2014. Simultaneous removal of sulfide, nitrate and acetate under denitrifying sulfide removal condition: modeling and experimental validation. *J Hazard Mater* 264:16-24.

Ye, R. W., B. A. Averill, and J. M. Tiedje. 1994. Denitrification: production and consumption of nitric oxide. *Appl Environ Microbiol* 60(4):1053-1058.

Yoo, G., and H. Kang. 2012. Effects of biochar addition on greenhouse gas emissions and microbial responses in a short-term laboratory experiment. *J Environ Qual* 41(4):1193-1202.

Zehnder, A. J. B. 1988. *Biology of anaerobic microorganisms*. No. Book, Whole. Wiley, New York.

Zhang, H., R. P. Voroney, and G. W. Price. 2014. Effects of biochar amendments on soil microbial biomass and activity. *J Environ Qual* 43(6):2104-2114.

Zhang, L. 2015. Exploring N and P Reduction in Bioreactors. ProQuest Dissertations Publishing,

Zimmerman, A. R. 2010. Abiotic and Microbial Oxidation of Laboratory-Produced Black Carbon (Biochar). *Environ Sci Technol* 44(4):1295-1301.

Zumft, W. G. 1997. Cell biology and molecular basis of denitrification. *Microbiol Mol Biol Rev* 61(4):533-616.

Appendix A: R Code Used for Statistical Analysis

A1. File: Time Series Models and ezANOVA.r

```
#########################################################################
#                            Setup and Data Import
#########################################################################
require(ggplot2)
require(ez)
require(gridExtra)

Time_Series = read.table("Stacked_N2O_pH.csv", sep=',', header=T)
# Time_Series = read.table("Stacked_N2O_pH_No_Acid.csv", sep=',', header=T)

#########################################################################
# T140 N2O concentration in rep 3 saturated the detector and resulted in inability to
# measure sample N2O at that teplicate. Approximate method detection ceiling is 50ppm
# Subsetting Data and running a local regression and predicting the value to fill in

local_N2O <-(subset(Time_Series, Column == 16))
attach(local_N2O)
lo <- loess(N2O~Time, span=0.35, control=loess.control(surface="direct"), se=T)

# Missing Value computed with LOESS Fit of Individual Column N2O Data
# Predicted value computed with : predict(lo, newdata=140)
# This yielded a value of 54.31367 ppm in line with the assumptions
# about the method detection limits. This value will be only used on
# analyses which require data for all values in the matrix

Time_Series[57,6] <- predict(lo, newdata=140)
detach(local_N2O)

#########################################################################
# log transforming concentration data and removal of -Infintite values
#########################################################################

N2Otrans<-log(Time_Series$N2O)
Time_Series$N2Otrans<-N2Otrans
Time_Series[mapply(is.infinite, Time_Series)] <- NA
# colMeans(Time_Series, na.rm=TRUE)
```

```
Time_Series<-within(Time_Series, {
    Treatment<-factor(Treatment)
    Time_Num<-Time #Need this later
    Time<-factor(Time)
    Column<-factor(Column)
    pH.cat<-factor(pH.cat)
    Combo<-factor(Combo)
})


#########################################################################
#                     ANOVA - (ANalysis Of VAriance)
#########################################################################

# Optionally visualize data with boxplots

# boxplot(Peak.N2O~Treatment*ph.cat,xlab='Treatment',ylab='N2O Production')
# title("Comparison of N2O Production by Treatment")

# One-way ANOVAs:
# Tests null hypothesis that at least one factor's impact is different from 0
# We use the variables Treatment and pH.cat as factors here with the fuction factor()

# One-way ANOVA without equal varience assumption
# oneway.test(DV~factor(1))

# Non-parametric version of ANOVA known as Kruskal-Wallis Test
# kruskal.test(DV~factor(1))

# Two-way ANOVAS:
# Test null hypothesis against multiple factors
#"BWT~factor(SMOKE)*factor(RACE)" is called the "model specification formula"
#A+B gives main effects; A:B gives the interaction; A*B gives both A*B=A+B+A:B

# IMPORTANT
# NEED TO COMPARE ezANOVA TO aov to make sure things are fitting ok
#
# AOV (base function)
# model <- aov(Performance ~ Classifier + Error(factor(Dataset)), data=data)
# summary(model)
#
# ezANOVA (library)
```

```
# ezANOVA(data=data, dv=.(Performance), within=.(Classifier), wid=.(Dataset), detailed=TRUE)

# Repeated measures ANOVA with ezANOVA
print(ezANOVA(data=Time_Series, dv=N2O, wid=Time, within=.(pH.cat, Treatment), detailed=1, type=2))

print(ezANOVA(data=Time_Series, dv=N2O, wid=Time, within=.(pH.cat), detailed=1, type=2))
print(ezANOVA(data=Time_Series, dv=N2O, wid=Time, within=.(Treatment), detailed=1, type=2))
print(ezANOVA(data=Time_Series, dv=N2O, wid=Time, within=.(Combo), detailed=1, type=2))

print(ezANOVA(data=Time_Series, dv=N2O, wid=Treatment, within=pH.cat, detailed=1, type=2))
print(ezANOVA(data=Time_Series, dv=N2O, wid=Treatment, within=Time, detailed=1, type=2))
print(ezANOVA(data=Time_Series, dv=N2O, wid=Treatment, within=.(pH.cat, Time), detailed=1, type=2))

print(ezANOVA(data=Time_Series, dv=N2O, wid=pH.cat, within=Treatment, detailed=1, type=2))
print(ezANOVA(data=Time_Series, dv=N2O, wid=pH.cat, within=Time, detailed=1, type=2))
print(ezANOVA(data=Time_Series, dv=N2O, wid=pH.cat, within=.(Treatment, Time), detailed=1, type=2))


# General ANOVAs across Time by column
Whole_Treat<-aov(Time_Series$N2O~Time_Series$Treatment)
summary(Whole_Treat)
TukeyHSD(Whole_Treat)

Whole_pH<-aov(Time_Series$N2O~Time_Series$pH.cat)
summary(Whole_pH)
TukeyHSD(Whole_pH)

Whole_Combo<-aov(Time_Series$N2O~Time_Series$Combo)
summary(Whole_Combo)
TukeyHSD(Whole_Combo)

# Whole_Treat_pH<-aov(Time_Series$N2O~Time_Series$Treatment*Time_Series$pH.cat)
# TukeyHSD(Whole_Treat_pH) # Same as Combo

######################################################################
#   Linear Models - N2O and logN2O by Time, pH group, and Treatment
######################################################################

#Linear Model of N2O over time by pH over time
results=lm(N2O~Time_Num*pH, Treatment=='BC', data=Time_Series)
summary(results)

results_log=lm(Time_Series$N2Otrans~Time_Series$Time_Num*Time_Series$pH*Time_Series$Treatment)
summary(results_log)
```

```
#########################################################################
#                     Pairwise Differencing
#########################################################################

#subsetting by timestep

T1<-subset(Time_Series, Time==0.5)
T2<-subset(Time_Series, Time==3)
T3<-subset(Time_Series, Time==6)
T4<-subset(Time_Series, Time==9)
T5<-subset(Time_Series, Time==12)
T6<-subset(Time_Series, Time==18)
T7<-subset(Time_Series, Time==24)
T8<-subset(Time_Series, Time==32)
T9<-subset(Time_Series, Time==40)
T10<-subset(Time_Series, Time==48)
T11<-subset(Time_Series, Time==56)
T12<-subset(Time_Series, Time==64)
T13<-subset(Time_Series, Time==72)
T14<-subset(Time_Series, Time==80)
T15<-subset(Time_Series, Time==92)
T16<-subset(Time_Series, Time==104)
T17<-subset(Time_Series, Time==116)
T18<-subset(Time_Series, Time==128)
T19<-subset(Time_Series, Time==140)

#Tukey's Tests
#May find and replace N2O here with the N2Otrans as needed...

#Tukey's Test by Matrix Material
T1N2<-aov(T1$N2O~T1$Treatment)
T1N2.HSD<-TukeyHSD(T1N2)
T1N2.HSD

T2N2<-aov(T2$N2O~T2$Treatment)
T2N2.HSD<-TukeyHSD(T2N2)
T2N2.HSD

T3N2<-aov(T3$N2O~T3$Treatment)
T3N2.HSD<-TukeyHSD(T3N2)
T3N2.HSD
```

```
T4N2<-aov(T4$N2O~T4$Treatment)
T4N2.HSD<-TukeyHSD(T4N2)
T4N2.HSD

T5N2<-aov(T5$N2O~T5$Treatment)
T5N2.HSD<-TukeyHSD(T5N2)
T5N2.HSD

T6N2<-aov(T6$N2O~T6$Treatment)
T6N2.HSD<-TukeyHSD(T6N2)
T6N2.HSD

T7N2<-aov(T7$N2O~T7$Treatment)
T7N2.HSD<-TukeyHSD(T7N2)
T7N2.HSD

T8N2<-aov(T8$N2O~T8$Treatment)
T8N2.HSD<-TukeyHSD(T8N2)
T8N2.HSD

T9N2<-aov(T9$N2O~T9$Treatment)
T9N2.HSD<-TukeyHSD(T9N2)
T9N2.HSD

T10N2<-aov(T10$N2O~T10$Treatment)
T10N2.HSD<-TukeyHSD(T10N2)
T10N2.HSD

T11N2<-aov(T11$N2O~T11$Treatment)
T11N2.HSD<-TukeyHSD(T11N2)
T11N2.HSD

T12N2<-aov(T12$N2O~T12$Treatment)
T12N2.HSD<-TukeyHSD(T12N2)
T12N2.HSD

T13N2<-aov(T13$N2O~T13$Treatment)
T13N2.HSD<-TukeyHSD(T13N2)
T13N2.HSD

T14N2<-aov(T14$N2O~T14$Treatment)
T14N2.HSD<-TukeyHSD(T14N2)
T14N2.HSD
```

```
T15N2<-aov(T15$N2O~T15$Treatment)
T15N2.HSD<-TukeyHSD(T15N2)
T15N2.HSD

T16N2<-aov(T16$N2O~T16$Treatment)
T16N2.HSD<-TukeyHSD(T16N2)
T16N2.HSD

T17N2<-aov(T17$N2O~T17$Treatment)
T17N2.HSD<-TukeyHSD(T17N2)
T17N2.HSD

T18N2<-aov(T18$N2O~T18$Treatment)
T18N2.HSD<-TukeyHSD(T18N2)
T18N2.HSD

T19N2<-aov(T19$N2O~T19$Treatment)
T19N2.HSD<-TukeyHSD(T19N2)
T19N2.HSD

#Tukey's Test by pH Group
T1N3<-aov(T1$N2O~T1$pH.cat)
T1N3.HSD<-TukeyHSD(T1N3)
T1N3.HSD

T2N3<-aov(T2$N2O~T2$pH.cat)
T2N3.HSD<-TukeyHSD(T2N3)
T2N3.HSD

T3N3<-aov(T3$N2O~T3$pH.cat)
T3N3.HSD<-TukeyHSD(T3N3)
T3N3.HSD

T4N3<-aov(T4$N2O~T4$pH.cat)
T4N3.HSD<-TukeyHSD(T4N3)
T4N3.HSD

T5N3<-aov(T5$N2O~T5$pH.cat)
T5N3.HSD<-TukeyHSD(T5N3)
T5N3.HSD

T6N3<-aov(T6$N2O~T6$pH.cat)
T6N3.HSD<-TukeyHSD(T6N3)
T6N3.HSD
```

```
T7N3<-aov(T7$N2O~T7$pH.cat)
T7N3.HSD<-TukeyHSD(T7N3)
T7N3.HSD

T8N3<-aov(T8$N2O~T8$pH.cat)
T8N3.HSD<-TukeyHSD(T8N3)
T8N3.HSD

T9N3<-aov(T9$N2O~T9$pH.cat)
T9N3.HSD<-TukeyHSD(T9N3)
T9N3.HSD

T10N3<-aov(T10$N2O~T10$pH.cat)
T10N3.HSD<-TukeyHSD(T10N3)
T10N3.HSD

T11N3<-aov(T11$N2O~T11$pH.cat)
T11N3.HSD<-TukeyHSD(T11N3)
T11N3.HSD

T12N3<-aov(T12$N2O~T12$pH.cat)
T12N3.HSD<-TukeyHSD(T12N3)
T12N3.HSD

T13N3<-aov(T13$N2O~T13$pH.cat)
T13N3.HSD<-TukeyHSD(T13N3)
T13N3.HSD

T14N3<-aov(T14$N2O~T14$pH.cat)
T14N3.HSD<-TukeyHSD(T14N3)
T14N3.HSD

T15N3<-aov(T15$N2O~T15$pH.cat)
T15N3.HSD<-TukeyHSD(T15N3)
T15N3.HSD

T16N3<-aov(T16$N2O~T16$pH.cat)
T16N3.HSD<-TukeyHSD(T16N3)
T16N3.HSD

T17N3<-aov(T17$N2O~T17$pH.cat)
T17N3.HSD<-TukeyHSD(T17N3)
T17N3.HSD
```

```
T18N3<-aov(T18$N2O~T18$pH.cat)
T18N3.HSD<-TukeyHSD(T18N3)
T18N3.HSD

T19N3<-aov(T19$N2O~T19$pH.cat)
T19N3.HSD<-TukeyHSD(T19N3)
T19N3.HSD

#Tukey's Test by Combo
T1N4<-aov(T1$N2O~T1$Combo)
T1N4.HSD<-TukeyHSD(T1N4)
T1N4.HSD

T2N4<-aov(T2$N2O~T2$Combo)
T2N4.HSD<-TukeyHSD(T2N4)
T2N4.HSD

T3N4<-aov(T3$N2O~T3$Combo)
T3N4.HSD<-TukeyHSD(T3N4)
T3N4.HSD

T4N4<-aov(T4$N2O~T4$Combo)
T4N4.HSD<-TukeyHSD(T4N4)
T4N4.HSD

T5N4<-aov(T5$N2O~T5$Combo)
T5N4.HSD<-TukeyHSD(T5N4)
T5N4.HSD

T6N4<-aov(T6$N2O~T6$Combo)
T6N4.HSD<-TukeyHSD(T6N4)
T6N4.HSD

T7N4<-aov(T7$N2O~T7$Combo)
T7N4.HSD<-TukeyHSD(T7N4)
T7N4.HSD

T8N4<-aov(T8$N2O~T8$Combo)
T8N4.HSD<-TukeyHSD(T8N4)
T8N4.HSD

T9N4<-aov(T9$N2O~T9$Combo)
T9N4.HSD<-TukeyHSD(T9N4)
```

```
T9N4.HSD

T10N4<-aov(T10$N2O~T10$Combo)
T10N4.HSD<-TukeyHSD(T10N4)
T10N4.HSD

T11N4<-aov(T11$N2O~T11$Combo)
T11N4.HSD<-TukeyHSD(T11N4)
T11N4.HSD

T12N4<-aov(T12$N2O~T12$Combo)
T12N4.HSD<-TukeyHSD(T12N4)
T12N4.HSD

T13N4<-aov(T13$N2O~T13$Combo)
T13N4.HSD<-TukeyHSD(T13N4)
T13N4.HSD

T14N4<-aov(T14$N2O~T14$Combo)
T14N4.HSD<-TukeyHSD(T14N4)
T14N4.HSD

T15N4<-aov(T15$N2O~T15$Combo)
T15N4.HSD<-TukeyHSD(T15N4)
T15N4.HSD

T16N4<-aov(T16$N2O~T16$Combo)
T16N4.HSD<-TukeyHSD(T16N4)
T16N4.HSD

T17N4<-aov(T17$N2O~T17$Combo)
T17N4.HSD<-TukeyHSD(T17N4)
T17N4.HSD

T18N4<-aov(T18$N2O~T18$Combo)
T18N4.HSD<-TukeyHSD(T18N4)
T18N4.HSD

T19N4<-aov(T19$N2O~T19$Combo)
T19N4.HSD<-TukeyHSD(T19N4)
T19N4.HSD
```

```
#########################################################################
#                    N2O Differencing Combo Plots
#########################################################################

# Create 15 total plots to represent differencing of each of the different treatment combos
# I am using grid.extra and ggplot2 for more polished plots with additional options

pd <- position_dodge(5)

Time_Series<-within(Time_Series, {
  Treatment<-factor(Treatment)
  Column<-factor(Column)
  pH.cat<-factor(pH.cat)
  Combo<-factor(Combo)
})

#########################################################################
#Untransformed Version

# Differencing - All replicates subtracted from each other
AC_WC__AC_BC <- c((subset(Time_Series, Column ==  '1')$N2O - subset(Time_Series, Column ==
'3')$N2O),(subset(Time_Series, Column ==  '1')$N2O - subset(Time_Series, Column == '15')$N2O),(subset(Time_Series,
Column ==  '1')$N2O - subset(Time_Series, Column == '16')$N2O),(subset(Time_Series, Column ==  '13')$N2O -
subset(Time_Series, Column == '15')$N2O),(subset(Time_Series, Column ==  '13')$N2O - subset(Time_Series, Column ==
'16')$N2O),(subset(Time_Series, Column ==  '14')$N2O - subset(Time_Series, Column == '16')$N2O))

AC_WC__UB_WC <- c((subset(Time_Series, Column ==  '1')$N2O - subset(Time_Series, Column ==
'5')$N2O),(subset(Time_Series, Column ==  '1')$N2O - subset(Time_Series, Column == '9')$N2O),(subset(Time_Series,
Column ==  '1')$N2O - subset(Time_Series, Column == '17')$N2O),(subset(Time_Series, Column ==  '13')$N2O -
subset(Time_Series, Column == '9')$N2O),(subset(Time_Series, Column ==  '13')$N2O - subset(Time_Series, Column ==
'17')$N2O),(subset(Time_Series, Column ==  '14')$N2O - subset(Time_Series, Column == '17')$N2O))

AC_WC__UB_BC <- c((subset(Time_Series, Column ==  '1')$N2O - subset(Time_Series, Column ==
'7')$N2O),(subset(Time_Series, Column ==  '1')$N2O - subset(Time_Series, Column == '11')$N2O),(subset(Time_Series,
Column ==  '1')$N2O - subset(Time_Series, Column == '18')$N2O),(subset(Time_Series, Column ==  '13')$N2O -
subset(Time_Series, Column == '11')$N2O),(subset(Time_Series, Column ==  '13')$N2O - subset(Time_Series, Column ==
'18')$N2O),(subset(Time_Series, Column ==  '14')$N2O - subset(Time_Series, Column == '18')$N2O))

AC_WC__BU_WC <- c((subset(Time_Series, Column ==  '1')$N2O - subset(Time_Series, Column ==
'2')$N2O),(subset(Time_Series, Column ==  '1')$N2O - subset(Time_Series, Column == '6')$N2O),(subset(Time_Series,
Column ==  '1')$N2O - subset(Time_Series, Column == '10')$N2O),(subset(Time_Series, Column ==  '13')$N2O -
subset(Time_Series, Column == '6')$N2O),(subset(Time_Series, Column ==  '13')$N2O - subset(Time_Series, Column ==
'10')$N2O),(subset(Time_Series, Column ==  '14')$N2O - subset(Time_Series, Column == '10')$N2O))
```

```
AC_WC__BU_BC <- c((subset(Time_Series, Column ==  '1')$N2O - subset(Time_Series, Column ==
'4')$N2O),(subset(Time_Series, Column ==  '1')$N2O - subset(Time_Series, Column == '8')$N2O),(subset(Time_Series,
Column ==  '1')$N2O - subset(Time_Series, Column == '12')$N2O),(subset(Time_Series, Column ==  '13')$N2O -
subset(Time_Series, Column == '8')$N2O),(subset(Time_Series, Column ==  '13')$N2O - subset(Time_Series, Column ==
'12')$N2O),(subset(Time_Series, Column ==  '14')$N2O - subset(Time_Series, Column == '12')$N2O))

AC_BC__UB_WC <- c((subset(Time_Series, Column ==  '3')$N2O - subset(Time_Series, Column ==
'5')$N2O),(subset(Time_Series, Column ==  '3')$N2O - subset(Time_Series, Column == '9')$N2O),(subset(Time_Series,
Column ==  '3')$N2O - subset(Time_Series, Column == '17')$N2O),(subset(Time_Series, Column ==  '15')$N2O -
subset(Time_Series, Column == '9')$N2O),(subset(Time_Series, Column ==  '15')$N2O - subset(Time_Series, Column ==
'17')$N2O),(subset(Time_Series, Column ==  '16')$N2O - subset(Time_Series, Column == '17')$N2O))

AC_BC__UB_BC <- c((subset(Time_Series, Column ==  '3')$N2O - subset(Time_Series, Column ==
'7')$N2O),(subset(Time_Series, Column ==  '3')$N2O - subset(Time_Series, Column == '11')$N2O),(subset(Time_Series,
Column ==  '3')$N2O - subset(Time_Series, Column == '18')$N2O),(subset(Time_Series, Column ==  '15')$N2O -
subset(Time_Series, Column == '11')$N2O),(subset(Time_Series, Column ==  '15')$N2O - subset(Time_Series, Column ==
'18')$N2O),(subset(Time_Series, Column ==  '16')$N2O - subset(Time_Series, Column == '18')$N2O))

AC_BC__BU_WC <- c((subset(Time_Series, Column ==  '3')$N2O - subset(Time_Series, Column ==
'2')$N2O),(subset(Time_Series, Column ==  '3')$N2O - subset(Time_Series, Column == '6')$N2O),(subset(Time_Series,
Column ==  '3')$N2O - subset(Time_Series, Column == '10')$N2O),(subset(Time_Series, Column ==  '15')$N2O -
subset(Time_Series, Column == '6')$N2O),(subset(Time_Series, Column ==  '15')$N2O - subset(Time_Series, Column ==
'10')$N2O),(subset(Time_Series, Column ==  '16')$N2O - subset(Time_Series, Column == '10')$N2O))

AC_BC__BU_BC <- c((subset(Time_Series, Column ==  '3')$N2O - subset(Time_Series, Column ==
'4')$N2O),(subset(Time_Series, Column ==  '3')$N2O - subset(Time_Series, Column == '8')$N2O),(subset(Time_Series,
Column ==  '3')$N2O - subset(Time_Series, Column == '12')$N2O),(subset(Time_Series, Column ==  '15')$N2O -
subset(Time_Series, Column == '8')$N2O),(subset(Time_Series, Column ==  '15')$N2O - subset(Time_Series, Column ==
'12')$N2O),(subset(Time_Series, Column ==  '16')$N2O - subset(Time_Series, Column == '12')$N2O))

UB_WC__UB_BC <- c((subset(Time_Series, Column ==  '5')$N2O - subset(Time_Series, Column ==
'7')$N2O),(subset(Time_Series, Column ==  '5')$N2O - subset(Time_Series, Column == '11')$N2O),(subset(Time_Series,
Column ==  '5')$N2O - subset(Time_Series, Column == '18')$N2O),(subset(Time_Series, Column ==  '9')$N2O -
subset(Time_Series, Column == '11')$N2O),(subset(Time_Series, Column ==  '9')$N2O - subset(Time_Series, Column ==
'18')$N2O),(subset(Time_Series, Column ==  '17')$N2O - subset(Time_Series, Column == '18')$N2O))

UB_WC__BU_WC <- c((subset(Time_Series, Column ==  '5')$N2O - subset(Time_Series, Column ==
'2')$N2O),(subset(Time_Series, Column ==  '5')$N2O - subset(Time_Series, Column == '6')$N2O),(subset(Time_Series,
Column ==  '5')$N2O - subset(Time_Series, Column == '10')$N2O),(subset(Time_Series, Column ==  '9')$N2O -
subset(Time_Series, Column == '6')$N2O),(subset(Time_Series, Column ==  '9')$N2O - subset(Time_Series, Column ==
'10')$N2O),(subset(Time_Series, Column ==  '17')$N2O - subset(Time_Series, Column == '10')$N2O))

UB_WC__BU_BC <- c((subset(Time_Series, Column ==  '5')$N2O - subset(Time_Series, Column ==
'4')$N2O),(subset(Time_Series, Column ==  '5')$N2O - subset(Time_Series, Column == '8')$N2O),(subset(Time_Series,
```

```
Column ==  '5')$N2O - subset(Time_Series, Column == '12')$N2O),(subset(Time_Series, Column ==  '9')$N2O -
subset(Time_Series, Column == '8')$N2O),(subset(Time_Series, Column ==  '9')$N2O - subset(Time_Series, Column ==
'12')$N2O),(subset(Time_Series, Column ==  '17')$N2O - subset(Time_Series, Column == '12')$N2O))

UB_BC__BU_WC <- c((subset(Time_Series, Column ==  '7')$N2O - subset(Time_Series, Column ==
'2')$N2O),(subset(Time_Series, Column ==  '7')$N2O - subset(Time_Series, Column == '6')$N2O),(subset(Time_Series,
Column ==  '7')$N2O - subset(Time_Series, Column == '10')$N2O),(subset(Time_Series, Column ==  '11')$N2O -
subset(Time_Series, Column == '6')$N2O),(subset(Time_Series, Column ==  '11')$N2O - subset(Time_Series, Column ==
'10')$N2O),(subset(Time_Series, Column ==  '18')$N2O - subset(Time_Series, Column == '10')$N2O))

UB_BC__BU_BC <- c((subset(Time_Series, Column ==  '7')$N2O - subset(Time_Series, Column ==
'4')$N2O),(subset(Time_Series, Column ==  '7')$N2O - subset(Time_Series, Column == '8')$N2O),(subset(Time_Series,
Column ==  '7')$N2O - subset(Time_Series, Column == '12')$N2O),(subset(Time_Series, Column ==  '11')$N2O -
subset(Time_Series, Column == '8')$N2O),(subset(Time_Series, Column ==  '11')$N2O - subset(Time_Series, Column ==
'12')$N2O),(subset(Time_Series, Column ==  '18')$N2O - subset(Time_Series, Column == '12')$N2O))

BU_WC__BU_BC <- c((subset(Time_Series, Column ==  '2')$N2O - subset(Time_Series, Column ==
'4')$N2O),(subset(Time_Series, Column ==  '2')$N2O - subset(Time_Series, Column == '8')$N2O),(subset(Time_Series,
Column ==  '2')$N2O - subset(Time_Series, Column == '12')$N2O),(subset(Time_Series, Column ==  '6')$N2O -
subset(Time_Series, Column == '8')$N2O),(subset(Time_Series, Column ==  '6')$N2O - subset(Time_Series, Column ==
'12')$N2O),(subset(Time_Series, Column ==  '10')$N2O - subset(Time_Series, Column == '12')$N2O))


#Appending to data frame
Time_Series$AC_WC__AC_BC <- AC_WC__AC_BC
Time_Series$AC_WC__UB_WC <- AC_WC__UB_WC
Time_Series$AC_WC__UB_BC <- AC_WC__UB_BC
Time_Series$AC_WC__BU_WC <- AC_WC__BU_WC
Time_Series$AC_WC__BU_BC <- AC_WC__BU_BC
Time_Series$AC_BC__UB_WC <- AC_BC__UB_WC
Time_Series$AC_BC__UB_BC <- AC_BC__UB_BC
Time_Series$AC_BC__BU_WC <- AC_BC__BU_WC
Time_Series$AC_BC__BU_BC <- AC_BC__BU_BC
Time_Series$UB_WC__UB_BC <- UB_WC__UB_BC
Time_Series$UB_WC__BU_WC <- UB_WC__BU_WC
Time_Series$UB_WC__BU_BC <- UB_WC__BU_BC
Time_Series$UB_BC__BU_WC <- UB_BC__BU_WC
Time_Series$UB_BC__BU_BC <- UB_BC__BU_BC
Time_Series$BU_WC__BU_BC <- BU_WC__BU_BC

# Generate Plots (Untransformed)
Plot_AC_WC__AC_BC <- ggplot(Time_Series, aes(x=Time_Num, y= AC_WC__AC_BC)) + geom_point(position=pd, size=2, shape=21,
fill='white') + xlab('AC_WC  minus  AC_BC') + ylab(expression(paste(Delta, '  ', N[2], 'O conc.'))) +
scale_x_continuous(breaks=0:150*30) + coord_cartesian(xlim = c(-5, 155)) + theme_bw() +  theme(axis.title.x =
```

```
element_text(size=13,face='bold')) + theme(axis.title.y = element_text(size=13,face='bold'), axis.title.x =
element_text(vjust=-0.5), axis.title.y = element_text(hjust=-0.5)) + annotate('point', x=140,
y=min(Time_Series$AC_WC__AC_BC, na.rm=TRUE), size=8, shape='+', col='darkred')

Plot_AC_WC__UB_WC <- ggplot(Time_Series, aes(x=Time_Num, y= AC_WC__UB_WC)) + geom_point(position=pd, size=2, shape=21,
fill='white') + xlab('AC_WC  minus  UB_WC') + ylab(expression(paste(Delta, '  ', N[2], 'O conc.'))) +
scale_x_continuous(breaks=0:150*30) + coord_cartesian(xlim = c(-5, 155)) + theme_bw() +  theme(axis.title.x =
element_text(size=13,face='bold')) + theme(axis.title.y = element_text(size=13,face='bold'), axis.title.x =
element_text(vjust=-0.5), axis.title.y = element_text(hjust=-0.5))

Plot_AC_WC__UB_BC <- ggplot(Time_Series, aes(x=Time_Num, y= AC_WC__UB_BC)) + geom_point(position=pd, size=2, shape=21,
fill='white') + xlab('AC_WC  minus  UB_BC') + ylab(expression(paste(Delta, '  ', N[2], 'O conc.'))) +
scale_x_continuous(breaks=0:150*30) + coord_cartesian(xlim = c(-5, 155)) + theme_bw() +  theme(axis.title.x =
element_text(size=13,face='bold')) + theme(axis.title.y = element_text(size=13,face='bold'), axis.title.x =
element_text(vjust=-0.5), axis.title.y = element_text(hjust=-0.5))

Plot_AC_WC__BU_WC <- ggplot(Time_Series, aes(x=Time_Num, y= AC_WC__BU_WC)) + geom_point(position=pd, size=2, shape=21,
fill='white') + xlab('AC_WC  minus  BU_WC') + ylab(expression(paste(Delta, '  ', N[2], 'O conc.'))) +
scale_x_continuous(breaks=0:150*30) + coord_cartesian(xlim = c(-5, 155)) + theme_bw() +  theme(axis.title.x =
element_text(size=13,face='bold')) + theme(axis.title.y = element_text(size=13,face='bold'), axis.title.x =
element_text(vjust=-0.5), axis.title.y = element_text(hjust=-0.5))

Plot_AC_WC__BU_BC <- ggplot(Time_Series, aes(x=Time_Num, y= AC_WC__BU_BC)) + geom_point(position=pd, size=2, shape=21,
fill='white') + xlab('AC_WC  minus  BU_BC') + ylab(expression(paste(Delta, '  ', N[2], 'O conc.'))) +
scale_x_continuous(breaks=0:150*30) + coord_cartesian(xlim = c(-5, 155)) + theme_bw() +  theme(axis.title.x =
element_text(size=13,face='bold')) + theme(axis.title.y = element_text(size=13,face='bold'), axis.title.x =
element_text(vjust=-0.5), axis.title.y = element_text(hjust=-0.5))

Plot_AC_BC__UB_WC <- ggplot(Time_Series, aes(x=Time_Num, y= AC_BC__UB_WC)) + geom_point(position=pd, size=2, shape=21,
fill='white') + xlab('AC_BC  minus  UB_WC') + ylab(expression(paste(Delta, '  ', N[2], 'O conc.'))) +
scale_x_continuous(breaks=0:150*30) + coord_cartesian(xlim = c(-5, 155)) + theme_bw() +  theme(axis.title.x =
element_text(size=13,face='bold')) + theme(axis.title.y = element_text(size=13,face='bold'), axis.title.x =
element_text(vjust=-0.5), axis.title.y = element_text(hjust=-0.5)) + annotate('point', x=c(40,92,128),
y=min(Time_Series$AC_BC__UB_WC, na.rm=TRUE), size=8, shape='+', col='darkred') + annotate('point', x=c(64,116,140),
y=min(Time_Series$AC_BC__UB_WC, na.rm=TRUE), size=8, shape='*', col='darkblue')

Plot_AC_BC__UB_BC <- ggplot(Time_Series, aes(x=Time_Num, y= AC_BC__UB_BC)) + geom_point(position=pd, size=2, shape=21,
fill='white') + xlab('AC_BC  minus  UB_BC') + ylab(expression(paste(Delta, '  ', N[2], 'O conc.'))) +
scale_x_continuous(breaks=0:150*30) + coord_cartesian(xlim = c(-5, 155)) + theme_bw() +  theme(axis.title.x =
element_text(size=13,face='bold')) + theme(axis.title.y = element_text(size=13,face='bold'), axis.title.x =
element_text(vjust=-0.5), axis.title.y = element_text(hjust=-0.5)) + annotate('point', x=c(32,40,92,128),
y=min(Time_Series$AC_BC__UB_BC, na.rm=TRUE), size=8, shape='+', col='darkred') + annotate('point', x=c(64,116,140),
y=min(Time_Series$AC_BC__UB_BC, na.rm=TRUE), size=8, shape='*', col='darkblue')
```

```
Plot_AC_BC__BU_WC <- ggplot(Time_Series, aes(x=Time_Num, y= AC_BC__BU_WC)) + geom_point(position=pd, size=2, shape=21,
fill='white') + xlab('AC_BC  minus  BU_WC') + ylab(expression(paste(Delta, '  ', N[2], 'O conc.'))) +
scale_x_continuous(breaks=0:150*30) + coord_cartesian(xlim = c(-5, 155)) + theme_bw() +  theme(axis.title.x =
element_text(size=13,face='bold')) + theme(axis.title.y = element_text(size=13,face='bold'), axis.title.x =
element_text(vjust=-0.5), axis.title.y = element_text(hjust=-0.5)) + annotate('point', x=c(32,40,92,128),
y=min(Time_Series$AC_BC__BU_WC, na.rm=TRUE), size=8, shape='+', col='darkred') + annotate('point', x=c(64,116,140),
y=min(Time_Series$AC_BC__BU_WC, na.rm=TRUE), size=8, shape='*', col='darkblue')

Plot_AC_BC__BU_BC <- ggplot(Time_Series, aes(x=Time_Num, y= AC_BC__BU_BC)) + geom_point(position=pd, size=2, shape=21,
fill='white') + xlab('AC_BC  minus  BU_BC') + ylab(expression(paste(Delta, '  ', N[2], 'O conc.'))) +
scale_x_continuous(breaks=0:150*30) + coord_cartesian(xlim = c(-5, 155)) + theme_bw() +  theme(axis.title.x =
element_text(size=13,face='bold')) + theme(axis.title.y = element_text(size=13,face='bold'), axis.title.x =
element_text(vjust=-0.5), axis.title.y = element_text(hjust=-0.5)) + annotate('point', x=c(24,32,40,92,128),
y=min(Time_Series$AC_BC__BU_BC, na.rm=TRUE), size=8, shape='+', col='darkred') + annotate('point', x=c(64,116,140),
y=min(Time_Series$AC_BC__BU_BC, na.rm=TRUE), size=8, shape='*', col='darkblue')

Plot_UB_WC__UB_BC <- ggplot(Time_Series, aes(x=Time_Num, y= UB_WC__UB_BC)) + geom_point(position=pd, size=2, shape=21,
fill='white') + xlab('UB_WC  minus  UB_BC') + ylab(expression(paste(Delta, '  ', N[2], 'O conc.'))) +
scale_x_continuous(breaks=0:150*30) + coord_cartesian(xlim = c(-5, 155)) + theme_bw() +  theme(axis.title.x =
element_text(size=13,face='bold')) + theme(axis.title.y = element_text(size=13,face='bold'), axis.title.x =
element_text(vjust=-0.5), axis.title.y = element_text(hjust=-0.5))

Plot_UB_WC__BU_WC <- ggplot(Time_Series, aes(x=Time_Num, y= UB_WC__BU_WC)) + geom_point(position=pd, size=2, shape=21,
fill='white') + xlab('UB_WC  minus  BU_WC') + ylab(expression(paste(Delta, '  ', N[2], 'O conc.'))) +
scale_x_continuous(breaks=0:150*30) + coord_cartesian(xlim = c(-5, 155)) + theme_bw() +  theme(axis.title.x =
element_text(size=13,face='bold')) + theme(axis.title.y = element_text(size=13,face='bold'), axis.title.x =
element_text(vjust=-0.5), axis.title.y = element_text(hjust=-0.5))

Plot_UB_WC__BU_BC <- ggplot(Time_Series, aes(x=Time_Num, y= UB_WC__BU_BC)) + geom_point(position=pd, size=2, shape=21,
fill='white') + xlab('UB_WC  minus  BU_BC') + ylab(expression(paste(Delta, '  ', N[2], 'O conc.'))) +
scale_x_continuous(breaks=0:150*30) + coord_cartesian(xlim = c(-5, 155)) + theme_bw() +  theme(axis.title.x =
element_text(size=13,face='bold')) + theme(axis.title.y = element_text(size=13,face='bold'), axis.title.x =
element_text(vjust=-0.5), axis.title.y = element_text(hjust=-0.5))

Plot_UB_BC__BU_WC <- ggplot(Time_Series, aes(x=Time_Num, y= UB_BC__BU_WC)) + geom_point(position=pd, size=2, shape=21,
fill='white') + xlab('UB_BC  minus  BU_WC') + ylab(expression(paste(Delta, '  ', N[2], 'O conc.'))) +
scale_x_continuous(breaks=0:150*30) + coord_cartesian(xlim = c(-5, 155)) + theme_bw() +  theme(axis.title.x =
element_text(size=13,face='bold')) + theme(axis.title.y = element_text(size=13,face='bold'), axis.title.x =
element_text(vjust=-0.5), axis.title.y = element_text(hjust=-0.5))

Plot_UB_BC__BU_BC <- ggplot(Time_Series, aes(x=Time_Num, y= UB_BC__BU_BC)) + geom_point(position=pd, size=2, shape=21,
fill='white') + xlab('UB_BC  minus  BU_BC') + ylab(expression(paste(Delta, '  ', N[2], 'O conc.'))) +
scale_x_continuous(breaks=0:150*30) + coord_cartesian(xlim = c(-5, 155)) + theme_bw() +  theme(axis.title.x =
```

```
element_text(size=13,face='bold')) + theme(axis.title.y = element_text(size=13,face='bold'), axis.title.x =
element_text(vjust=-0.5), axis.title.y = element_text(hjust=-0.5))

Plot_BU_WC__BU_BC <- ggplot(Time_Series, aes(x=Time_Num, y= BU_WC__BU_BC)) + geom_point(position=pd, size=2, shape=21,
fill='white') + xlab('BU_WC  minus  BU_BC') + ylab(expression(paste(Delta, '  ', N[2], 'O conc.'))) +
scale_x_continuous(breaks=0:150*30) + coord_cartesian(xlim = c(-5, 155)) + theme_bw() +  theme(axis.title.x =
element_text(size=13,face='bold')) + theme(axis.title.y = element_text(size=13,face='bold'), axis.title.x =
element_text(vjust=-0.5), axis.title.y = element_text(hjust=-0.5))

grid.arrange(Plot_AC_WC__AC_BC,Plot_AC_WC__UB_WC,Plot_AC_WC__UB_BC,Plot_AC_WC__BU_WC,Plot_AC_WC__BU_BC,Plot_AC_BC__UB_W
C,Plot_AC_BC__UB_BC,Plot_AC_BC__BU_WC,Plot_AC_BC__BU_BC,Plot_UB_WC__UB_BC,Plot_UB_WC__BU_WC,Plot_UB_WC__BU_BC,Plot_UB_B
C__BU_WC,Plot_UB_BC__BU_BC,Plot_BU_WC__BU_BC, nrow = 3, ncol = 5)

######################################################################
# Encode differences into lists - Log Transformed Version
# Results not significant - excluding from final analysis
#
# AC_WC__AC_BC <- (subset(Time_Series, Combo ==  'AC_WC')$N2Otrans - subset(Time_Series, Combo == 'AC_BC')$N2Otrans)
# AC_WC__UB_WC <- (subset(Time_Series, Combo ==  'AC_WC')$N2Otrans - subset(Time_Series, Combo == 'UB_WC')$N2Otrans)
# AC_WC__UB_BC <- (subset(Time_Series, Combo ==  'AC_WC')$N2Otrans - subset(Time_Series, Combo == 'UB_BC')$N2Otrans)
# AC_WC__BU_WC <- (subset(Time_Series, Combo ==  'AC_WC')$N2Otrans - subset(Time_Series, Combo == 'BU_WC')$N2Otrans)
# AC_WC__BU_BC <- (subset(Time_Series, Combo ==  'AC_WC')$N2Otrans - subset(Time_Series, Combo == 'BU_BC')$N2Otrans)
# AC_BC__UB_WC <- (subset(Time_Series, Combo ==  'AC_BC')$N2Otrans - subset(Time_Series, Combo == 'UB_WC')$N2Otrans)
# AC_BC__UB_BC <- (subset(Time_Series, Combo ==  'AC_BC')$N2Otrans - subset(Time_Series, Combo == 'UB_BC')$N2Otrans)
# AC_BC__BU_WC <- (subset(Time_Series, Combo ==  'AC_BC')$N2Otrans - subset(Time_Series, Combo == 'BU_WC')$N2Otrans)
# AC_BC__BU_BC <- (subset(Time_Series, Combo ==  'AC_BC')$N2Otrans - subset(Time_Series, Combo == 'BU_BC')$N2Otrans)
# UB_WC__UB_BC <- (subset(Time_Series, Combo ==  'UB_WC')$N2Otrans - subset(Time_Series, Combo == 'UB_BC')$N2Otrans)
# UB_WC__BU_WC <- (subset(Time_Series, Combo ==  'UB_WC')$N2Otrans - subset(Time_Series, Combo == 'BU_WC')$N2Otrans)
# UB_WC__BU_BC <- (subset(Time_Series, Combo ==  'UB_WC')$N2Otrans - subset(Time_Series, Combo == 'BU_BC')$N2Otrans)
# UB_BC__BU_WC <- (subset(Time_Series, Combo ==  'UB_BC')$N2Otrans - subset(Time_Series, Combo == 'BU_WC')$N2Otrans)
# UB_BC__BU_BC <- (subset(Time_Series, Combo ==  'UB_BC')$N2Otrans - subset(Time_Series, Combo == 'BU_BC')$N2Otrans)
# BU_WC__BU_BC <- (subset(Time_Series, Combo ==  'BU_WC')$N2Otrans - subset(Time_Series, Combo == 'BU_BC')$N2Otrans)
#
# #Append to the data frame
# Time_Series$AC_WC__AC_BC <- AC_WC__AC_BC
# Time_Series$AC_WC__UB_WC <- AC_WC__UB_WC
# Time_Series$AC_WC__UB_BC <- AC_WC__UB_BC
# Time_Series$AC_WC__BU_WC <- AC_WC__BU_WC
# Time_Series$AC_WC__BU_BC <- AC_WC__BU_BC
# Time_Series$AC_BC__UB_WC <- AC_BC__UB_WC
# Time_Series$AC_BC__UB_BC <- AC_BC__UB_BC
# Time_Series$AC_BC__BU_WC <- AC_BC__BU_WC
# Time_Series$AC_BC__BU_BC <- AC_BC__BU_BC
# Time_Series$UB_WC__UB_BC <- UB_WC__UB_BC
```

```
# Time_Series$UB_WC__BU_WC <- UB_WC__BU_WC
# Time_Series$UB_WC__BU_BC <- UB_WC__BU_BC
# Time_Series$UB_BC__BU_WC <- UB_BC__BU_WC
# Time_Series$UB_BC__BU_BC <- UB_BC__BU_BC
# Time_Series$BU_WC__BU_BC <- BU_WC__BU_BC
#
# #Generate Plots (transformed)
# Plot_AC_WC__AC_BC <- ggplot(Time_Series, aes(x=Time_Num, y= AC_WC__AC_BC)) + geom_point(position=pd, size=3,
shape=21, fill='white') + xlab('AC_WC  minus  AC_BC') + ylab(expression(paste(Delta,' log ( ', N[2], 'O ) conc.'))) +
scale_x_continuous(breaks=0:140*30) + theme_bw() +  theme(axis.title.x = element_text(size=13,face='bold')) +
theme(axis.title.y = element_text(size=13,face='bold'), axis.title.x = element_text(vjust=-0.5), axis.title.y =
element_text(hjust=-0.5))
# Plot_AC_WC__UB_WC <- ggplot(Time_Series, aes(x=Time_Num, y= AC_WC__UB_WC)) + geom_point(position=pd, size=3,
shape=21, fill='white') + xlab('AC_WC  minus  UB_WC') + ylab(expression(paste(Delta,' log ( ', N[2], 'O ) conc.'))) +
scale_x_continuous(breaks=0:140*30) + theme_bw() +  theme(axis.title.x = element_text(size=13,face='bold')) +
theme(axis.title.y = element_text(size=13,face='bold'), axis.title.x = element_text(vjust=-0.5), axis.title.y =
element_text(hjust=-0.5)) + annotate('point', x=c(72, 80), y=min(Time_Series$AC_WC__UB_WC, na.rm=TRUE), size=8,
shape='+', col='darkred') + annotate('point', x=c(64,92), y=min(Time_Series$AC_WC__UB_WC, na.rm=TRUE), size=8,
shape='*', col='darkblue')
# Plot_AC_WC__UB_BC <- ggplot(Time_Series, aes(x=Time_Num, y= AC_WC__UB_BC)) + geom_point(position=pd, size=3,
shape=21, fill='white') + xlab('AC_WC  minus  UB_BC') + ylab(expression(paste(Delta,' log ( ', N[2], 'O ) conc.'))) +
scale_x_continuous(breaks=0:140*30) + theme_bw() +  theme(axis.title.x = element_text(size=13,face='bold')) +
theme(axis.title.y = element_text(size=13,face='bold'), axis.title.x = element_text(vjust=-0.5), axis.title.y =
element_text(hjust=-0.5)) + annotate('point', x=40, y=min(Time_Series$AC_WC__UB_BC, na.rm=TRUE), size=8, shape ='*',
col='darkblue')
# Plot_AC_WC__BU_WC <- ggplot(Time_Series, aes(x=Time_Num, y= AC_WC__BU_WC)) + geom_point(position=pd, size=3,
shape=21, fill='white') + xlab('AC_WC  minus  BU_WC') + ylab(expression(paste(Delta,' log ( ', N[2], 'O ) conc.'))) +
scale_x_continuous(breaks=0:140*30) + theme_bw() +  theme(axis.title.x = element_text(size=13,face='bold')) +
theme(axis.title.y = element_text(size=13,face='bold'), axis.title.x = element_text(vjust=-0.5), axis.title.y =
element_text(hjust=-0.5)) + annotate('point', x=40, y=min(Time_Series$AC_WC__BU_WC, na.rm=TRUE), size=8, shape ='*',
col='darkblue')
# Plot_AC_WC__BU_BC <- ggplot(Time_Series, aes(x=Time_Num, y= AC_WC__BU_BC)) + geom_point(position=pd, size=3,
shape=21, fill='white') + xlab('AC_WC  minus  BU_BC') + ylab(expression(paste(Delta,' log ( ', N[2], 'O ) conc.'))) +
scale_x_continuous(breaks=0:140*30) + theme_bw() +  theme(axis.title.x = element_text(size=13,face='bold')) +
theme(axis.title.y = element_text(size=13,face='bold'), axis.title.x = element_text(vjust=-0.5), axis.title.y =
element_text(hjust=-0.5)) + annotate('point', x=40, y=min(Time_Series$AC_WC__BU_BC, na.rm=TRUE), size=8, shape ='*',
col='darkblue')
# Plot_AC_BC__UB_WC <- ggplot(Time_Series, aes(x=Time_Num, y= AC_BC__UB_WC)) + geom_point(position=pd, size=3,
shape=21, fill='white') + xlab('AC_BC  minus  UB_WC') + ylab(expression(paste(Delta,' log ( ', N[2], 'O ) conc.'))) +
scale_x_continuous(breaks=0:140*30) + theme_bw() +  theme(axis.title.x = element_text(size=13,face='bold')) +
theme(axis.title.y = element_text(size=13,face='bold'), axis.title.x = element_text(vjust=-0.5), axis.title.y =
element_text(hjust=-0.5)) + annotate('point', x=c(64, 80, 92), y=min(Time_Series$AC_BC__UB_WC, na.rm=TRUE), size=8,
shape ='*', col='darkblue')
```

```
# Plot_AC_BC__UB_BC <- ggplot(Time_Series, aes(x=Time_Num, y= AC_BC__UB_BC)) + geom_point(position=pd, size=3,
shape=21, fill='white') + xlab('AC_BC  minus  UB_BC') + ylab(expression(paste(Delta,' log ( ', N[2], 'O ) conc.'))) +
scale_x_continuous(breaks=0:140*30) + theme_bw() +  theme(axis.title.x = element_text(size=13,face='bold')) +
theme(axis.title.y = element_text(size=13,face='bold'), axis.title.x = element_text(vjust=-0.5), axis.title.y =
element_text(hjust=-0.5)) + annotate('point', x=40, y=min(Time_Series$AC_BC__UB_BC, na.rm=TRUE), size=8, shape ='*',
col='darkblue')
# Plot_AC_BC__BU_WC <- ggplot(Time_Series, aes(x=Time_Num, y= AC_BC__BU_WC)) + geom_point(position=pd, size=3,
shape=21, fill='white') + xlab('AC_BC  minus  BU_WC') + ylab(expression(paste(Delta,' log ( ', N[2], 'O ) conc.'))) +
scale_x_continuous(breaks=0:140*30) + theme_bw() +  theme(axis.title.x = element_text(size=13,face='bold')) +
theme(axis.title.y = element_text(size=13,face='bold'), axis.title.x = element_text(vjust=-0.5), axis.title.y =
element_text(hjust=-0.5)) + annotate('point', x=18, y=min(Time_Series$AC_BC__BU_WC, na.rm=TRUE), size=8, shape ='*',
col='darkblue') + annotate('point', x=40, y=min(Time_Series$AC_BC__BU_WC, na.rm=TRUE), size=6, shape='#',
col='darkgreen')
# Plot_AC_BC__BU_BC <- ggplot(Time_Series, aes(x=Time_Num, y= AC_BC__BU_BC)) + geom_point(position=pd, size=3,
shape=21, fill='white') + xlab('AC_BC  minus  BU_BC') + ylab(expression(paste(Delta,' log ( ', N[2], 'O ) conc.'))) +
scale_x_continuous(breaks=0:140*30) + theme_bw() +  theme(axis.title.x = element_text(size=13,face='bold')) +
theme(axis.title.y = element_text(size=13,face='bold'), axis.title.x = element_text(vjust=-0.5), axis.title.y =
element_text(hjust=-0.5)) + annotate('point', x=40, y=min(Time_Series$AC_BC__BU_BC, na.rm=TRUE), size=8, shape ='*',
col='darkblue')
# Plot_UB_WC__UB_BC <- ggplot(Time_Series, aes(x=Time_Num, y= UB_WC__UB_BC)) + geom_point(position=pd, size=3,
shape=21, fill='white') + xlab('UB_WC  minus  UB_BC') + ylab(expression(paste(Delta,' log ( ', N[2], 'O ) conc.'))) +
scale_x_continuous(breaks=0:140*30) + theme_bw() +  theme(axis.title.x = element_text(size=13,face='bold')) +
theme(axis.title.y = element_text(size=13,face='bold'), axis.title.x = element_text(vjust=-0.5), axis.title.y =
element_text(hjust=-0.5))
# Plot_UB_WC__BU_WC <- ggplot(Time_Series, aes(x=Time_Num, y= UB_WC__BU_WC)) + geom_point(position=pd, size=3,
shape=21, fill='white') + xlab('UB_WC  minus  BU_WC') + ylab(expression(paste(Delta,' log ( ', N[2], 'O ) conc.'))) +
scale_x_continuous(breaks=0:140*30) + theme_bw() +  theme(axis.title.x = element_text(size=13,face='bold')) +
theme(axis.title.y = element_text(size=13,face='bold'), axis.title.x = element_text(vjust=-0.5), axis.title.y =
element_text(hjust=-0.5))
# Plot_UB_WC__BU_BC <- ggplot(Time_Series, aes(x=Time_Num, y= UB_WC__BU_BC)) + geom_point(position=pd, size=3,
shape=21, fill='white') + xlab('UB_WC  minus  BU_BC') + ylab(expression(paste(Delta,' log ( ', N[2], 'O ) conc.'))) +
scale_x_continuous(breaks=0:140*30) + theme_bw() +  theme(axis.title.x = element_text(size=13,face='bold')) +
theme(axis.title.y = element_text(size=13,face='bold'), axis.title.x = element_text(vjust=-0.5), axis.title.y =
element_text(hjust=-0.5))
# Plot_UB_BC__BU_WC <- ggplot(Time_Series, aes(x=Time_Num, y= UB_BC__BU_WC)) + geom_point(position=pd, size=3,
shape=21, fill='white') + xlab('UB_BC  minus  BU_WC') + ylab(expression(paste(Delta,' log ( ', N[2], 'O ) conc.'))) +
scale_x_continuous(breaks=0:140*30) + theme_bw() +  theme(axis.title.x = element_text(size=13,face='bold')) +
theme(axis.title.y = element_text(size=13,face='bold'), axis.title.x = element_text(vjust=-0.5), axis.title.y =
element_text(hjust=-0.5))
# Plot_UB_BC__BU_BC <- ggplot(Time_Series, aes(x=Time_Num, y= UB_BC__BU_BC)) + geom_point(position=pd, size=3,
shape=21, fill='white') + xlab('UB_BC  minus  BU_BC') + ylab(expression(paste(Delta,' log ( ', N[2], 'O ) conc.'))) +
scale_x_continuous(breaks=0:140*30) + theme_bw() +  theme(axis.title.x = element_text(size=13,face='bold')) +
theme(axis.title.y = element_text(size=13,face='bold'), axis.title.x = element_text(vjust=-0.5), axis.title.y =
element_text(hjust=-0.5))
```

```
# Plot_BU_WC__BU_BC <- ggplot(Time_Series, aes(x=Time_Num, y= BU_WC__BU_BC)) + geom_point(position=pd, size=3,
shape=21, fill='white') + xlab('BU_WC  minus  BU_BC') + ylab(expression(paste(Delta,' log ( ', N[2], 'O ) conc.'))) +
scale_x_continuous(breaks=0:140*30) + theme_bw() +  theme(axis.title.x = element_text(size=13,face='bold')) +
theme(axis.title.y = element_text(size=13,face='bold'), axis.title.x = element_text(vjust=-0.5), axis.title.y =
element_text(hjust=-0.5))
#
grid.arrange(Plot_AC_WC__AC_BC,Plot_AC_WC__UB_WC,Plot_AC_WC__UB_BC,Plot_AC_WC__BU_WC,Plot_AC_WC__BU_BC,Plot_AC_BC__UB_W
C,Plot_AC_BC__UB_BC,Plot_AC_BC__BU_WC,Plot_AC_BC__BU_BC,Plot_UB_WC__UB_BC,Plot_UB_WC__BU_WC,Plot_UB_WC__BU_BC,Plot_UB_B
C__BU_WC,Plot_UB_BC__BU_BC,Plot_BU_WC__BU_BC, nrow = 3, ncol = 5)
```

A2. File: Combined ANOVA and Tukey's Analysis.r

```
#####################################################################
#                          Setup and Data Import
#####################################################################
getwd()
setwd("C:\\Users\\jmdavis4\\Google Drive\\Research\\R Code")

require(ggplot2)
require(gridExtra)

## Summary function definitions here...
## Summarizes data.
## Gives count, mean, standard deviation, standard error of the mean, and confidence
## interval (default 95%).
##   data: a data frame.
##   measurevar: the name of a column that contains the variable to be summariezed
##   groupvars: a vector containing names of columns that contain grouping variables
##   na.rm: a boolean that indicates whether to ignore NA's
##   conf.interval: the percent range of the confidence interval (default is 95%)

summarySE <- function(data=NULL, measurevar, groupvars=NULL, na.rm=FALSE, conf.interval=.95) {
  library(doBy)

  # New version of length which can handle NA's: if na.rm==T, don't count them
  length2 <- function (x, na.rm=FALSE) {
    if (na.rm) sum(!is.na(x))
    else       length(x)
  }
```

```
  # Collapse the data
  formula <- as.formula(paste(measurevar, paste(groupvars, collapse=" + "), sep=" ~ "))
  datac <- summaryBy(formula, data=data, FUN=c(length2,mean,sd), na.rm=na.rm)

  # Rename columns
  names(datac)[ names(datac) == paste(measurevar, ".mean",    sep="") ] <- measurevar
  names(datac)[ names(datac) == paste(measurevar, ".sd",      sep="") ] <- "sd"
  names(datac)[ names(datac) == paste(measurevar, ".length2", sep="") ] <- "N"

  datac$se <- datac$sd / sqrt(datac$N)  # Calculate standard error of the mean

  # Confidence interval multiplier for standard error
  # Calculate t-statistic for confidence interval:
  # e.g., if conf.interval is .95, use .975 (above/below), and use df=N-1
  ciMult <- qt(conf.interval/2 + .5, datac$N-1)
  datac$ci <- datac$se * ciMult

  return(datac)
}

# Can change the next two lines to test with or without acid columns

file = read.table("Combined Data.csv", sep=',', header=T) #Normal
# file = read.table("Combined Data No Acid.csv", sep=',', header=T) #Excludes Acid Column
combined_genes = read.table("Combined Genes.csv", sep=',', header=T) #For total micro ANOVAs
# combined_genes = read.table("Combined Genes No Acid.csv", sep=',', header=T) #Excludes Acid Column

#####################################################################
#           Gene Tests for Normality in Treatment
#####################################################################

# Testing normality of microbial data by Treatment pH category before doing ANOVA

shapiro.test(subset(file, Treatment == "WC" & pH.cat == "AC")$NirK.mean)
shapiro.test(subset(file, Treatment == "WC" & pH.cat == "UB")$NirK.mean)
shapiro.test(subset(file, Treatment == "WC" & pH.cat == "BU")$NirK.mean)
shapiro.test(subset(file, Treatment == "WC" & pH.cat == "AC")$NirS.mean) #not normal - tested for outliers and removed
from main plot
shapiro.test(subset(file, Treatment == "WC" & pH.cat == "UB")$NirS.mean)
shapiro.test(subset(file, Treatment == "WC" & pH.cat == "BU")$NirS.mean)
shapiro.test(subset(file, Treatment == "WC" & pH.cat == "AC")$NosZ.mean)
shapiro.test(subset(file, Treatment == "WC" & pH.cat == "UB")$NosZ.mean)
shapiro.test(subset(file, Treatment == "WC" & pH.cat == "BU")$NosZ.mean)
```

```
shapiro.test(subset(file, Treatment == "WC" & pH.cat == "BU")$NirS_div_NirK)
shapiro.test(subset(file, Treatment == "WC" & pH.cat == "BU")$NosZ_div_NirS)
shapiro.test(subset(file, Treatment == "WC" & pH.cat == "BU")$NosZ_div_NirK)
shapiro.test(subset(file, Treatment == "WC" & pH.cat == "BU")$NosZ_div_NirKS)
shapiro.test(subset(file, Treatment == "WC" & pH.cat == "UB")$NirS_div_NirK)
shapiro.test(subset(file, Treatment == "WC" & pH.cat == "UB")$NosZ_div_NirS)
shapiro.test(subset(file, Treatment == "WC" & pH.cat == "UB")$NosZ_div_NirK)
shapiro.test(subset(file, Treatment == "WC" & pH.cat == "UB")$NosZ_div_NirKS)
shapiro.test(subset(file, Treatment == "WC" & pH.cat == "AC")$NirS_div_NirK)
shapiro.test(subset(file, Treatment == "WC" & pH.cat == "AC")$NosZ_div_NirS)
shapiro.test(subset(file, Treatment == "WC" & pH.cat == "AC")$NosZ_div_NirK)
shapiro.test(subset(file, Treatment == "WC" & pH.cat == "AC")$NosZ_div_NirKS)

shapiro.test(subset(file, Treatment == "BC" & pH.cat == "AC")$NirK.mean)
shapiro.test(subset(file, Treatment == "BC" & pH.cat == "UB")$NirK.mean) #not normal - tested for outliers and removed
from main plot
shapiro.test(subset(file, Treatment == "BC" & pH.cat == "BU")$NirK.mean)
shapiro.test(subset(file, Treatment == "BC" & pH.cat == "AC")$NirS.mean) #not normal -  tested for outliers and removed
from main plot
shapiro.test(subset(file, Treatment == "BC" & pH.cat == "UB")$NirS.mean)
shapiro.test(subset(file, Treatment == "BC" & pH.cat == "BU")$NirS.mean)
shapiro.test(subset(file, Treatment == "BC" & pH.cat == "AC")$NosZ.mean)
shapiro.test(subset(file, Treatment == "BC" & pH.cat == "UB")$NosZ.mean)
shapiro.test(subset(file, Treatment == "BC" & pH.cat == "BU")$NosZ.mean)

shapiro.test(subset(file, Treatment == "BC" & pH.cat == "BU")$NirS_div_NirK)
shapiro.test(subset(file, Treatment == "BC" & pH.cat == "BU")$NosZ_div_NirS)
shapiro.test(subset(file, Treatment == "BC" & pH.cat == "BU")$NosZ_div_NirK)
shapiro.test(subset(file, Treatment == "BC" & pH.cat == "BU")$NosZ_div_NirKS)
shapiro.test(subset(file, Treatment == "BC" & pH.cat == "UB")$NirS_div_NirK)
shapiro.test(subset(file, Treatment == "BC" & pH.cat == "UB")$NosZ_div_NirS)
shapiro.test(subset(file, Treatment == "BC" & pH.cat == "UB")$NosZ_div_NirK)
shapiro.test(subset(file, Treatment == "BC" & pH.cat == "UB")$NosZ_div_NirKS)
shapiro.test(subset(file, Treatment == "BC" & pH.cat == "AC")$NirS_div_NirK)
shapiro.test(subset(file, Treatment == "BC" & pH.cat == "AC")$NosZ_div_NirS)
shapiro.test(subset(file, Treatment == "BC" & pH.cat == "AC")$NosZ_div_NirK)
shapiro.test(subset(file, Treatment == "BC" & pH.cat == "AC")$NosZ_div_NirKS)
```

```
#########################################################################
#                     ANOVA - (ANalysis Of VAriance)
#########################################################################

# Optionally visualize data with boxplots

# boxplot(Peak.N2O~Treatment*ph.cat,xlab='Treatment',ylab='N2O Production')
# title("Comparison of N2O Production by Treatment")

# One-way ANOVAs:
# Tests null hypothesis that at least one factor's impact is different from 0
# We use the variables Treatment and pH.cat as factors here with the fuction factor()

# One-way ANOVA without equal varience assumption
# oneway.test(DV~factor(1))

# Two-way ANOVAS:
# Test null hypothesis against multiple factors
#"BWT~factor(SMOKE)*factor(RACE)" is called the "model specification formula"
#A+B gives main effects; A:B gives the interaction; A*B gives both A*B=A+B+A:B


#Gene 1-Ways
#########################################################################

#Gene by pH Group
ANOVA_NirK.mean_pH.cat <- aov(file$NirK.mean~factor(file$pH.cat))
ANOVA_NirS.mean_pH.cat <- aov(file$NirS.mean~factor(file$pH.cat))
ANOVA_NosZ.mean_pH.cat <- aov(file$NosZ.mean~factor(file$pH.cat))
ANOVA_NirS_div_NirK_pH.cat <- aov(file$NirS_div_NirK~factor(file$pH.cat))
ANOVA_NosZ_div_NirK_pH.cat <- aov(file$NosZ_div_NirK~factor(file$pH.cat))
ANOVA_NosZ_div_NirS_pH.cat <- aov(file$NosZ_div_NirS~factor(file$pH.cat))
ANOVA_NosZ_div_NirKS_pH.cat <- aov(file$NosZ_div_NirKS~factor(file$pH.cat))
#summaries
summary(ANOVA_NirK.mean_pH.cat)
summary(ANOVA_NirS.mean_pH.cat)
summary(ANOVA_NosZ.mean_pH.cat)
summary(ANOVA_NirS_div_NirK_pH.cat)
summary(ANOVA_NosZ_div_NirK_pH.cat)
summary(ANOVA_NosZ_div_NirS_pH.cat)
summary(ANOVA_NosZ_div_NirKS_pH.cat)
```

```
#Gene by Treatment
ANOVA_NirK.mean_Treatment <- aov(file$NirK.mean~factor(file$Treatment))
ANOVA_NirS.mean_Treatment <- aov(file$NirS.mean~factor(file$Treatment))
ANOVA_NosZ.mean_Treatment <- aov(file$NosZ.mean~factor(file$Treatment))
ANOVA_NirS_div_NirK_Treatment <- aov(file$NirS_div_NirK~factor(file$Treatment))
ANOVA_NosZ_div_NirK_Treatment <- aov(file$NosZ_div_NirK~factor(file$Treatment))
ANOVA_NosZ_div_NirS_Treatment <- aov(file$NosZ_div_NirS~factor(file$Treatment))
ANOVA_NosZ_div_NirKS_Treatment <- aov(file$NosZ_div_NirKS~factor(file$Treatment))
#summaries
summary(ANOVA_NirK.mean_Treatment)
summary(ANOVA_NirS.mean_Treatment)
summary(ANOVA_NosZ.mean_Treatment)
summary(ANOVA_NirS_div_NirK_Treatment)
summary(ANOVA_NosZ_div_NirK_Treatment)
summary(ANOVA_NosZ_div_NirS_Treatment)
summary(ANOVA_NosZ_div_NirKS_Treatment)

#Peak N2O by Gene
ANOVA_Peak.N2O_NirK.mean <- aov(file$Peak.N2O~factor(file$NirK.mean))
ANOVA_Peak.N2O_NirS.mean <- aov(file$Peak.N2O~factor(file$NirS.mean))
ANOVA_Peak.N2O_NosZ.mean <- aov(file$Peak.N2O~factor(file$NosZ.mean))
ANOVA_Peak.N2O_NirS_div_NirK <- aov(file$Peak.N2O~factor(file$NirS_div_NirK))
ANOVA_Peak.N2O_NosZ_div_NirK <- aov(file$Peak.N2O~factor(file$NosZ_div_NirK))
ANOVA_Peak.N2O_NosZ_div_NirS <- aov(file$Peak.N2O~factor(file$NosZ_div_NirS))
ANOVA_Peak.N2O_NosZ_div_NirKS <- aov(file$Peak.N2O~factor(file$NosZ_div_NirKS))
#summaries
summary(ANOVA_Peak.N2O_NirK.mean)
summary(ANOVA_Peak.N2O_NirS.mean)
summary(ANOVA_Peak.N2O_NosZ.mean)
summary(ANOVA_Peak.N2O_NirS_div_NirK)
summary(ANOVA_Peak.N2O_NosZ_div_NirK)
summary(ANOVA_Peak.N2O_NosZ_div_NirS)
summary(ANOVA_Peak.N2O_NosZ_div_NirKS)

#Total Abundance - only valid for the genes of interest... need 16s rRNA or EuBac for all bacteria
ANOVA_Combined.mean_pH.cat <- aov(combined_genes$Combined_Genes~factor(combined_genes$pH.cat))
summary(ANOVA_Combined.mean_pH.cat)
plot(TukeyHSD(ANOVA_Combined.mean_pH.cat))

ANOVA_Combined.Treatment <- aov(combined_genes$Combined_Genes~factor(combined_genes$Treatment))
summary(ANOVA_Combined.Treatment)
plot(TukeyHSD(ANOVA_Combined.Treatment))
```

```
# 2-Ways ANOVAs
#########################################################################
# Notes on Summarizing 2-Way ANOVA
# summary(ANOVA_Save) # Summarizes all
# summary(aov(DV~factor(1)+factor(2))) # Summarizes main effects only


#Gene by Matrix and pH Group
ANOVA2_NirK.mean_pH.cat_Treatment <- aov(file$NirK.mean~factor(file$pH.cat)*factor(file$Treatment))
ANOVA2_NirS.mean_pH.cat.Treatment <- aov(file$NirS.mean~factor(file$pH.cat)*factor(file$Treatment))
ANOVA2_NosZ.mean_pH.cat.Treatment <- aov(file$NosZ.mean~factor(file$pH.cat)*factor(file$Treatment))
ANOVA2_NirS_div_NirK_pH.cat.Treatment <- aov(file$NirS_div_NirK~factor(file$pH.cat)*factor(file$Treatment))
ANOVA2_NosZ_div_NirK_pH.cat.Treatment <- aov(file$NosZ_div_NirK~factor(file$pH.cat)*factor(file$Treatment))
ANOVA2_NosZ_div_NirS_pH.cat.Treatment <- aov(file$NosZ_div_NirS~factor(file$pH.cat)*factor(file$Treatment))
ANOVA2_NosZ_div_NirKS_pH.cat.Treatment <- aov(file$NosZ_div_NirKS~factor(file$pH.cat)*factor(file$Treatment))
#summaries
summary(ANOVA2_NirK.mean_pH.cat_Treatment)
summary(ANOVA2_NirS.mean_pH.cat.Treatment)
summary(ANOVA2_NosZ.mean_pH.cat.Treatment)
summary(ANOVA2_NirS_div_NirK_pH.cat.Treatment)
summary(ANOVA2_NosZ_div_NirK_pH.cat.Treatment)
summary(ANOVA2_NosZ_div_NirS_pH.cat.Treatment)
summary(ANOVA2_NosZ_div_NirKS_pH.cat.Treatment)


#########################################################################
#           Pairwise Comparisons of ANOVA - Tukey's Test
#########################################################################
# Use contrasts to test differences between treatment pairs
# Pairwise Comparisons: Tukey Procedure controls multiple comparison problem
# TukeyHSD(ANOVA_SAVE)
# plot(ANOVA_SAVE(a.1))

# Comparisons
TukeyHSD(ANOVA_NirK.mean_pH.cat)
TukeyHSD(ANOVA_NirS.mean_pH.cat)
TukeyHSD(ANOVA_NosZ.mean_pH.cat)
TukeyHSD(ANOVA_NirS_div_NirK_pH.cat)
TukeyHSD(ANOVA_NosZ_div_NirK_pH.cat)
TukeyHSD(ANOVA_NosZ_div_NirS_pH.cat)
TukeyHSD(ANOVA_NosZ_div_NirKS_pH.cat)
TukeyHSD(ANOVA_NirK.mean_Treatment)
TukeyHSD(ANOVA_NirS.mean_Treatment)
TukeyHSD(ANOVA_NosZ.mean_Treatment)
```

```
TukeyHSD(ANOVA_NirS_div_NirK_Treatment)
TukeyHSD(ANOVA_NosZ_div_NirK_Treatment)
TukeyHSD(ANOVA_NosZ_div_NirS_Treatment)
TukeyHSD(ANOVA_NosZ_div_NirKS_Treatment)


# 1-Way pairwise comparisons Plots - I should probably only do these for areas where ANOVA
# Significant interactions. Those might actually be worth putting in somewhere

par(mfrow=c(1,3))
GenePlot1 <- plot(TukeyHSD(ANOVA_NirK.mean_pH.cat), cex.axis = 1.2)
GenePlot2 <- plot(TukeyHSD(ANOVA_NirS.mean_pH.cat), cex.axis = 1.2)
GenePlot3 <- plot(TukeyHSD(ANOVA_NosZ.mean_pH.cat), cex.axis = 1.2)


# plot(TukeyHSD(ANOVA_NirS_div_NirK_pH.cat))
# plot(TukeyHSD(ANOVA_NosZ_div_NirK_pH.cat))
# plot(TukeyHSD(ANOVA_NosZ_div_NirS_pH.cat))
# plot(TukeyHSD(ANOVA_NosZ_div_NirKS_pH.cat))
#
# plot(TukeyHSD(ANOVA_NirK.mean_Treatment))
# plot(TukeyHSD(ANOVA_NirS.mean_Treatment))
# plot(TukeyHSD(ANOVA_NosZ.mean_Treatment))
# plot(TukeyHSD(ANOVA_NirS_div_NirK_Treatment))
# plot(TukeyHSD(ANOVA_NosZ_div_NirK_Treatment))
# plot(TukeyHSD(ANOVA_NosZ_div_NirS_Treatment))
# plot(TukeyHSD(ANOVA_NosZ_div_NirKS_Treatment))


# 2-Way pairwise comparisons
# TukeyHSD(ANOVA2_SAVE) #Produces Multiple Sets of Pairs
# plot(TukeyHSD(ANOVA2_SAVE,'factor(1):factor(2)'))

# These plots just have too much going on. Better to put in a table I think


#####################################################################
#                     Peak Comparisons
#####################################################################

peakN2O_Treat<-aov(file$Peak.N2O~file$Treatment)
peakN2O_Treat.HSD<-TukeyHSD(peakN2O_Treat)
peakN2O_Treat.HSD
```

```
peakN2O_pH<-aov(file$Peak.N2O~file$pH.cat)
peakN2O_pH.HSD<-TukeyHSD(peakN2O_pH)
peakN2O_pH.HSD

peakTime_Treat<-aov(file$Peak.Time~file$Treatment)
peakTime_Treat.HSD<-TukeyHSD(peakTime_Treat)
peakTime_Treat.HSD

peakTime_pH<-aov(file$Peak.Time~file$pH.cat)
peakTime_pH.HSD<-TukeyHSD(peakTime_pH)
peakTime_pH.HSD


#########################################################################
#                     Kruskal-Wallis Tests
#########################################################################
#
# # Non-parametric version of ANOVA known as Kruskal-Wallis Test
# # kruskal.test(DV~factor(1))
# # This could be fun to explore in a later paper
# # Can't we do more than this?
#
# #Gene copy number by mean pH
# kruskal.test(file$NirK.mean~factor(file$pH.cat))
# kruskal.test(file$NirS.mean~factor(file$pH.cat))
# kruskal.test(file$NosZ.mean~factor(file$pH.cat))
# kruskal.test(file$NirS_div_NirK~factor(file$pH.cat))
# kruskal.test(file$NosZ_div_NirK~factor(file$pH.cat))
# kruskal.test(file$NosZ_div_NirS~factor(file$pH.cat))
# kruskal.test(file$NosZ_div_NirKS~factor(file$pH.cat))
#
# #Gene copy number by mean pH
# kruskal.test(file$NirK.mean~factor(file$Treatment))
# kruskal.test(file$NirS.mean~factor(file$Treatment))
# kruskal.test(file$NosZ.mean~factor(file$Treatment))
# kruskal.test(file$NirS_div_NirK~factor(file$Treatment))
# kruskal.test(file$NosZ_div_NirK~factor(file$Treatment))
# kruskal.test(file$NosZ_div_NirS~factor(file$Treatment))
# kruskal.test(file$NosZ_div_NirKS~factor(file$Treatment))
#
# #Testing of N2O by pH group and Treatment
# kruskal.test(file$Peak.N2O~factor(file$pH.cat))
# kruskal.test(file$Peak.N2O~factor(file$Treatment))
```

```
#########################################################################
#   Linear Models - N2O and logN2O by Time, pH group, and Treatment
#########################################################################
# Not used in final analysis
#
# attach(file)
# Results_NirK.mean<- lm(Peak.N2O~NirK.mean)
# Results_NirS.mean<- lm(Peak.N2O~NirS.mean)
# Results_NosZ.mean<- lm(Peak.N2O~NosZ.mean)
# Results_NirS_div_NirK<- lm(Peak.N2O~NirS_div_NirK)
# Results_NosZ_div_NirK<- lm(Peak.N2O~NosZ_div_NirK)
# Results_NosZ_div_NirS<- lm(Peak.N2O~NosZ_div_NirS)
# Results_NosZ_div_NirKS<- lm(Peak.N2O~NosZ_div_NirKS)
# detach(file)
#
# # results_log=lm(Time_Series$N2Otrans~Time_Series$Time_Num*Time_Series$pH.cat*Time_Series$Treatment)
#
# summary(Results_NirK.mean)
# summary(Results_NirS.mean)
# summary(Results_NosZ.mean)
# summary(Results_NirS_div_NirK)
# summary(Results_NosZ_div_NirK)
# summary(Results_NosZ_div_NirS)
# summary(Results_NosZ_div_NirKS)
```

A3. File: Original LOESS Model.r

```
#########################################################################
#                          Setup and Data Import
#########################################################################
getwd()
setwd("C:\\Users\\jmdavis4\\Google Drive\\Research\\R Code")
require(ggplot2)
require(gridExtra)
require(locfit)
require(pastecs)

phData <- read.table('Stacked_pH.csv', sep=',', header=T)
##N2OData <- read.table('Stacked_N2O.csv', sep=',', header=T)
```

```
N2OData_Acid <- read.table('N2O_Acid.csv', sep=',', header=T)
N2OData_Unbuffered <- read.table('N2O_Unbuffered.csv', sep=',', header=T)
N2OData_Buffered <- read.table('N2O_Buffered.csv', sep=',', header=T)

## Summary function definitions here...
## Summarizes data.
## Gives count, mean, standard deviation, standard error of the mean, and confidence
## interval (default 95%).
##   data: a data frame.
##   measurevar: the name of a column that contains the variable to be summariezed
##   groupvars: a vector containing names of columns that contain grouping variables
##   na.rm: a boolean that indicates whether to ignore NA's
##   conf.interval: the percent range of the confidence interval (default is 95%)
summarySE <- function(data=NULL, measurevar, groupvars=NULL, na.rm=FALSE, conf.interval=.95) {
  library(doBy)

  # New version of length which can handle NA's: if na.rm==T, don't count them
  length2 <- function (x, na.rm=FALSE) {
    if (na.rm) sum(!is.na(x))
    else       length(x)
  }

  # Collapse the data
  formula <- as.formula(paste(measurevar, paste(groupvars, collapse=" + "), sep=" ~ "))
  datac <- summaryBy(formula, data=data, FUN=c(length2,mean,sd), na.rm=na.rm)

  # Rename columns
  names(datac)[ names(datac) == paste(measurevar, ".mean",    sep="") ] <- measurevar
  names(datac)[ names(datac) == paste(measurevar, ".sd",      sep="") ] <- "sd"
  names(datac)[ names(datac) == paste(measurevar, ".length2", sep="") ] <- "N"

  datac$se <- datac$sd / sqrt(datac$N)  # Calculate standard error of the mean

  # Confidence interval multiplier for standard error
  # Calculate t-statistic for confidence interval:
  # e.g., if conf.interval is .95, use .975 (above/below), and use df=N-1
  ciMult <- qt(conf.interval/2 + .5, datac$N-1)
  datac$ci <- datac$se * ciMult

  return(datac)
}

N2OData_Acid_sorted <- summarySE(N2OData_Acid, measurevar = "N2O", groupvars=c("Time","Treatment"))
N2OData_Buffered_sorted <- summarySE(N2OData_Buffered, measurevar = "N2O", groupvars=c("Time","Treatment"))
```

```
N2OData_Unbuffered_sorted <- summarySE(N2OData_Unbuffered, measurevar = "N2O", groupvars=c("Time","Treatment"))

AC_WC <- subset(N2OData_Acid_sorted, Treatment == "WC")
AC_BC <- subset(N2OData_Acid_sorted, Treatment == "BC")

UB_WC <- subset(N2OData_Unbuffered_sorted, Treatment == "WC")
UB_BC <- subset(N2OData_Unbuffered_sorted, Treatment == "BC")

BU_WC <- subset(N2OData_Buffered_sorted, Treatment == "WC")
BU_BC <- subset(N2OData_Buffered_sorted, Treatment == "BC")

#####################################################################
#                LOESS fit of N2O over Time
#####################################################################

#Use span=n to adjust smoothing of fit - lower values are tighter... consider 0.25-0.5

#Acid Run

attach(N2OData_Acid_sorted)
plotbyfactor(Time,N2O,Treatment, pch=c(20,20), cex=1.5,xlim=c(0,140),ylim=c(0,40),ylab='N2O Concentration (mg/L)',
             xlab='Time',main='Concentration vs. Time \n Loess with Confidence Intervals', col=c('blue','red'))
legend(0,40,c("AC_BC","AC_WC"),pch=c(20,20),col=c('blue','red'))
detach(N2OData_Acid_sorted)

attach(AC_BC)
loess2<-predict(loess(N2O~Time, span=0.35), se=T)
lines(Time,loess2$fit,col='blue')
lines(Time,loess2$fit+1.96*loess2$s, lty=2,col='blue')
lines(Time,loess2$fit-1.96*loess2$s, lty=2,col='blue')
detach(AC_BC)


lo <- loess(N2O~Time, span=0.35, control=loess.control(surface="direct"), se=T)
predict(lo, newdata=140)

attach(AC_WC)
loess1<-predict(loess(N2O~Time, span=0.5), se=T)
lines(Time,loess1$fit,col='red')
lines(Time,loess1$fit+1.96*loess1$s, lty=2,col='red')
lines(Time,loess1$fit-1.96*loess1$s, lty=2,col='red')
detach(AC_WC)

Acid_Plot <- recordPlot()
```

```
#Unbuffered Run

attach(N2OData_Unbuffered_sorted)
plotbyfactor(Time,N2O,Treatment, pch=c(20,20), cex=1.5,xlim=c(0,140),ylim=c(0,5),ylab='N2O Concentration (mg/L)',
             xlab='Time',main='Concentration vs. Time \n Loess with Confidence Intervals', col=c('blue','red'))
legend(0,5,c("UB_BC","UB_WC"),pch=c(20,20),col=c('blue','red'))
detach(N2OData_Unbuffered_sorted)

attach(UB_BC)
loess3<-predict(loess(N2O~Time, span=0.3), se=T)
lines(Time,loess3$fit, col='blue')
lines(Time,loess3$fit+1.96*loess3$s, lty=2,col='blue')
lines(Time,loess3$fit-1.96*loess3$s, lty=2,col='blue')
detach(UB_BC)

attach(UB_WC)
loess4<-predict(loess(N2O~Time, span=0.3), se=T)
lines(Time,loess4$fit,col='red')
lines(Time,loess4$fit+1.96*loess4$s, lty=2,col='red')
lines(Time,loess4$fit-1.96*loess4$s, lty=2,col='red')
detach(UB_WC)

Unbuffered_Plot <- recordPlot()

#Buffered Run

attach(N2OData_Buffered_sorted)
plotbyfactor(Time,N2O,Treatment, pch=c(20,20), cex=1.5,xlim=c(0,140),ylim=c(0,1.5),ylab='N2O Concentration (mg/L)',
             xlab='Time',main='Concentration vs. Time \n Loess with Confidence Intervals', col=c('blue','red'))
legend(0,1.5,c("BU_BC","BU_WC"),pch=c(20,20),col=c('blue','red'))
detach(N2OData_Buffered_sorted)

attach(BU_BC)
loess5<-predict(loess(N2O~Time, span=0.35), se=T)
lines(Time,loess5$fit, col='blue')
lines(Time,loess5$fit+1.96*loess5$s, lty=2,col='blue')
lines(Time,loess5$fit-1.96*loess5$s, lty=2,col='blue')
detach(BU_BC)

attach(BU_WC)
loess6<-predict(loess(N2O~Time, span=0.35), se=T)
lines(Time,loess6$fit,col='red')
lines(Time,loess6$fit+1.96*loess6$s, lty=2,col='red')
```

```
lines(Time,loess6$fit-1.96*loess6$s, lty=2,col='red')
detach(BU_WC)

Buffered_Plot <- recordPlot()
```

A4. File: Summary Plots.r

```
#########################################################################
#                           Setup and Data Import
#########################################################################
getwd()
setwd("C:\\Users\\jmdavis4\\Google Drive\\Research\\R Code")
require(ggplot2)
require(gridExtra)
require(locfit)
require(pastecs)

phData <- read.table('Stacked_pH.csv', sep=',', header=T)
##N2OData <- read.table('Stacked_N2O.csv', sep=',', header=T)
N2OData_Acid <- read.table('N2O_Acid.csv', sep=',', header=T)
N2OData_Unbuffered <- read.table('N2O_Unbuffered.csv', sep=',', header=T)
N2OData_Buffered <- read.table('N2O_Buffered.csv', sep=',', header=T)

## Summary function definitions here...
## Summarizes data.
## Gives count, mean, standard deviation, standard error of the mean, and confidence
## interval (default 95%).
##   data: a data frame.
##   measurevar: the name of a column that contains the variable to be summariezed
##   groupvars: a vector containing names of columns that contain grouping variables
##   na.rm: a boolean that indicates whether to ignore NA's
##   conf.interval: the percent range of the confidence interval (default is 95%)
summarySE <- function(data=NULL, measurevar, groupvars=NULL, na.rm=FALSE, conf.interval=.95) {
  library(doBy)

  # New version of length which can handle NA's: if na.rm==T, don't count them
  length2 <- function (x, na.rm=FALSE) {
    if (na.rm) sum(!is.na(x))
    else       length(x)
  }

  # Collapse the data
  formula <- as.formula(paste(measurevar, paste(groupvars, collapse=" + "), sep=" ~ "))
  datac <- summaryBy(formula, data=data, FUN=c(length2,mean,sd), na.rm=na.rm)

  # Rename columns
  names(datac)[ names(datac) == paste(measurevar, ".mean",    sep="") ] <- measurevar
```

```
  names(datac)[ names(datac) == paste(measurevar, ".sd",      sep="") ] <- "sd"
  names(datac)[ names(datac) == paste(measurevar, ".length2", sep="") ] <- "N"

  datac$se <- datac$sd / sqrt(datac$N)  # Calculate standard error of the mean

  # Confidence interval multiplier for standard error
  # Calculate t-statistic for confidence interval:
  # e.g., if conf.interval is .95, use .975 (above/below), and use df=N-1
  ciMult <- qt(conf.interval/2 + .5, datac$N-1)
  datac$ci <- datac$se * ciMult

  return(datac)
}

#Q-Q plot with qline for ggplot2

qqplot.data <- function (vec) # argument: vector of numbers
{
  # following four lines from base R's qqline()
  y <- quantile(vec[!is.na(vec)], c(0.25, 0.75))
  x <- qnorm(c(0.25, 0.75))
  slope <- diff(y)/diff(x)
  int <- y[1L] - slope * x[1L]

  d <- data.frame(resids = vec)

  ggplot(d, aes(sample = resids)) + stat_qq() + geom_abline(slope = slope, intercept = int, linetype="dashed")
}

#Reading in summary dependant data now

file = read.table("Combined Data.csv", sep=',', header=T)
pHData_Sorted <- summarySE(phData, measurevar = "pH", groupvars=c("Time","Treatment"))

#####################################################################
#               pH QQ Plots, Summary, Normality
#####################################################################

stat.desc(subset(pHData_Sorted, Treatment == "AC_WC" | Treatment == "AC_BC")$pH)
stat.desc(subset(pHData_Sorted, Treatment == "UB_WC" | Treatment == "UB_BC")$pH)
stat.desc(subset(pHData_Sorted, Treatment == "BU_WC" | Treatment == "BU_BC")$pH)
shapiro.test(subset(pHData_Sorted, Treatment == "AC_WC" | Treatment == "AC_BC")$pH)
shapiro.test(subset(pHData_Sorted, Treatment == "UB_WC" | Treatment == "UB_BC")$pH)
shapiro.test(subset(pHData_Sorted, Treatment == "BU_WC" | Treatment == "BU_BC")$pH)
```

```
shapiro.test(subset(pHData_Sorted, Treatment == "AC_WC")$pH)
shapiro.test(subset(pHData_Sorted, Treatment == "UB_WC")$pH)
shapiro.test(subset(pHData_Sorted, Treatment == "BU_WC")$pH)
shapiro.test(subset(pHData_Sorted, Treatment == "AC_BC")$pH)
shapiro.test(subset(pHData_Sorted, Treatment == "UB_BC")$pH)
shapiro.test(subset(pHData_Sorted, Treatment == "BU_BC")$pH)

pH_QQ1 <- qqplot.data(subset(pHData_Sorted, Treatment == "AC_WC" | Treatment == "AC_BC")$pH) + ggtitle("Acidified
Treatment") + ylab("pH")
pH_QQ2 <- qqplot.data(subset(pHData_Sorted, Treatment == "UB_WC" | Treatment == "UB_BC")$pH) + ggtitle("Unbuffered
Treatment") + ylab("pH")
pH_QQ3 <- qqplot.data(subset(pHData_Sorted, Treatment == "BU_WC" | Treatment == "BU_BC")$pH) + ggtitle("Buffered
Treatment") + ylab("pH")

grid.arrange(pH_QQ1, pH_QQ2, pH_QQ3, ncol=3)


#########################################################################
#                        pH and N2O Time Series
#########################################################################

#To add a LOESS fit to ggplot, use the geom_smooth() function in the ggplot call. Adjust fit with span=n
#e.g. ggplot(data, aes(x=x, y=y)) + geom_smooth() + theme_bw()

pd <- position_dodge(.1) # move them .05 to the left and right

#N2OData_sorted <- summarySE(N2OData, measurevar = "N2O", groupvars=c("Time","Treatment","Matrix"))

N2OData_Acid_sorted <- summarySE(N2OData_Acid, measurevar = "N2O", groupvars=c("Time","Treatment"))
N2OData_Buffered_sorted <- summarySE(N2OData_Buffered, measurevar = "N2O", groupvars=c("Time","Treatment"))
N2OData_Unbuffered_sorted <- summarySE(N2OData_Unbuffered, measurevar = "N2O", groupvars=c("Time","Treatment"))

ggplot(pHData_Sorted, aes(x=Time, y=pH, colour=Treatment, group=Treatment)) +
  geom_errorbar(aes(ymin=pH-se, ymax=pH+se), width=7, linetype=5, alpha=0.7, position=pd) +
  geom_line(position=pd, alpha=0.5) + geom_point(position=pd, size=2, shape=21, fill="white") + expand_limits(y=0) +
  scale_y_continuous(breaks=0:9*1) + scale_x_continuous(breaks=0:140*10) + xlab("Time (hrs)") +
  scale_color_hue(name="Treatment", l=40) + ggtitle("Time series of pH by treatment\n") +
  theme_bw() + theme(plot.title = element_text(face="bold"), legend.direction="horizontal",
legend.justification=c(1,0), legend.position=c(1,0))

N2O_plot1 <- ggplot(N2OData_Acid_sorted, aes(x=Time, y=N2O, colour=Treatment)) +
  geom_errorbar(aes(ymin=N2O-se, ymax=N2O+se), width=4, linetype=5, alpha=0.7, position=pd) +
  geom_line(position=pd) + geom_point(position=pd, size=3, shape=21, fill="white") +
```

```
  scale_x_continuous(breaks=0:140*10) + scale_y_continuous(breaks=0:11*5) + coord_cartesian(ylim = c(-2.5, 57.5)) +
  xlab("Time (hrs)") + ylab(expression(paste(N[2], "O (ppm)"))) +
  scale_color_hue(name="Treatment", l=40) + ggtitle(expression(paste("Change in Headspace ", N[2], "O Over Time
(Acid)"))) +
  theme_bw() + theme(plot.title = element_text(face="bold"), legend.justification=c(1,1), legend.position=c(1,1))

N2O_plot2 <- ggplot(N2OData_Unbuffered_sorted, aes(x=Time, y=N2O, colour=Treatment)) +
  geom_errorbar(aes(ymin=N2O-se, ymax=N2O+se), width=4, linetype=5, alpha=0.7, position=pd) +
  geom_line(position=pd) + geom_point(position=pd, size=3, shape=21, fill="white") +
  scale_x_continuous(breaks=0:140*10) + scale_y_continuous(breaks=0:11*.6) + coord_cartesian(ylim = c(-0.3, 6.9)) +
  xlab("Time (hrs)") + ylab(expression(paste(N[2], "O (ppm)"))) +
  scale_color_hue(name="Treatment", l=40) + ggtitle(expression(paste("Change in Headspace ", N[2], "O Over Time
(Unbuffered)"))) +
  theme_bw() + theme(plot.title = element_text(face="bold"), legend.justification=c(1,1), legend.position=c(1,1))

N2O_plot3 <- ggplot(N2OData_Buffered_sorted, aes(x=Time, y=N2O, colour=Treatment)) +
  geom_errorbar(aes(ymin=N2O-se, ymax=N2O+se), width=4, linetype=5, alpha=0.7, position=pd) +
  geom_line(position=pd) + geom_point(position=pd, size=3, shape=21, fill="white") +
  scale_x_continuous(breaks=0:140*10) + scale_y_continuous(breaks=0:11*.1) + coord_cartesian(ylim = c(-0.05, 1.15)) +
  xlab("Time (hrs)") + ylab(expression(paste(N[2], "O (ppm)"))) +
  scale_color_hue(name="Treatment", l=40) + ggtitle(expression(paste("Change in Headspace ", N[2], "O Over Time
(Buffered)"))) +
  theme_bw() + theme(plot.title = element_text(face="bold"), legend.justification=c(1,1), legend.position=c(1,1))

grid.arrange(N2O_plot1,N2O_plot2,N2O_plot3, ncol=3)

#LOESS fits

APlot <- ggplot(N2OData_Acid_sorted, aes(x=Time, y=N2O, colour=Treatment)) +
  geom_line(position=pd, alpha=0.5) + geom_point(position=pd, size=3, shape=21, fill="white") +
  scale_x_continuous(breaks=0:140*10) + scale_y_continuous(breaks=0:6*6) + coord_cartesian(ylim = c(-2.5, 39)) +
  xlab("Time (hrs)") + ylab(expression(paste(N[2], "O (ppm)"))) + geom_smooth(span=0.35, aes(fill=Treatment)) +
  scale_color_hue(name="Treatment", l=40) + ggtitle("Acid Treatment - mean pH = 2.56 (AC)") +
  theme_bw() + theme(plot.title = element_text(face="bold"), legend.justification=c(0,1), legend.position=c(0,1))

UPlot <- ggplot(N2OData_Unbuffered_sorted, aes(x=Time, y=N2O, colour=Treatment)) +
  geom_line(position=pd, alpha=0.5) + geom_point(position=pd, size=3, shape=21, fill="white") +
  scale_x_continuous(breaks=0:140*10) + scale_y_continuous(breaks=0:6*.6) + coord_cartesian(ylim = c(-0.3, 3.9)) +
  xlab("Time (hrs)") + ylab(expression(paste(N[2], "O (ppm)"))) + geom_smooth(span=0.35, aes(fill=Treatment)) +
  scale_color_hue(name="Treatment", l=40) + ggtitle("Unbuffered Treatment - mean pH = 6.70 (UB)") +
  theme_bw() + theme(plot.title = element_text(face="bold"), legend.justification=c(1,1), legend.position=c(1,1))

BPlot <- ggplot(N2OData_Buffered_sorted, aes(x=Time, y=N2O, colour=Treatment)) +
  geom_line(position=pd, alpha=0.5) + geom_point(position=pd, size=3, shape=21, fill="white") +
```

```
  scale_x_continuous(breaks=0:140*10) + scale_y_continuous(breaks=0:6*.2) + coord_cartesian(ylim = c(-0.05, 1.3)) +
  xlab("Time (hrs)") + ylab(expression(paste(N[2], "O (ppm)"))) + geom_smooth(span=0.35, aes(fill=Treatment)) +
  scale_color_hue(name="Treatment", l=40) + ggtitle("Buffered Treatment - mean pH = 8.08 (BU)") +
  theme_bw() + theme(plot.title = element_text(face="bold"), legend.justification=c(1,1), legend.position=c(1,1))

##Combined LOESS Plots

#Keying data

N2ODataAcid_sorted$Treatment <- sub("^", "AC_", N2ODataAcid_sorted$Treatment)
N2ODataBuffered_sorted$Treatment <- sub("^", "BU_", N2ODataBuffered_sorted$Treatment)
N2ODataUnbuffered_sorted$Treatment <- sub("^", "UB_", N2ODataUnbuffered_sorted$Treatment)

Combine <- rbind(N2ODataUnbuffered_sorted, N2ODataBuffered_sorted)
TotalPlot <- rbind(N2ODataAcid_sorted, N2ODataUnbuffered_sorted, N2ODataBuffered_sorted)

ComboPlot <- ggplot(Combine, aes(x=Time, y=N2O, colour=Treatment)) +
  geom_line(position=pd, alpha=0.5) + geom_point(position=pd, size=3, shape=21, fill="white") +
  scale_x_continuous(breaks=0:140*10) + scale_y_continuous(breaks=0:6*.6) + coord_cartesian(ylim = c(-0.3, 3.9)) +
  xlab("Time (hrs)") + ylab(expression(paste(N[2], "O (ppm)"))) + geom_smooth(span=0.4,aes(fill=Treatment)) +
  scale_color_hue(name="Treatment", l=40) +
  theme_bw() + theme(plot.title = element_text(face="bold"), legend.justification=c(1,1), legend.position=c(1,1))

APlot <- ggplot(N2ODataAcid_sorted, aes(x=Time, y=N2O, colour=Treatment)) +
  geom_line(position=pd, alpha=0.5) + geom_point(position=pd, size=3, shape=21, fill="white") +
  scale_x_continuous(breaks=0:140*10) + scale_y_continuous(breaks=0:6*6) + coord_cartesian(ylim = c(-2.5, 39)) +
  xlab("Time (hrs)") + ylab(expression(paste(N[2], "O (ppm)"))) + geom_smooth(span=0.4, aes(fill=Treatment)) +
  scale_color_hue(name="Treatment", l=40) +
  theme_bw() + theme(plot.title = element_text(face="bold"), legend.justification=c(0,1), legend.position=c(0,1))

grid.arrange(APlot, ComboPlot, ncol = 2)

#TotalPlot
CriticalPlot <- ggplot(TotalPlot, aes(x=Time, y=N2O, colour=Treatment)) +
  geom_line(position=pd, alpha=0.5) + geom_point(position=pd, size=3, shape=21, fill="white") +
  scale_x_continuous(breaks=0:32*4) + scale_y_continuous(breaks=0:5*1) + coord_cartesian(xlim = c(-1, 34),
  ylim = c(-1, 5.1)) +xlab("Time (hrs)") + ylab(expression(paste(N[2], "O (ppm)"))) +
  geom_smooth(span=0.367, aes(fill=Treatment))+ guides(col = guide_legend(ncol = 2)) +
  scale_color_hue(name="Treatment", l=40) +   theme_bw() + theme(plot.title = element_text(face="bold"),
  legend.justification=c(1,1), legend.position=c(1,1))

grid.arrange(APlot, ComboPlot, CriticalPlot, ncol = 3)
```

```
#########################################################################
#                       pH and N2O Interaction Plots
#########################################################################

# # Standard - means without bars
#
# interaction.plot(Treatment, pH.cat, Peak.N2O, type="b", col=c(1:3),leg.bty="o",
#                  leg.bg="beige", pch=c(18,24,22), xlab="Treatment",
#                  ylab=expression(paste("Peak Headspace ", N[2], "O (ppm)")),
#                  main=expression(paste(N[2], "O Treatment Interaction Plot")), trace.label ="pH Group")
#
#
# # SciPlot - standard interaction plot plus error bars
#
# library(sciplot)
# data(file)
# lineplot.CI(Treatment, Peak.N2O, group = pH.cat, data = file, , col=c(1:3), leg.bty="o",
#             leg.bg="beige", pch=c(18,24,22), xlab="Treatment", x.leg=1.95, y.leg=42,
#             ylab=expression(paste("Peak Headspace ", N[2], "O (ppm)")),
#             main=expression(paste(N[2], "O Treatment Interaction Plot")), trace.label ="pH Group")

# GGplot for N2O pH interaction

GasSum <- summarySE(file, measurevar="Peak.N2O", groupvars=c("Treatment", "pH.cat"))

pd <- position_dodge(0.0)

ggplot(GasSum, aes(x=Treatment, y=Peak.N2O, colour=pH.cat, group=pH.cat, ymax=50.01)) +
  geom_errorbar(aes(ymin=Peak.N2O-se, ymax=Peak.N2O+se), width = 0.1, linetype=5, alpha=0.7, position=pd) +
  geom_line(position=pd, alpha =0.7) + geom_point(position=pd, size=3, shape=21, fill="white") +
  xlab("Matrix Material") + ylab(expression(paste("Peak Headspace ", N[2], "O (ppm)"))) + coord_cartesian(xlim =
c(0.75, 2.25)) +
  scale_colour_hue(name="pH Range", breaks=c("AC", "UB", "BU"), labels=c("Acidified", "Unbuffered", "Buffered"), l=40)
+
  ggtitle(expression(paste(N[2], "O Treatment Interaction Plot"))) +  theme_bw() +
  theme(legend.justification=c(1,0), legend.position=c(1,0.55), panel.grid.major = element_blank(),
        panel.grid.minor = element_blank(), axis.title=element_text(size= rel(1.5)),
        axis.text=element_text(size= rel(1.3)), plot.title=element_text(size= rel(1.5)))

#########################################################################
#                       Gene Interaction Plots
#########################################################################
# ggplot code is below for producing log-transformed interaction plots...
# I feel like these aren't different enough to use after What I saw
```

```
#
# pd <- position_dodge(0.1)
#
# file$logNirK.mean <- log10(file$NirK.mean)
# file$logNirS.mean <- log10(file$NirS.mean)
# file$logNosZ.mean <- log10(file$NosZ.mean)
#
# NirKSum <- summarySE(file, measurevar="logNirK.mean", groupvars=c("Treatment", "pH.cat"))
# NirSSum <- summarySE(file, measurevar="logNirS.mean", groupvars=c("Treatment", "pH.cat"))
# NosZSum <- summarySE(file, measurevar="logNosZ.mean", groupvars=c("Treatment", "pH.cat"))
#
# NirKPlot <-  ggplot(NirKSum, aes(x=Treatment, y=logNirK.mean, colour=pH.cat, group=pH.cat)) +
#   geom_errorbar(aes(ymin=logNirK.mean-se, ymax=logNirK.mean+se), width = 0.1, linetype=5, alpha=0.7, position=pd) +
#   geom_line(position=pd, alpha =0.7) + geom_point(position=pd, size=3, shape=21, fill="white") +
#   xlab("Matrix Material") + scale_y_continuous(expression(paste("Log10 ",italic("nirK")," copies"))) +
#   scale_colour_hue(name="pH Range", breaks=c("AC", "UB", "BU"), labels=c("Acidified", "Unbuffered", "Buffered"),
#   l=40) + coord_cartesian(ylim = c(3.75, 8.25)) + theme_bw() +
#   theme(legend.position = "none", panel.grid.major = element_blank(),
#         panel.grid.minor = element_blank(), axis.title=element_text(size= rel(1.5)),
#         axis.text=element_text(size= rel(1.3)), plot.title=element_text(size= rel(1.5)))
#
# NirSPlot <-  ggplot(NirSSum, aes(x=Treatment, y=logNirS.mean, colour=pH.cat, group=pH.cat)) +
#   geom_errorbar(aes(ymin=logNirS.mean-se, ymax=logNirS.mean+se), width = 0.1, linetype=5, alpha=0.7, position=pd) +
#   geom_line(position=pd, alpha =0.7) + geom_point(position=pd, size=3, shape=21, fill="white") +
#   xlab("Matrix Material") + scale_y_continuous(expression(paste("Log10 ",italic("nirS")," copies"))) +
#   scale_colour_hue(name="pH Range", breaks=c("AC", "UB", "BU"), labels=c("Acidified", "Unbuffered", "Buffered"),
#   l=40) + coord_cartesian(ylim = c(3.75, 8.25)) + theme_bw() +
#   theme(legend.position = "none", panel.grid.major = element_blank(),
#         panel.grid.minor = element_blank(), axis.title=element_text(size= rel(1.5)),
#         axis.text=element_text(size= rel(1.3)), plot.title=element_text(size= rel(1.5)))
#
# NosZPlot <-  ggplot(NosZSum, aes(x=Treatment, y=logNosZ.mean, colour=pH.cat, group=pH.cat)) +
#   geom_errorbar(aes(ymin=logNosZ.mean-se, ymax=logNosZ.mean+se), width = 0.1, linetype=5, alpha=0.7, position=pd) +
#   geom_line(position=pd, alpha =0.7) + geom_point(position=pd, size=3, shape=21, fill="white") +
#   xlab("Matrix Material") + scale_y_continuous(expression(paste("Log10 ",italic("nosZ")," copies"))) +
#   scale_colour_hue(name="pH Range", breaks=c("AC", "UB", "BU"), labels=c("Acidified", "Unbuffered", "Buffered"),
#   l=40) + coord_cartesian(ylim = c(3.75, 8.25)) + theme_bw() +
#   theme(legend.position = "none", panel.grid.major = element_blank(),
#         panel.grid.minor = element_blank(), axis.title=element_text(size= rel(1.5)),
#         axis.text=element_text(size= rel(1.3)), plot.title=element_text(size= rel(1.5)))
#
# grid.arrange(NirKPlot, NirSPlot, NosZPlot, ncol=3)
```